National Library of Canada

Cataloguing Branch
Canadian Theses Division

Ottawa, Canada
K1A 0N4

Bibliothèque nationale du Canada

Direction du catalogage
Division des thèses canadiennes

## NOTICE

The quality of this microfiche is heavily dependent upon the quality of the original thesis submitted for microfilming. Every effort has been made to ensure the highest quality of reproduction possible.

If pages are missing, contact the university which granted the degree.

Some pages may have indistinct print especially if the original pages were typed with a poor typewriter ribbon or if the university sent us a poor photocopy.

Previously copyrighted materials (journal articles, published tests, etc.) are not filmed.

Reproduction in full or in part of this film is governed by the Canadian Copyright Act, R.S.C. 1970, c. C-30. Please read the authorization forms which accompany this thesis.

THIS DISSERTATION
HAS BEEN MICROFILMED
EXACTLY AS RECEIVED

## AVIS

La qualité de cette microfiche dépend grandement de la qualité de la thèse soumise au microfilmage. Nous avons tout fait pour assurer une qualité supérieure de reproduction.

S'il manque des pages, veuillez communiquer avec l'université qui a conféré le grade.

La qualité d'impression de certaines pages peut laisser à désirer, surtout si les pages originales ont été dactylographiées à l'aide d'un ruban usé ou si l'université nous a fait parvenir une photocopie de mauvaise qualité.

Les documents qui font déjà l'objet d'un droit d'auteur (articles de revue, examens publiés, etc.) ne sont pas microfilmés.

La reproduction, même partielle, de ce microfilm est soumise à la Loi canadienne sur le droit d'auteur, SRC 1970, c. C-30. Veuillez prendre connaissance des formules d'autorisation qui accompagnent cette thèse.

LA THÈSE A ÉTÉ
MICROFILMÉE TELLE QUE
NOUS L'AVONS REÇUE

# THEORETICAL AND EXPERIMENTAL INVESTIGATION OF STAPLED CONNECTIONS

Matthew-Andrew Kalosinakis

A Thesis

in the

Centre for

Building Studies

Faculty of Engineering

Presented in Partial Fulfillment of the Requirements
for the degree Master of Engineering at
Concordia University
Montreal, Quebec, Canada

June 1978

© Matthew-Andrew Kalosinakis

## ABSTRACT

THEORETICAL AND EXPERIMENTAL

INVESTIGATION OF STAPLED CONNECTIONS

Matthew-Andrew Kalosinakis

An experimental and theoretical investigation was carried out on stapled connections to determine their performance and potential uses for load-carrying applications in the building industry.

The first part of the experimental investigation was carried out on a set of stapled connections using aluminum extrusions to connect aluminum sandwich panels in a half-scale panelized model. The results showed that:

i) these connections behaved much like nailed wood connections but having greater stiffness and capacity.

ii) the stiffness and capacity are substantially reduced by gaps between the flange of the connection and the facing of the panel.

iii) the load-deformation relationship is non linear but it can be considered elastic except for residual deformations resulting after initial load cycles.

Based upon the above results, the theory by Kuenzi[27] for nailed connections was adopted and modified to satisfy the conditions of the stapled connections. In this theory, the principal parameters affecting the behaviour of stapled connections were identified.

In the second part of the experimental investigation, these parameters were varied to verify the theory and to develop design formulae.

## ACKNOWLEDGEMENTS

The author wishes to express his gratitude to his thesis supervisor, Dr. P.P. Fazio, Director of the Centre for Building Studies, Concordia University, for his guidance and advice throughout the course of the research work.

The valuable advice and ideas of Professor C. Marsh and Mr. S. Rizzo are greatly appreciated.

The financial support of the National Research Council and les subventions de formation de chercheurs et d'action concertée (FCAC) is acknowledged.

The author also wishes to thank the staff of the Structures Laboratory and the Machine Shop for their assistance and wishes to thank P. O'Cain for typing his thesis.

TABLE OF CONTENTS

# LIST OF TABLES

## LIST OF FIGURES

## NOTATIONS

| | |
|---|---|
| b | width of a member |
| c | constant |
| D | diameter of staple leg |
| E | modulus of elasticity |
| F | force on aluminium sheet |
| $F_B$ | bearing strength of aluminum |
| $F_u$ | ultimate strength of aluminum |
| $F_y$ | yield strength of aluminum or steel |
| $F_{us}$ | ultimate shear strength of aluminium |
| $F_{ys}$ | yield shear strength of aluminum |
| $f_1$ | capacity of a single fastener at 0.015 in deformation |
| K | stiffness |
| k | $K_o b$ (lbs/in$^2$) particular foundation modulus comprising the width of the beam |
| $K_o$ | (lbs/in$^3$) elastic bearing modulus of foundation |
| $K_s$ | stiffness of aluminum sheet on bearing |
| L | length of a member |
| M | moment at any point |
| $M_F$ | moment at fixed end of staple |
| $M_o$ | moment at x = 0 |
| N | normal load . number of fasteners |
| P | force . load |
| $\bar{p}$ | K.y (lbs/in) foundation reaction |
| $P_a$ | allowable load |

| | |
|---|---|
| $P_{cr}$ | creep load |
| P.015 | load at .015 inch deformation |
| P.030 | load at .030 inch deformation |
| P.L. | proportional limit |
| Q | shear force |
| $Q_o$ | shear at x = 0 |
| q | external distributed load |
| R | constant |
| r | fastener spacing |
| t | thickness |
| y | deflection at a point |
| $y_o$ | deflection at x = 0 |
| $\Delta$ | total deformation |
| $\delta$ | maximum deformation of the staple leg |
| $\delta_o$ | initial slippage |
| $\theta$ | slope |
| $\theta_o$ | slope at x = 0 |
| $\lambda$ | characteristic of the differential equation |

# CHAPTER I

## INTRODUCTION

Low cost housing is the issue to which many researchers have lately devoted a large part of their research effort. Prefabrication of building components appears to be a very appealing construction method for reducing cost and overcoming adverse weather conditions during construction. One of the projects on low cost housing undertaken at the Centre for Building Studies, of Concordia University in Montreal, is the modular construction of buildings from panels with aluminum face and lightweight core. Part of the studies is the investigation of the structural performance of the proposed building. To this end, a half-scale building model was constructed to be tested. The panels were connected with aluminum extrusions, the flanges of which were stapled to the facings. This type of connection can be effected quickly and cheaply. Moreover, it helps to prevent delamination around the periphery of the panels. The model was subjected to vertical and lateral loads. The results from the lateral loading showed deflection values to be higher than predicted by theory, which assumed fixed connections. The investigation reported herein was carried out to determine the behaviour of the stapled connections. Such investigation must consider all types of forces to which the connections on the model were subjected. These forces include shear, tension and combination of shear and compression. It is customary to determine the performance and the capacity of a

connection by examining the resulting deformations in relation to the imposed loading conditions. Here, the deformation of a connection is defined as the relative movement of the connected members. This deformation could be due to the connected members or the fasteners, or the combination of both.

The work in this thesis extends beyond the experimental investigation of this particular connection. It also includes a theoretical and experimental study of a connection using the same parts but with applications outside building. In the theoretical study, the approach outlined by Kuenzi [27] was adopted. In this theoretical development, the staple is regarded as a beam on elastic foundation. Other theory used in this thesis is the theory of beams on elastic foundations by M. Hetenyi[1]. The above theories and a few others used are explained in the thesis. Due to the fast, inexpensive, and versatile application of staples and their advantageous structural characteristics as compared to other nailed fasteners, the stapled connection becomes very attractive and structurally efficient for many applications in the building industry such as buildings, warehouses, workshops, factories, mobile homes, vehicles, containers and many others. These applications are documented in literature of companies listed in the last page of reference [7]. This work was undertaken by the author with the purpose to investigate the performance of the stapled connection, to evaluate and implement it as a low cost, efficient and versatile structural connection having numerous applications.

# CHAPTER 2

# STATE OF THE ART

## 2.1 Staples and their Applications

A fairly complete listing of all the staples available on the North American market is presented in ref (7). In this publication, the staples are specified (Fig. 2.1) according the the shape, size, point, material and purpose. The industry of fasteners composed of an appreciable number of large companies which exhibit a large variety of staples, staple machines and stapling procedures. A better idea of what is available on the the market may be obtained by referring to the ordering system published by SENCO and shown in Table (2.1). The present applications of staples are limited and they are mostly used to replace nails wherever the staples prove to be more practical and better functioning. The principal uses of staples are, however, in furniture fastening and material handling where they are used for assembling panels, boxes and containers.

Table 2.1

7-DIGIT STAPLE ORDERING SYSTEM

| 1st DIGIT CRN WID THK (") (.000)(.000) | 2nd & 3rd DIGIT LEG LGTH | 4th DIGIT POINT | 5th DIGIT METAL | 6th DIGIT FINISH | 7th DIGIT FEATURES |
|---|---|---|---|---|---|
| A 7/16 .030 .0215 | 01 1/4 17 1/2 | A Blunt | A Std. Carb. Galv. | A Plain | |
| B 1/2 .030 .0215 | 02 5/16 18 1/2 | B Chisel | C Std. Carb. Liq. | B Sencote | |
| C 9/16 .030 .0215 | 03 3/8 19 1/2 | C Ins. Ch. | DtUltra H Carb. Liq. | C Painted | |
| D* 5/8 .030 .0215 | 04 7/16 20 1/2 | D Out. Ch. | F Med. Carb. | D Ptd. & Senc. | P Bulk Pack |
| E 5/8 .050 .019 | 05 1/2 21 2 | F Divergent | G Stain. St.-Std. | | |
| F 1/2 .050 .019 | 06 9/16 22 2 1/2 | G Out. Ch. Div. | J Monel | | |
| G 1/2 .045 .023 | 07 5/8 23 2 1/2 | H Cross Cut Ch. | K St. Core Alum. | | |
| H 5/8 .050 .019 | 08 7/16 24 2 1/2 | J Cr. Cut Ch. Div. | M Aluminum | | |
| J 5/8 .075 .023 | 09 1/2 26 2 3/4 | K Spear | N Bronze | | |
| K 1/2 .045 .030 | 10 5/8 27 3 | L Ch. Div. | R Brite Basic | | |
| L 1/2 .050 .044 | 11 3/4 28 3 1/2 | M Self Clinch | | | |
| M 3/4 .050 .044 | 12 7/8 29 3 1/2 | N Sharp Ch. | | | |
| N 5/8 .062 .055 | 13 1 | | | | |
| P 1 .062 .055 | 14 1 1/2 | | | | |
| Q 5/8 .074 .067 | 15 1 1/4 | | | | |
| S †5/8 .062 .075 | 16 1 3/4 | | | | |
| W 7/16 .032 .025 | | | | | |

Example —
To order 1/2" staples,
crown 7/16"
wire width .045",
wire thickness .023":
G = 7/16" crown, .045 x .023"
08 = 1/2" leg length
B = Chisel point
A = Standard carbon galvanized wire
A = Plain finish
You will order G 08 BAA

*Use this digit only when ordering special 5/8" long staple for use in Model JN2330 tool.
†Available in Fine Wire only.

ORDERING SYSTEM FOR SENCO STAPLES

In construction, staples are mainly used as secondary fasteners, that is, for fastening shingles and wood, whereby using staples, wood splitting is largely eliminated. They are also used for fastening sheathing, insulation, partitions, plywood boards, etc. There are many advantages in using staples to replace nails or other fasteners, improved production efficiency, ease of handling, speed and availability, all of which make staples more economical than other fasteners.

The most commonly used sizes of staples in construcion today are gages sixteen, fifteen, and fourteen with varying length, crown width and point (Fig. 2.1). The materials commonly employed in manufacturing these staples are steel and aluminium.

The staplers available on the market for construction are either pheumatic or hammer operated. They can be portable of light weight, or stationary. The operation of such tools is fairly easy and does not require particular skills. The names of the major companies that manufacture staples and staplers in North America can be found on the last page of references (7).

## 2.2 Review of Research Work on Staples

The staple is a fastener, mainly used to replace nails or to extend the application of nailed fasteners. It works in a similar fashion to a nail for withdrawal resistance and resistance to lateral loads. However, nails and staples differ in the resistance to pull through the fastened material since the nail's capacity to resist pull through is based on its head, while for

the staple it is based on whole crown. This feature makes the staple highly attractive for fastening weak materials, thin sheets or plates. The research work done so far on staples includes principally tests on certain products of some companies. Most of the publications available for research done on staples have been made available by the Virginia Polytechnic Institute Wood Research Division, in U.S.A. The material presented in these publications deals mostly with the withdrawal resistance of the staple legs, and the resistance of the crown to pull through the fastened material. A few of the subjects of this material deal with the capacity of the staples to transmit lateral load. The results published are all experimental and no theoretical investigation of the staple behaviour is included. It should be mentioned that all the tests on staples have been done by Prof. George Stern of the Virginia Polytechnic Institute. Prof. Stern performed a large number of experimental measurements on staples, fastening wood to wood. Regarding the lateral load transmission of staples, some test results are quoted from Ref. (8, 9, 11) and are presented here:

1) The allowable lateral load transmitted by a staple is governed by the 3/2 power of the staple-leg diameter, provided the depth of penetration in the fastening member is sufficient; that is, amounts to a minimum of 10 to 14 staple-leg diameters depending on the wood species under consideration.

2) The general formula advanced by the U.S. Forests Products Laboratory for nails also applicable for staples for lateral load was derived by applying a reduction factor of 1.6 to the proportional limit loads and the reductions factors of 6 and 11 respectively to the ultimate load in seasoned soft woods and hard woods.

3) The testing procedure described in Ref. (8) is presented. The joints were loaded in the direction perpendicular to the grain of the fastened member as shown in Fig. (2.2). The joints were tested for their immediate and six week delayed static lateral load transmission at a constant rate of load application of 0.100 inches per minute. Automatically recorded load-deformation curves for the complete joints were obtained. Typical load deformation curves are presented in Fig. (2.3) which gives the load deformation curves for southern pine joints assembled with a single 2 1/2" long 8/16" crown, 15 gage SENCO staple laterally loaded immediately and six weeks after assembly in the direction perpendicular to the grain of the fastened member and parallel to the grain of the fastening member.

4) Fig. (2.4), from Ref. (9) presents the load deformation curves for nailed and stapled joints consisting of 5/8" yellow poplar deckboard and 1 1/4" x 3 5/8" hard maple stringer with the fastener loaded laterally immediately after assemblage. The fasteners used were 3" x 0.111" nails and 2" x 15-gage staples. The curves indicate that the stapled joint was 28% more rigid

than the nailed joint, if consideration is given to the rigidity of the joints, up to a total deformation of 0.400 inches.

5) Table 2.2 below, shows the average performance under lateral load of 2 1/2" x 15-gage duo-fast versus sencote staples.

Table 2.2

| Wood Species | Staple Type Time of Testing | Lateral (shear) in Pounds Sencote 1839 Immediate | Duo-fast 1845 E Immediate | Sencote 1839 Delayed | Duo-fast 1845 E Delayed |
|---|---|---|---|---|---|
| Green red oak | | 466 | 545 | 409 | 424 |
| Dry red oak | | 581 | 656 | 508 | 623 |
| Dry southern Pine | | 457 | 548 | 394 | 422 |
| Dry Douglas Fir | | 375 | 475 | 343 | 444 |
| Green Aspen | | 340 | 303 | 221 | 289 |

PERFORMANCE OF DUO-FAST VERSUS SENCOTE STAPLE

# CHAPTER 3

# EXPERIMENTAL INVESTIGATION OF A STAPLED CONNECTION

## 3.1 Description of the Connection

The type of connection examined here (Fig. 3.1) is a stapled assembly of sandwich panels with aluminum extrusions. The staples are placed in uniform spacing in a row along the edge of the panel. There are two types of extrusions used. The first has an I type cross section (Fig. 3.2) while the second (Fig. 3.3) is made of a hollow square cross section and eight flanges, two at each corner perpendicular to each other.

## 3.2 The Extrusions

The aluminum used for the extrusions is of the 6063-T5 produced by Alcan. It has the following mechanical properties:

Ultimate tensile strength : $F_u$ = 22.0 ksi

Yield tensile strength : $F_y$ = 16.0 ksi

Bearing Strength : $F_B$ = 46.0 ksi

There are two factors taken into consideration in deciding the dimensions and the shape of the extrusions. The first was the size of the panels and the geometry of the structure, and the other extruding processes and the head of the stapler. There are limitations and economic considerations in the extruding processes. For example, the thickness of 0.10 inches of the flanges was dictated by the overall dimensions of the section. There are also limitations of availability of staples, stapling machines and their capacity to penetrate the aluminum extrusion and the face of the sandwich panels. The two extrusions are discussed below.

Both designs were adopted for the experimental programme but could be refined for industrial applications.

The I-shaped extrusion is shown in Fig. 3.2 and the #-shaped extrusion in Fig. 3.3. The grooves along the edges of the flanges are made for two reasons. First, to reduce the thickness of the aluminum and thus permit the staple to penetrate it, second, the groove contour accommodates the stapler during stapling. The weight of the I-shaped extrusion is 0.990 lbs. per foot and it can connect two panels in the same plane.

The four-way extrusion (Fig. 3.3) is made of a hollow square cross section and eight flanges, two on each corner perpendicular to each other. The overall dimensions of the extrusion are 6.0" x 6.0" and the length of each flange is 1.86" and was dictated by the commercial stapler available. Its weight is 3.44 lbs. per foot and can connect two to four panels. The two panels can be either in the same plane or in two perpendicular planes.

## 3.3 The Staples

The staples used for the connection are U-shaped, made from high strength carbon steel, and they are galvanized. Their dimensions are: length = 5/8"; diameter = 0.057"; crown = 7/16". They were tested for ultimate capacity in shear according to ASTM B565 Standard. This was found to be 75,000 psi. The staples are usually furnished in collated sticks suitable for the stapler. Fig. (3.4) shows a typical pneumatic Senco stapler and some staples.

## 3.4 The Panels

The panels are made up of a rectangular frame of clear white pine, as shown in Fig. (3.5). The frame is connected with corrugated fasteners. Inside the frame there is a 2 inch thick styrofoam core having a density of 2 psf. The core has good insulation properties and provides high strength to weight ratio for the panel. The faces of the panel are made from 0.025" thick utility aluminum and they are glued with epoxy on the core and the frame.

Both the wood and the aluminum facing were tested for their mechanical properties according to ASTM D143, E8, E238 Standards and the results are presented below:

I) Wood (White Pine)

| | Compression parallel to the grain | Compression perpendicular to the grain |
|---|---|---|
| Modulus of Elasticity (psi) | $E_{11}$ = 1,000,000 | $E_1$ = 90,000 |
| Proportional Limit (psi) | $F_{11}$ = 4,500 | $F_1$ = 800 |
| Ultimate Strength (psi) | $F_{ul1}$ = 6,500 | - |
| Elastic Bearing Modulus lbs/in | $K_{oE}$ = 330,000 | $K_{op}$ = 150,000 |

Details of the elastic bearing modulus are given in section 3.6.1.

II) Aluminum Faces (Utility aluminum)

| | Tension | Shear | Bearing |
|---|---|---|---|
| Yield Strength (psi) | $F_y$ = 22,000 | $F_s$ = 12,000 | $F_B$ = 40,000 |
| Ultimate Strength (psi) | $F_u$ = 25,000 | $F_{su}$ = 15,000 | |
| Modulus of Elasticity (psi) | E = 10.7 x$10^6$ | | |

## 3.5 Description of the Connecting Method and its Effects

The connection of the members is done by using a pneumatic staple gun like the one shown in Fig. (3.4) connected to a 100 psi air pressure line. The panel is inserted in the extrusion which is approximately 0.08 to 0.1 inches wider than the thickness of the panel. To fill the tolerance gap between the extrusion and the panel, a plywood filler is inserted on one side of the connection. The staples are inserted through the aluminum extrusion from one end to the other. They penetrate first the aluminum extrusion then the face of the panel, and eventually are driven into the wood frame. The finished connection is shown in Fig. (3.1).

The spacing of the staples is 7/8 inches center to center. Since the crown width of the staple is 7/16 inches, it means that there is a staple leg at every 7/16 inches.

The spacing of the staples is within the specifications of CSA Standard 036, but the length to diameter ratio is much less than required by the specifications. It is required that the length of the staple or nail embedded in the wood to the diameter

ratio be not less than fourteen. In the present case, the ratios are: 0.54/.057 about nine and a half, and on the side with the plywood filler, 0.43/0.057 about seven and a half. It is interesting to observe the effect that the staple penetration has on each of the connection components. This is done by analysing the penetration in six steps. (referring to Fig. (3.6)) In stage one the staple is applied on the surface of the aluminum without force. In stage two, the staple starts to penetrate the aluminum extrusion deforming it permanently, the deformation of the extrusion results in the deformation of the aluminum sheet, as shown in stage 3. In stage 4, the staple penetrates the aluminum sheet. The protrusion formed around the hole of the extrusion penetrates the aluminum sheet which in turn penetrates the wood. In stage 5, the staple is completely inserted and the crown presses against the assembly which is further distorted. In stage 6, the pressure from the gun is released. The aluminum extrusion bounces back slightly creating a very small gap between the extrusion and the face sheet. It was noted that the bent aluminum sheet around the hole depresses into the wood by twice its thickness.

On the side where the plywood filler is used the aluminum extrusion is not in contact with the face of the panel but the final effect is almost the same. The disadvantage of using the plywood filler (see Fig. 3.7) is apparent prior to testing because this filler is not attached to any of the connected members and is thus free to move. Consequently the staple has a large part

of its length acting as a cantilever beam. Thus it will be under bending rather than pure shear.

## 3.6 Tests and Results

The tests performed within the framework of establishing the performance of the connection were divided into three groups. The aim of the first group is the identification of the mechanical properties of the materials used. The second group deals with the determination of the behaviour of the staples used for the connection. The third group examines the behaviour of the connection as used in the model building and under all anticipated loading conditions.

### 3.6.1 Identification of Mechanical Properties- Test Group one

All the components used in the connection were tested to identify their mechanical properties. These components are aluminum extrusions, staples, aluminum faces of panels and wood used for the frame of the panels. All the tests were performed according to ASTM standards mentioned in Sections 3.3 and 3.4. Besides the tests performed for determination of the commonly used properties, some tests were performed which were judged necessary for this particular case. These tests are mentioned here: one is the determination of the elastic bearing modulus of the wood, and the other is the bearing capacity of aluminum using staples.

a) Bearing capacity of aluminium using staples:

This test was required to define the force needed to yield the aluminum in bearing and the force required to tear the aluminum sheet when the staple leg was used. The calculated bearing yield capacity, using the results from the standard ASTM Test E238, was 57 lbs. for the staple leg diameter and the experimental 60 lbs. The ultimate capacity of the aluminum sheet in bearing using the staple leg was 180 lbs. The results from the ASTM Standard E 238 test using a pin of 0.25 inches diameter were 190 lbs. for yielding and 220 lbs. for the ultimate. It is seen that the ultimate capacity is almost the same. The reason for that is that the ultimate capacity is governed by the tearing of the aluminium sheet which is rather independent from the pin diameter. The P-$\delta$ relation for the bearing test when the staple was used is shown in Fig. (3.8).

b) Determination of the elastic bearing modulus of the wood ($K_o$):

The determination of ($K_o$) was done using steel plates two inches long with thickness varying from 0.035" to 0.180". The results were very inconsistent and largely scattered. Hence, it was decided to average those which had less deviation. At least seventy-five percent of the measured values were included. The values of elastic bearing moduli are given in Section 2.4 with the other properties of the wood.

### 3.6.2 Investigation of the Staple Behaviour - Test group two

The purpose of this group of tests was to find the behaviour and capacity of individual staples as well as their behaviour when many staples were put in a row.

The extrusion was stapled on the panel with the number of staples varying from two to twenty-six. The staples were put in one row. Two types of loadings were tested (see Fig. 3.9 A & B). For arrangement A, the direction of the load was in the same line with the staples and in the other, the load was perpendicular to the line of staples. In order to investigate the effect of the plywood filler in the performance of the connection, two connection arrangements were examined; i.e. with and without plywood filler. This was done where the load is in line with the staple row (see Fig. 3.9).

a) Load applied in line with the staples without plywood filler:

The number of staples used for this test were two, eight, twelve and twenty-six at a time. The load was applied gradually at a constant rate and the following observations were made:

The deformation, which is defined as the slippage of the extrusion relative to the panel, was recorded as the load was increasing. At the initial stage of loading there was a small slippage which made the connection appear to be very flexible.

It then became stiffer and eventually the load appeared to be in linear relation with the deformation. If the loading were stopped within the linear range of the P-$\delta$ relation and then removed, the curve shows always a residual permanent deformation. This permanent deformation increases with higher loads but decreases as the number of cycles of the same load increases. It is worth noting that most of the deformation recovery took place at the end of unloading. Every time that the connection was reloaded, it would follow the same path as in the previous loading cases. The load-deformation relation is linear up to a certain load when the slope of the curve starts to decrease. When the connection was unloaded from a level higher than the proportional limit, the results showed a large permanent deformation and the connection had become very flexible. If reloaded, it would not follow the same P-$\delta$ line, but it would show very large deformations at the beginning of loading, stiffen with the increased load for small range, and then become very flexible again. The load was increased until the connection failed completely.

The failure of the connection was reached with the withdrawal of the staples, and thus the ultimate capacity of the connection was dictated by its mechanical behaviour and not by the strength of any of its components.

The curves plotted in Fig. (3.10) show the load per staple leg versus the deformation for different number of staples in a row. The deformation being the slippage of the extrusion

relative to the panel. From Fig. (3.10) it can be seen that with increasing number of staples in a row, the slope of the load per staple leg versus the deformation curve becomes smaller, while the ultimate capacity of the staple leg remains fairly constant with increasing number of staples in a row. It can also be seen that the shapes of the curves are similar which means that regardless of the number of staples in a row, the load-deformation pattern will have the same shape. For better understanding of the effect of the connection length, the value of the slope in the linear range and the value of the proportional limit (see curves in Fig. 3.10) of the two-staple connection are taken as being one hundred percent. Then the values of the other curves are plotted as a percentage of the values of the two-staple connection curve in Fig. (3.11). This comparison shows the drop of efficiency per staple leg with increasing number of staples in a row. It is seen that for a large number of staples the curve becomes flat tending to a constant value of percentage.

The drop in stiffness is attributed to the unequal initial slippage of the staples which results in different load for each staple.

b) Load applied in line with the staples with plywood filler:

Tests were carried out according to the same procedures described previously. The number of staples tested were five and eight at a time. The results of the investigation are plotted in Fig. (3.12). This connection was much more flexible than the previous one and exhibited much larger deformation at the linear stage of loading. The linear portion of the curve

was much shorter and the transition of the slope much smoother. The other response characteristics were about the same as the previous case except for larger permanent deformations observed. The capacity of this connection dropped with increasing number of staples and it was much lower than that of the connection without filler.

A detailed examination of the two connections after the staples had pulled out showed that in the case of connection without filler, there was visible distortion in bearing on the aluminum face of the panel at the staple hole, while in the other, there was no noticable distortion.

c) Joint without filler subjected to load perpendicular to the line of staples:

Four groups of stapled connections were tested under this type of load. These groups had two, eight, eleven and thirteen staples respectively. The load per staple leg versus the derformation curves for the various groups are shown in Fig. (3.13). The behaviour of the connection under this load type was similar to that obtained when the load was applied in the line of the staples. The main difference being a smaller decrease in the slope of the curves with increasing number of staples. It can thus be stated that there is no significant drop in the capacity and the stiffness of the connection when the load is perpendicular to the line of the staples.

Figures (3.14 A, B, C) show the staples after they pulled out. Picture (A) compares a deformed staple with an unused one. The size of the staple is shown by the millimeter division

of the graph in the background. The angle at which the staples pulled out varied from 25° to 45°. It should be noted that in all tests the part of the staple in the extrusion remained fixed.

### 3.6.3 Investigation of the Connection Behaviour - Test group three

The purpose of these tests was to examine the connection used in the building model and describe its behaviour. The description of the connection has been presented at the beginning of this chapter. The conditions reproduced in the test were exactly the same as those encountered in the building model.

There were three kinds of tests performed in order to fully investigate the connection behaviour under all the anticipated loads. These are: shear, combined shear and compression and tension. The testing procedures and the results are presented in the following sections.

a) Shear Test

The assembly for this test is shown in Fig. (3.15). Two panels (24" x 12" x 2") were connected with an aluminum extrusion along the 24 inches side, both panels were in the same plane, the tolerance gap between the panels and the extrusion was filled with plywood fillers. There were twenty-seven staples on each face of the panels, a total of 108 staples. In this shear test, the load was applied to the aluminum extrusion as compression and it was transferred as shear through the staples to the panels.

Hence, the extrusions were under compression, the staples under shear and bending, and the panels under compression. Due to the length of the connection the distribution of the forces on the staples was not uniform. When the staples were loaded within the elastic range, maximum forces were at the staples close to the ends of the connection and minimum at those close to the center. As the load increased, the staples close to the ends reached their ultimate capacity first and began to deform under constant load. The additional load then transferred to the adjacent staples up to the point where all staples had reached their ultimate capacity and failure of the connection occurred. The load was applied at a constant rate of one thousand pounds per minute and the deformation was measured with a dial gage in 0.001" divisions as shown in Fig. (3.15). The deformation measured this way included the slippage of the extrusion and the deformation of the panels. Since the objective was to determine the slippage of the extrusion the contraction of the panel was substracted from the total deformation to find the slippage. Edgewise compressive tests were performed on the panels to determine their load-deformation relation. The load transferred to the panel by the connecting member varied from zero at the top of the panel to the total applied load at the bottom of the panel (see Fig. (3.15)). Hence, the contraction of the panel was taken as half of that measured in the edgewise compression test for the same load. Thus, to find the slippage of the connection, an amount half of the deformation measured in the edgwise compressive test corresponding to each applied load was substracted from the total

deformation measured in the shear test. The same correction was applied to all shear tests on the connection described in this thesis.

Load-deformation curves for the connection are shown in Figs. (3.16) and (3.17) where the load per panel is plotted against the deformation (slippage). At the initial loading stages, the connection appears to be very flexible and relatively large deformation occur (See Fig. (3.17)). This initial flexibility was also noticed when the staples themselves were tested (Section 3.6.2). As the load increases, the connection becomes stiffer and the load-deformation curve becomes a straight line. During testing the load on the connection was cycled. It can be seen that the load-deformation relation at unloading differs from the corresponding curve at loading. When the load is completely removed, a permanent deformation remains. This aspect would mean an undesirable characteristic of the connection. However, with repeated load cycles, the increment of the permanent deformation was found to decrease. The load was then continually increased until ultimate failure, at which point the staples first bent and then pulled out and the members came apart. The complete load deformation curve was plotted in Fig. (3.17).

For purposes of calculations, the curve is approximated with three straight lines. The second straight line, which is accepted as the load-deformation curve, is extrapolated, and the deformation corresponding to zero load is interpreted as initial slippage. Hence, the equation of the deformation in terms of

the load becomes:

$$\Delta = \frac{P}{150,000} + 0.008"$$

P = load in lbs.

$\Delta$ = deformation in inches.

b) Combined Shear and Compression

This series of tests was carried out to determine the effect of normal forces acting on the connections (Fig. (3.18)). These forces create friction between the components of the connection which should result in an increase in the stiffness of the connection. This increase in stiffness was initially observed in the building model. The test arrangement was the same as for the shear test (Fig. (3.15)) with the addition of the normal force, which was applied to the panels using a hydraulic jack (Fig. (3.18)).

The normal force was distributed along the edges of the panels using steel blocks which were attached to stiff steel channels. The test proceeded by first applying a constant normal force and then applying incremental shear loads as done in the shear test (Section 3.6.3 a). The normal load changes the behaviour of the connection, as seen by comparing Fig. (3.17) with (3.19). Because of the normal load, the connection now shows a higher stiffness at the initial stage of loading then decreases up to a certain load and the increases again. The stiffness of the connection increased with increasing normal force, as shown in the family of curves in Fig. (3.19).

In order to study the stiffening effect of the normal force on the behaviour of the connection, each of the curves shown in Fig. (3.19) is approximated with three straight lines AB, BC, CD. Line AB starts at zero load. The slopes of these three lines are designated as $B_1$, $B_2$ and $B_3$ respectively. It can be seen from Fig. (3.20) that the slopes of the P-$\delta$ curves increase with increasing normal load. The variation of the slopes with the normal load is shown in Fig. (3.20). As seen in this figure, the value of $B_1$ increases rapidly with increasing normal load. The values of $B_2$ and $B_3$ increase at a decaying rate following almost parallel paths. From this it can be concluded that the effect of the normal force is the introduction of friction which makes the connection very stiff at the beginning of loading and as soon as the frictional force is overcome, the load-deformation curve follows a stiffened path in the same way as it does when the normal force is not present. Due to this characteristic of the connection, the building model showed greater stiffness when the vertical load was applied before the lateral load, Ref (30). Other features of the connection, such as permanent deformation, loading and unloading curves remained the same as for the case of N=0.

c) Tension

The tension test demonstrated clearly the effect of the plywood filler. The testing arrangement is shown in Fig. (3.21) where a tested sample is photographed. To measure the deformation

dial gages were located at four points, two on each side of the connection, so that the relative displacement between the aluminum extrusions and the panels was measured at both sides of the panels.

The application of the load was at a constant rate of 1000 lbs/min and each connection was loaded repeatedly with increased load each time until failure was reached. Two arrangements with plywood fillers were tested. In the first arrangement both of the plywood fillers were placed on the same side of the connection and in the second, the fillers were placed on diagonally opposite sides. The results at failure are shown in Fig. (3.22 (A) and (B)). Greater deformation occurred where the fillers were used, hence, the total deformation consisted of elongation and rotation. The rotation was much larger for case (B). The behaviour of the connection is shown in Figs. (3.23) and (3.24). It can be seen that the load carrying capacity of connection (B) is considerably lower than that in (A). It should be noted that in Fig. (3.23) the load is plotted vs the average displacement of each panel relative to the extrusion and in Fig. (3.24) the load is plotted vs the total rotation ($2\theta$) of the connections. The calculations of the deformation from the measurements is shown in Fig. (3.25). Unlike the case of the shear test where relatively large displacements occurred at small loads in the tension test, the initial flexibility was much less, the connection then stiffened quickly and then became flexible again. The permanent deformation was present here too, and the loading and unloading paths were again

different, As in previous cases, the staples pulled out at ultimate failure.

3.6.4 Interpretation of the Results

The tests clearly show that the plywood filler used to fill the tolerance gap weakens considerably the connection, since the filler serves to increase the moment arm in the cantilevered staple and less of the staple leg penetrates the panel. It is, therefore, necessary to eliminate the gap between the panel and the extrusion if the capacity and the stiffness of the connection are to be improved. To investigate the performance of such a connection, the above connection was modified as shown in Fig. (3.26) to eliminate the gap. The modified connection uses two extruded aluminum components as compared to one originally used. The two extrusions are adjusted with bolts to fit exactly on the panels and then are stapled. This way, the gap and the problem of tolerances are completely eliminated within reasonable variation of panel thickness or misalignement.

a) Parameters affecting Performance of Connections

The following parameters determine the behaviour and capacity of the connections: the staple stiffness (EI), its length (L), its diameter (D), the thickness of the aluminum on the panel face, the wood used in the frame, and the extrusion thickness. During the tests, it was found that the aluminum extrusion thickness was sufficient to ensure fixity of the staple

crown to loads exceeding the ultimate capacity of the connection. Slight yielding due to bearing was observed when the staples bent to pull out from the panel. It may be concluded that the thickness of the aluminum which was slightly larger than the diameter of the staple, is sufficient to hold the staple crown fixed. The effect of the other parameters will be examined theoretically and experimentally in subsequent chapters.

3.6.5 Testing the Modified Connection under Shear

The testing arrangement and the cross section of the connection are shown in Fig. (3.27). The connection was tested under shear in the same manner as before (Section 3.6.3 a). The stiffness increased from 150,000 lbs/in to 265,000 lbs/in in the linear range (Fig. (3.28)) and the ultimate capacity more than doubled. In fact, the ultimate capacity occurred in the panels at points shown by the arrows on Fig. (3.27). For comparison, the load-deformation curves for the modified and the original connections are shown in Fig. (3.28). It can be seen from this figure that the jnitial displacement is less for the modified connection. The permanent deformation due to cycled loads was also less for connection (A).

The bolts are used to:

(i) align the extrusions before stapled and keep them aligned during stapling.

(ii) eliminate possible gap by keeping the extrusions tightly attached to the panels so the staples can achieve maximum capacity.

iii) keep the staples in position under large loads and excessive deformations and thus increase the ultimate capacity of the connection by a factor of roughly two, since the staples to pull-out have to cut through the wood and the aluminum face of the panel. Tensioning the bolts does not have much effect, and one cannot count on friction since the wood frame will creep and shrink and the friction will dissipate. For industrial applications, better designs can be achieved.

# CHAPTER 4

## THEORETICAL STUDY OF A STAPLED CONNECTION

The connection being investigated consists of aluminum sandwich panels (see Fig. (4.1)) having aluminium facings, styrofoam core, and wood framing connected to extruded aluminum members by staples. A theoretical examination of the behaviour and load carrying capacity of the connection was undertaken to study the effect of the various components and the overall behaviour of the connection so that it could be better understood, improved and optimized.

A mechanical model of the connection is shown in Fig. (4.2) in which the wood has been replaced by an elastic foundation, the aluminum face by a spring, and the staple by a beam with one end fixed on the aluminium plate. The assumption of fixity between the aluminum plate and the staple was found, from previous tests described in Chapter 3, to be appropriate if the thickness of the aluminum plate was at least equal to the diameter of the staple. Referring to the free body diagram of Fig. (4.2), it can be seen that:

$$H = F + P$$

$$F = K_s \delta \qquad P = f_n(\delta)$$

where

H is the applied force

F is the force resisted by the aluminum

P is the shear at the crown section

$K_s$ is the equivalent bearing stiffness of the aluminium facing.

$\delta$ is the resulting deformation at X = 0.0

It is now necessary to determine the factors that govern the P-$\delta$ relationship and establish such relationship mathematically to include the basic parameters which govern the staple behaviour.

The behaviour of the staple will be investigated by applying the already accepted theory developed by Kuenzi (Ref. 27) which regards it as a beam on elastic foundation.

## 4.1 Beam on an Elastic Foundation

Consider the beam AB shown in Fig. (4.3) supported by an elastic foundation along all its length (ref 1). When the beam is loaded, the reaction exerted by the foundation to the beam at a point, is proportional the deflection of the beam at that point and it can either be tension or compression. This foundation reaction is $P = K \cdot y$, based on the assumption that the supporting medium is elastic and follows Hooke's law.

$K_o$ = $(\frac{lbs/in^2}{in})$ foundation modulus

b = (in) width of the beam

$K = K_o b$ = $(lbs/in^2)$ particular foundation modulus comprising the width of the beam

y = (in) deflection at a point

$\bar{P}$ = $K \cdot y$ $(lbs/in)$ foundation reaction

q = $(lbs/in)$ external distributed load

P = lbs external concentrated load

$$dy/dx = \theta \quad \text{slope}$$

$$EI\frac{d^2y}{dx^2} = -M \quad \text{moment}$$

$$EI\frac{d^3y}{dx^3} = -Q \quad \text{shear}$$

Considering a segment of the beam AB as shown in Fig. (4.4) and applying equilibrium, then:

$$Q - (Q + dQ) + Kydx - qdx = 0 \tag{4.1}$$

hence

$$-\frac{dQ}{dx} = Ky - q$$

since

$$Q = \frac{dM}{dx}$$

$$\frac{dQ}{dx} = \frac{d^2M}{dx^2}$$

$$\frac{dQ}{dx} = \frac{d^2M}{dx^2} = Ky - q \tag{4.2}$$

since

$$EI\frac{d^2y}{dx^2} = -M \quad \text{therefore} \quad EI\frac{d^4y}{dx^4} = \frac{-d^2M}{dx^2}$$

hence

$$EI\frac{d^4y}{dx^4} = -Ky + q$$

With reference to Fig. (4.4), considering the case of external load $q = 0$, we obtain:

$$EI\frac{d^4y}{dx^4} = -Ky \tag{4.3}$$

Assuming a solution for y in the following form

$$y = e^{mx}$$

$$EIm^4e^{mx} = EI\frac{d^4y}{dx^4}$$

Substituting in the equation (4.3) gives

$$m^4e^{mx} + \frac{K}{EI}e^{mx} = 0$$

from which

$$m^4 = \frac{-K}{EI}$$

and its roots are

$$m_1 = -m_3 = (1+i)\sqrt[4]{\frac{K}{4EK}}$$

$$m_2 = -m_4 = (-1+i)\sqrt[4]{\frac{K}{4EK}}$$

let

$$\sqrt[4]{\frac{K}{4EI}} = \lambda$$

then

$$m_1 = -m_3 = \lambda(i+1)$$

$$m_2 = -m_4 = \lambda(-1+i)$$

and the general solution of Eqn. (4.1) becomes

$$y = A_1e^{m1x} + A_2e^{m2x} + A_3e^{m3x} + A_4e^{m4x} \tag{4.4}$$

using

$$e^{i\lambda x} = \cos\lambda x + i\sin\lambda x$$

$$e^{-i\lambda x} = \cos\lambda x - i\sin\lambda x$$

and then introducing the new constants $C_1$, $C_2$, $C_3$, $C_4$, where

$$C_1 = (A_1 + A_4) \quad C_2 = i(A_1 - A_4)$$
$$C_3 = (A_2 + A_3) \quad C_4 = i(A_2 - A_3)$$

The general solution (4.4) can now be written in the following form, where $\lambda$ is the characteristic of the equation and its units are length$^{-1}$.

$$y = e^{\lambda x}\{C_1\cos\lambda x + C_2 \sin\lambda x\} + e^{-\lambda x}\{C_3\cos\lambda x + C_4 \sin\lambda x\} \qquad (4.4)A$$

subsequently:

$$\frac{1}{\lambda}\frac{dy}{dx} = e^{\lambda x}\{C_1[\cos\lambda x - \sin\lambda x] + C_2[\cos\lambda x + \sin\lambda x]\}$$
$$-e^{-\lambda x}\{C_3[\cos\lambda x + \sin\lambda x] - C_4[\cos\lambda x - \sin\lambda x]\} \qquad (4.4)B$$

$$\frac{1}{2\lambda^2}\frac{d^2y}{dx^2} = -e^{\lambda x}(C_1\sin\lambda x - C_2\cos\lambda x) + e^{-\lambda x}(C_3\sin\lambda x - C_4\cos\lambda x) \qquad (4.4)C$$

$$\frac{1}{2\lambda^3}\frac{d^3y}{dx^3} = -e^{\lambda x}\{C_1[\cos\lambda x + \sin\lambda x] - C_2[\cos\lambda x - \sin\lambda x]\}$$
$$+e^{-\lambda x}\{C_3[\cos\lambda x - \sin\lambda x] + C_4[\cos\lambda x + \sin\lambda x]\} \qquad (4.4)D$$

The above equations, (4.4) A, B, C and D give the deflection, slope, moment and shear respectively at any point along the beam. The constants $C_1$, $C_2$, $C_3$, $C_4$ are determined by applying the boundary conditions for each particular case.

Referring to Fig. (4.2), we have to combine the reaction from the beam, representing the staple length, at x = 0.0, and the reaction from the spring, representing the aluminum face, to find the total reaction. This total force must balance the externally applied force. Three particular cases will be examined: in the first, the beam is considered to have an infinite length; in the second the beam is of finite length (L); and in the last case, the beam will have a finite length, but there will be a gap between the panel and the aluminum plate, which will result, as explained previously, in an unsupported portion of the beam (staple).

## 4.2 Case I - Beam with Infinite Length

This beam, according to the mechanical model which was previously constructed, has the following characteristics (Fig. 4.5). At x = 0 the beam can translate but cannot rotate. The length of the beam is approaching infinity and the load is applied as a concentrated force at x = 0.

Boundary conditions:

$$\text{at } x = 0 \quad dy/dx = 0 \quad \text{(a)}$$

$$\text{at } x \to \infty \quad y = 0 \quad \text{(b)}$$

$$\text{at } x = 0 \quad Q = P \quad \text{(c)}$$

Referring to the equation (4.4)A, it is seen that the condition (b) is satisfied if $C_1 = C_2 = 0$ which gives:

$$y = e^{-\lambda x}(C_3 \cos\lambda x + C_4 \sin\lambda x) \qquad (4.5)$$

application of the condition (a) gives

$$C_3 = C_4 = C$$

hence

$$y = C\, e^{-\lambda x} (\cos\lambda x + \sin\lambda x) \qquad (4.6)$$

for equilibirum (condition c) the summations of forces on the beam must be equal to the applied force P i.e. $P = \int_0^\infty Ky\,dx$

which, with reference to (4.6) can be written as:

$$P = \int_0^\infty KCe^{-\lambda x}(\cos\lambda x + \sin\lambda x)\, dx$$

which gives:

$$P = -K\, C\, \frac{1}{\lambda} \rightarrow C = -\frac{\lambda P}{K}$$

so the deflection becomes:

$$y = \frac{-\lambda P}{K} e^{-\lambda x}(\cos\lambda x + \sin\lambda x)$$

$$= -\frac{P}{4EI\lambda^3} e^{-\lambda x}(\cos\lambda x + \sin\lambda x)$$

the maximum deflection is at x = 0, i.e.

$$\max y_{x=0} = -\frac{P}{4EI\lambda^3} \qquad (4.7)$$

$$\theta = \frac{dy}{dx} = \frac{2P\lambda^2}{K} e^{-\lambda x} \sin\lambda x = \frac{P}{2EI\lambda^2} e^{-\lambda x} \sin\lambda x$$

$$M = -EI \frac{d^2y}{dx^2} = -\frac{Pe^{-\lambda x}}{2\lambda} (\cos\lambda x - \sin\lambda x)$$

$$Q = -EI \frac{d^3y}{dx^3} = Pe^{-\lambda x} \cos\lambda x \quad \text{and}$$

$$P = K_y = \frac{-EId^4y}{dx^4} = - P\lambda e^{-\lambda x}(\cos\lambda x + \sin\lambda x)$$

Interest is focused on Equation (4.7) which gives the relation P-δ. Substituting δ for y at x = 0 in Equation (4.7), one obtains:

$$P = -4EI\lambda^3\delta \qquad (4.7)A$$

The total reaction of the staple is the sum of the wood reaction (P) and the aluminum face reaction (F).

Therefore $H = F + P$

$$H = -K_s\delta - 4EI\lambda^3\delta \qquad (4.8)$$

The negative sign appears because H, F and P were assumed positive upwards while y was assumed positive downwards.

In order to apply the conditions for cases two and three, it was found more convenient to express the deflection, slope moment and shear in terms of their values at x =0, that is $y_o$, $\theta_o$, $M_o$, $Q_o$ respectively,

where

$y_o$ = deflection at x = 0

$\theta_o$ = rotation at x = 0

$M_o$ = moment at x = 0

$Q_o$ = shear at x = 0.

Refering to Equations (4.4)A through (4.4)D, it can be found that

$$y_o = C_1 + C_2$$

$$\theta_o = \lambda(C_1 + C_2 - C_3 + C_4)$$

$$M_o = 2\lambda^2EI(-C_2 + C_4)$$

$$Q_o = 2\lambda^3EI(C_1 - C_2 - C_3 - C_4)$$

from which

$$C_1 = \frac{1}{2} y_o + \frac{1}{4\lambda} \theta_o + \frac{1}{8\lambda^3 EI} Q_o$$

$$C_2 = \frac{1}{4\lambda} \theta_o - \frac{1}{4\lambda^2 EI} M_o - \frac{1}{8\lambda^3 EI} Q_o$$

$$C_3 = \frac{1}{2} y_o - \frac{1}{4\lambda} \theta_o - \frac{1}{8\lambda^3 EI} Q_o$$

$$C_4 = \frac{1}{4\lambda} \theta_o + \frac{1}{4\lambda^2 EI} M_o - \frac{1}{8\lambda^3 EI} Q_o$$

After substituting the C's and putting $\frac{1}{2}(e^{\lambda x} + e^{-\lambda x}) = \cosh\lambda x$ and $\frac{1}{2}(e^{\lambda x} - e^{-\lambda x}) = \sinh\lambda x$ it gives:

$$y_x = y_o F_1(\lambda x) + \frac{1}{\lambda} \theta_o F_2(\lambda x) - \frac{1}{\lambda^2 EI} M_o F_3(\lambda x) - \frac{1}{\lambda^3 EI} Q_o F_4(\lambda x) \qquad (4.9)A$$

$$\theta_x = \theta_o F_1(\lambda x) - \frac{1}{\lambda EI} M_o F_2(\lambda x) - \frac{1}{\lambda^2 EI} Q_o F_3(\lambda x) - 4\lambda y_o F_4(\lambda x) \qquad (4.9)B$$

$$M_x = M_o F_1(\lambda x) + \frac{1}{\lambda} Q_o F_2(\lambda x) + \frac{k}{\lambda^2} y_o F_3(\lambda x) + \frac{k}{\lambda^3} \theta_o F_4(\lambda x) \qquad (4.9)C$$

$$Q_x = Q_o F_1(\lambda x) + \frac{k}{\lambda} y_o F_2(\lambda x) + \frac{k}{\lambda^2} \theta_o F_3(\lambda x) - 4\lambda M_o F_4(\lambda x) \qquad (4.9)D$$

where

$$F_1(\lambda x) = \cosh\lambda x . \cos\lambda x$$

$$F_2(\lambda x) = \frac{1}{2}(\cosh\lambda x . \sin\lambda x + \sinh\lambda x . \cos\lambda x)$$

$$F_3(\lambda x) = \frac{1}{2}(\sinh\lambda x . \sin\lambda x)$$

$$F_4(\lambda x) = \frac{1}{4}(\cosh\lambda x.\sin\lambda x - \sinh\lambda x.\cos\lambda x)$$

4.3 Case II - Beam with Finite Length

The conditions for this case are as in case one, but the length of the beam is now finite (L).

Boundary conditions:

a) $Q_o = P$ b) $\theta_o = 0$

c) $Q_L = 0$ d) $M_L = 0$

After the application of the first two boundary conditions the equation is reduced to the form:

$$y = y_o F_1(\lambda x) - \frac{1}{\lambda^2}\frac{M_o}{EI} F_3(\lambda x) - \frac{1}{\lambda^3 EI} P F_4(\lambda x)$$

with $y_o$ and $M_o$ remaining unknown.

Evaluating the F's at X = L then

$$F_1 = F_1(\lambda L) = \cosh\lambda L \cdot \cos\lambda L$$

$$F_2 = F_2(\lambda L) = \frac{1}{2}(\cosh\lambda L \cdot \sin\lambda L + \sinh\lambda L \cdot \cos\lambda L)$$

$$F_3 = F_3(\lambda L) = \frac{1}{2}\sinh\lambda L \cdot \sin\lambda L$$

$$F_4 = F_4(\lambda L) = \frac{1}{4}(\cosh\lambda L \cdot \sin\lambda L - \sinh\lambda L \cdot \cos\lambda L)$$

Applying the boundary conditions (c) and d) gives:

$$F_1 M_o + \frac{k}{\lambda^2} F_3 y_o = -\frac{F_2}{\lambda} P$$

$$-4\lambda F_4 + \frac{k}{\lambda} F_2 Y_o = -F_1 P$$

which can be written in the following matrix form in order to solve for $M_o$ at $y_o$:

$$\begin{bmatrix} F_1 & \frac{k}{\lambda^2} F_3 \\ -4\lambda F_4 & \frac{k}{\lambda} F_2 \end{bmatrix} \begin{bmatrix} M_o \\ y_o \end{bmatrix} = \begin{bmatrix} -\frac{F_2}{\lambda} P \\ -F_1 P \end{bmatrix}$$

from which

$$M_o = \frac{\frac{P}{\lambda}(F_3F_1 - F_2^2)}{F_1F_2 + 4F_3F_4} \tag{4.10}$$

$$y_o = \frac{P(-4F_2F_4 - F_1^2)}{\frac{k}{\lambda}(F_1F_2 + 4F_3F_4)} \tag{4.11}$$

and

$$\theta_o = 0$$

$$Q_o = 0$$

The values of deflection, slope, shear and moment can be obtained from Equations (4.9)A to (4.9)D using the values given above for $y_o$, $\theta_o$, $Q_o$, $M_o$.

Of primary interest is the P-$\delta$ relationship (where $\delta = y_{x=0}$) for finding the total resistance of the staple. Thus from (4.11):

$$P = \frac{\frac{k}{\lambda}(F_1F_2 + 4F_3F_4)}{(-4F_2F_4 - F_1^2)}\,\delta$$

The total resistance of the staple is

$$H = F + P = -K_s\delta + \frac{\frac{k}{\lambda}(F_1F_2 + 4F_3F_4)}{(-4F_2F_4 - F_1^2)}\,\delta$$

## 4.4 Case III - Partially Supported Beam

The third case can be described as follows:

A beam of finite length is partially supported by an elastic foundation. The supported part starts at $x = 0$ and extends to $X = L_2$ at the end of the beam, while the unsupported part starts at $x = 0$ and extends to $-L_1$ at the left end of the beam (see Fig. (4.6)). The left end of the beam is free to translate but cannot rotate, and the load is applied at the left end as a concentrated force.

For the interval $-L_1 \leq x \leq 0$

$$M = M_F - H(x + L_1)$$

$$EI\frac{d^2y}{dx^2} = M_F - H(x + L_1)$$

$$EI\frac{dy}{dx} = EI\theta = M_F x - \frac{H}{2}(x + L_1)^2 + C_1$$

at $x = -L_1$ $\quad \theta = 0$

hence $-M_F L_1 + C_1 = 0 \qquad C_1 = M_F L_1$

$$\theta_x = \frac{1}{EI}\left(M_F x - \frac{H}{2}(x + L_1)^2 + M_F L_1\right)$$

$$EIy = \frac{M_F x^2}{2} - \frac{H}{6}(x + L_1)^2 + M_F L_1 x + C_2$$

$$y_x = \frac{1}{EI}\left(\frac{M_F x^2}{2} - \frac{H}{6}(x + L_1)^3 + M_F L_1 x + C_2\right) \qquad (4.12)$$

$M_F$ and $C_2$ are unknown.

For the interval $0 \leq x \leq L_2$

$$y_x = y_o F_1(\lambda x) + \frac{1}{\lambda}\theta_o F_2(\lambda x) - \frac{1}{\lambda^2 EI} M_o F_3(\lambda x)$$

$$- \frac{1}{\lambda^3 EI} Q_o F_4(\lambda x)$$

Call

$$F_1(\lambda L_2) = F_1$$

$$F_2(\lambda L_2) = F_2$$

$$F_3(\lambda L_2) = F_3$$

$$F_4(\lambda L_2) = F_4$$

for $x = L_2$

and evaluate for x = 0

$$F_1(\lambda,0) = 1.0$$

$$F_2(\lambda,0) = F_3(\lambda,0) = F_4(\lambda,0) = 0.0$$

There are six unknowns for both intervals, so six boundary conditions are needed for their evaluation. The boundary conditions are the following:

a) at $x = 0$ $\quad Q = Q_o = -H + K_s y_o$

b) at $x = L_2$ $\quad M = 0.0$

c) at $x = L_2$ $\quad Q = 0.0$

d) at $x = 0$ $\quad y_L = Y_R = y_o$

e) at $x = 0$ $\quad M_L = M_R = M_o$

f) at $x = 0$ $\quad \theta_L = \theta_R = \theta_o$

The subscripts L, R signify left and right respectively. Applying the boundary conditions in the order presented above, we obtain the following equations:

a) $$\frac{-K_s C_2}{EI} + Q_o = -H \left(1 + \frac{L_1^3 k_s}{6EI}\right)$$

b) $$F_1 M_o + \frac{F_2}{\lambda} Q_o + \frac{kF_4}{\lambda^3} \theta_o + \frac{k}{\lambda^2} F_3 y_o = 0$$

c) $$-4\lambda F_4 M_o + F_1 Q_o + \frac{k}{\lambda^2} F_3 \theta_o + \frac{k}{\lambda} F_2 y_o = 0$$

d) $$\frac{-C_2}{EI} + y_o = -\frac{HL_1^3}{6EI}$$

e) $$-M_F + M_o = -HL_1$$

f) $$\frac{-M_F L_1}{EI} + \theta_o = \frac{-HL_1^2}{2EI}$$

Writing the equations in a matrix form:

$$\begin{bmatrix} 0.0 & \frac{-k_s}{EI} & 0.0 & 1.0 & 0.0 & 0.0 \\ 0.0 & 0.0 & F_1 & \frac{F_2}{\lambda} & \frac{kF_4}{\lambda^3} & \frac{kF_3}{\lambda^2} \\ 0.0 & 0.0 & -4\lambda F_4 & F_1 & \frac{kF_3}{\lambda^2} & \frac{kF_2}{\lambda} \\ 0.0 & \frac{-1}{EI} & 0.0 & 0.0 & 0.0 & 1.0 \\ -1.0 & 0.0 & 1.0 & 0.0 & 0.0 & 0.0 \\ \frac{-L_1}{EI} & 0.0 & 0.0 & 0.0 & 1.0 & 0.0 \end{bmatrix} \cdot \begin{bmatrix} M_F \\ C_2 \\ M_o \\ Q_o \\ \theta_o \\ y_o \end{bmatrix} = \begin{bmatrix} -H(1+\frac{K_s L_1^3}{6EI}) \\ 0.0 \\ 0.0 \\ \frac{-HL_1^3}{6EI} \\ -HL_1 \\ \frac{-HL_1^2}{2EI} \end{bmatrix}$$

The input variable in the preceding matrix for given geometric conditions, is the applied force H, whereby the maximum displacement is given by equation (4.12) at $x = -L_1$. Thus, the force displacement relation is established.

In all the previous cases, the developed relations hold for the elastic range of the staple once the staple has yielded, the equations previously developed cannot be used further. It has been assumed that the elastic range of the other components of the connection is not exceeded. If it is exceeded, the values of K's in the matrix must be modified.

# CHAPTER 5

## EXPERIMENTAL INVESTIGATION OF A STAPLED CONNECTION VARYING THE PARAMETERS IDENTIFIED IN THE THEORY

In all three cases discussed previously in Chapter 4, the parameters which affect the behaviour and capacity of the staple are:

a) Length (L)

b) Diameter (D)

c) Modulus of elasticity of staple material (E)

d) Elastic bearing modulus of wood ($K_o$)

e) The yield bearing strength of the aluminum facing ($f_s$)

f) Yield strength of the staple material ($f_y$)

g) The thickness of the aluminum facing

The above parameters are discussed in the following sections.

a) Length of the Staple

For a staple of infinite length, under lateral load supported by wood only, the P - $\delta$ relation is given by equation (4.7), where $\delta = y_{x=0}$ , $\delta = -\frac{P}{4EI\lambda^3} = -\frac{\lambda}{K} P$.

If one assumes P and $\delta$ both positive in the same direction, then:

$$\delta = P/_{4EI\lambda^3} = \frac{\lambda}{K} P \qquad (5.1)$$

since

$$\lambda = \sqrt[4]{\frac{K}{4EI}}$$

$$\frac{\lambda}{K} = \frac{(K/_{4EI})^{1/4}}{K} = \frac{1}{(4EI)^{1/4} K^{3/4}}$$

Substituting for $K = K_o D$ and $I = \frac{\pi D^4}{64}$

$$\frac{\lambda}{K} = \frac{1}{(4EI\frac{\pi D^4}{64})^{1/4}(K_o D)^{3/4}} = \frac{1}{\frac{E^{1/4}\pi^{1/4}D^{7/4}K_o^{3/4}}{2}}$$

Hence, by substituting $\frac{\lambda}{K}$ to Eqn. (5.1), we obtain

$$\delta = \frac{P}{\frac{E^{1/4}\pi^{1/4}D^{7/4}K_o^{3/4}}{2}} \tag{5.2}$$

For a staple of finite length, under lateral load supported by wood only, the P - $\delta$ relation is given by equation (4.11) where $\delta = y_o$.

$$\delta = \frac{\lambda}{K} P\left(\frac{-4F_2F_4 - F_1^2}{F_1F_2 + 4F_3F_4}\right)$$

since

$$\frac{\lambda}{K} = \frac{2}{E^{1/4}\pi^{1/4}D^{7/4}K_o^{3/4}}$$

$$\delta = \frac{2P}{E^{1/4}\pi^{1/4}D^{7/4}K_o^{3/4}} \left(\frac{-4F_2F_4 - F_1^2}{F_1F_2 + 4F_3F_4}\right)$$

if P and $\delta$ are assumed both possitive in the same direction, then

$$\frac{P}{\delta} = -\frac{E^{1/4}\pi^{1/4}D^{7/4}K_o^{3/4}}{2} \left(\frac{F_1F_2 + 4F_3F_4}{-4F_2F_4 - F_1^2}\right) \tag{5.3}$$

It is shown in Appendix I that the ratio of the F's in Equation (5.3) is almost equal to -1.0 if L/D > 14.0.

Hence, if L/D is kept greater than 14.0 the length of the staple can be eliminated from being a variable affecting its P-δ relation and Equation (5.3) can be written

$$\frac{P}{\delta} = \frac{E^{1/4}\pi^{1/4}D^{7/4}K_o^{3/4}}{2} \qquad (5.4)$$

which is the same with Equation (5.2) for a staple of infinite length. Equation (5.4) has three variables, E, D and $K_o$, and these are described here.

b) Diameter of the Staple D

According to Equation (5.4) the P/δ relation is a function of the diameter to the power (7/4) this should be verified experimentally.

c) The Modulus of Elasticity of the Staple Material (E).

Since the staples are made from steel E = 29-30x$10^6$psi and is constant.

d) The Elastic Bearing Modulus of Wood ($K_o$)

The wood elastic bearing modulus is a controversial parameter for which different references give different values which may differ by a factor of three, Ref. (3,4,5). It was decided to adopt the values given by Wilkinson in Ref. (5), which for loading parallel to the grain gives

$$K_o = 2{,}144{,}000\ G$$

where G = specific gravity of the wood.

The wood used in this case is white pine (G = 0.38). The value of $K_o$, according to Wilkinson (5), changes depending on the relative stiffness of the members connected. To account for that variation, Wilkinson introduced a factor $\beta_1$ which can be obtained from a graph relating the ratio (r) of the elastic bearing moduli of the two connected members to $\beta_1$. In our case, the conditions for using this graph are not satisfied, so $\beta_1$ must be found experimentally. Hence, the P - $\delta$ relationship of equation (5.4) becomes:

$$\frac{P}{\delta} = \frac{E^{1/4}\pi^{1/4}D^{7/4}K_o^{3/4}\beta_1}{2} \qquad (5.5)$$

Substituting for E, $\pi$ and $K_o$ Equation (5.5) yields:

$$\frac{P}{\delta} = 1{,}334{,}500\ \beta_1 D^{7/4}. \qquad (5.6)$$

To the above relation we must include the contribution of the aluminium facing

$$F = K_s\delta \qquad \frac{F}{\delta} = K_s$$

Where the factor $K_s$ depends on the thickness of the aluminium face, for a given type of aluminum, and the diameter of the staple. According to the work of Hrenikoff (31) on rivets, the value of $K_s$ depends on the diameter of the rivet only, if the thickness of the plate, on which the rivet bears, is large. If the thickness

of the plate is small, then the value of $K_s$ depends of the diameter and the hyperbolic tangent of the ratio of the thickness of the plate to the diameter of the rivet. The formulae given by Hrenikoff were derived theoretically as he mentions without experimental verification. In the same reference, the work of others is presented who found the value of $K_s$ as a linear function of the bearing area from experimental data. Due to distortion created on the aluminum facing during the insertion of the staple, as explained in Chapter 3, the value of $K_s$ cannot be determined theoretically. In this work it is assumed that the value of $K_s$ is a function of the staple diameter and the aluminum facing thickness (5.7) with unknown exponents and coefficient which have to be found experimentally.

$$K_s = R\, D^z t_s^w \tag{5.7}$$

Thus, the combined effect of the wood (5.6) and aluminium (5.7) yields:

$$\frac{P}{\delta} = 1{,}334{,}500\ \beta_1 D^{7/4} + R D^z t_s^w \tag{5.8}$$

It can be seen from equation (5.8) that the total stiffness ($P/\delta$) of the staple leg varies according to diameter of the staple and the thickness of the aluminum for a particular wood species and a particular aluminum type. Equation (5.8) contains four unknowns $\beta_1$, R, z and w which must be determined from the experimental results.

The last three parameters:

e) The Yield Bearing Strength of the Aluminum Facing;
f) Yield Strength of the Staple Material; and
g) The Thickness of the Aluminum Facing

affect lateral load transmission capacity of the staple leg and are discussed below.

The lateral load transmission capacity of a staple leg in wood is a function of the $D^{3/2}$ and the wood density. This relationship has been developed by the U.S. Forest Product Laboratory. In general, the lateral load resistance of a nailed fastener in a particular wood is given by:

$$P_{uw} = C_w D^{3/2} \tag{5.9}$$

The coefficient $C_w$ depends on the wood species and also incorporates the strength of the steel. The reasons that $C_w$ does not change with the strength of the steel are:

(i) the strength of the standard fasteners does not vary considerably, hence, it can be incorporated in $C_w$ as constant; and

(ii) the wood species and the diameter of the fastener affected its lateral resistance far more than the strength of the steel from which the fastener is made.

The total lateral resistance of the staple leg includes the resistance of the wood (5.9) and the resistance of the aluminum.

The resistance of the aluminum is given by the product of the bearing area and the bearing strength of aluminum. Since the aluminum on which the staple bears is distorted its resistance

cannot be predicted. Hence, it was decided to express the resistance of the aluminum (5.11) as a function of the bearing area ($Dt_s$) multiplied by an unknown coefficient ($C_s$) to account for the bearing strength of the aluminum.

$$P_{us} = C_s D t_s \tag{5.10}$$

The combined effect of equations (5.9) and (5.10) yields

$$P_u = C_w D^{3/2} + C_s D t_s \tag{5.11}$$

The capacity of the staple leg to transmit lateral load given by Equation (5.11), which like the stiffness of the staple leg given by Equation (5.8), varies according to the diameter of the staple and the thickness of the aluminum facing for a particular wood species and aluminum type. The values of $C_w$ and $C_s$ of equation (5.11) need to be determined from the experimental results. Case three, examined in Chapter 4, for the staple with the overhanging part, cannot be analyzed here parametrically. This case, as well as the two previous ones were examined with the use of the computer. The equations of Chapter 4 were programmed to give the deflection of the staple, the shear, the moment, the force on the wood, and the force on aluminum for ideal conditions neglecting the distortion of the aluminum facing. The $P - \delta$ relation was investigated varying all the parameters identified at the beginning of Chapter 5. All the variables, when increased, increase the capacity and stiffness of the staple leg, as can be seen by Equations (5.1) to (5.11). The only variable than can be excluded is the staple

length. Case three had the same behaviour as the two others except that the overhanging part resulted in large moments with small loads and consequently early yielding of the staple leg occured. Therefore, it is advised that the overhanging part should be eliminated in practice. It should be mentioned that according to the output from the computer, the first part to yield is the aluminum and second the staple. In any case, the output from the computer was for an idealized connection, but it gives an idea of how the variables effect the behaviour and capacity of the staple.

## 5.1 Tests and Results for Single Staples

The purpose of the tests is to verify the theory and to determine the values of the coefficients of Equations (5.8) and (5.11). As mentioned in the previous section, two parameters need to be varied to find the values of the unknowns and verify that the effect of these parameters is as predicted by the theory. These parameters are the diameter of the staple leg and the thickness of the aluminum facing. The selection of staple gages and aluminum thickness was made from available commercial products. The selected values are shown in Table (5.1). Four samples were made for each parameter variation, a total of forty-eight samples. The testing arrangement is shown in Fig. (5.1).

In preceding tests (Chapter 3), the load was applied at a constant rate and the deflection was observed and recorded. The loading continued until the connection had failed by separation of the connected members. The load required to separate the members was recorded.

TABLE 5.1

| STAPLE<br>gage (parameter)<br>length<br>crown | 16<br>7/8"<br>7/16" | 15<br>1 1/8"<br>7/16" | 14<br>1 1/4"<br>7/16" |
|---|---|---|---|
| aluminium<br>plate<br>thickness | .064" | .080" | .080" |
| aluminium<br>face thickness<br>(parameter) | .025"<br>.032"<br>.050"<br>.064" | .025"<br>.032"<br>.050"<br>.064" | .025"<br>.032"<br>.050"<br>.064" |

SELECTED VALUES FOR THE PARAMETERS (GAGE, ALUMINIUM FACE THICKNESS). THE STAPLES USED ARE SENCO AND POWER LINE. THE ALUMINUM USED IS UTILITY ALUMINIUM, ALLOY 3003-H16.

In these tests, during cycling of the load, it was observed that continuous deformation of the connection occurred at loads lower than previously recorded ultimate loads. When the load was increased, the rate of continuous deformation under constant load also increased. It was thus decided for the present group of tests to apply the load incrementally and observe the behaviour of the connection at each load increment. The connection was considered as having failed as soon as creep began to occur. The term creep refers to the point at which the connection continues to deform without any increase of the load. THe load on each connection was first cycled at some levels to let the connection stabilize then the load was increased in increments until creep occurred (Fig. (5.2)). The general behaviour of this stapled assembly is similar to that of a nailed connection (Ref, 3). In particular, the following observations were made. Each connection showed a slightly higher flexibility at the beginning of loading. The amount of this flexibility decreased with increasing thickness of aluminum face and staple diameter. Each connection was loaded several times to various loads and several times to the creep load. Permanent deformation occurred after each unloading (see Fig. (5.2)). This permanent deformation decreased with the number of loadings and with increased thickness of the aluminum facing. Fig. (5.3) shows the relation between the load per staple leg and its resulting deformation, for each staple gage and aluminum thickness ($t_s$). In Fig. (5.4) the creep load per staple is plotted against the aluminum face thickness for various staple gages. It can be seen that the creep load varies linearly with the thickness of the aluminum facing.

The family of curves shown in Fig. (5.5) presents the creep load versus the staple diameter for various aluminum face thicknesses. It is seen that the creep load is not a linear function of the staple diameter but it varies with the $D^{3/2}$ as a result of the resistance of the wood. Fig. (5.6) shows the slope of P-$\delta$ relation versus the diameter of the staple for various aluminum thicknesses. The slope of the P-$\delta$ relation is not a linear function of the diameter.

Using the above graphs the coefficients of Equations (5.8) and (5.11) were determined in the following manner:

First, for Equation (5.11), in order to find $C_w$, the values from the ($t_o$) curve of Fig. (5.5) were plotted against $D^{3/2}$. A straight line resulted. The slope of this line yields the value of $C_w$ = 2700 (lbs/in$^{3/2}$).

In order to find the value of $C_s$, the load given by the curves $t_1$, $t_2$, $t_3$ and $t_4$ minus the load given by the ($t_o$) curve was plotted against ($Dt_s$). This difference ($P_{cr}$-$P_{uw}$) gives the load resisted by the aluminum facing. The values of the load resisted by the aluminum versus the bearing area ($Dt_s$) were on a straight line, the slope of which was the value of $C_s$ = 15,750 (lbs/in$^2$).

Hence, Equation (5.11) becomes

$$P_u = P_{cr} = 15{,}750\, Dt_s + 2700\, D^{3/2} \qquad (5.12)$$

The unknowns of Equation (5.8) are determined using the stiffness values (K) of Fig. (5.6). The value of the coefficient $\beta_1$ is determined by plotting the K values of curve ($t_o$) versus $D^{7/4}$. The slope of the resulting straight line yields M = 325,000 which is equal to 1,334,500 $\beta_1$ in Eqn. 5.8. Hence, $\beta_1$ = 325,000/1,334,500 = 0.244. For the second part of Eqn. (5.8), the three unknowns, r, z and w must be found. Preliminary values of 1.0 were assumed for z and w. Then the K values of the curves $t_1$, $t_2$, $t_3$ and $t_4$ from Fig. (5.6) minus the K values of curve ($t_o$) were plotted versus the bearing area of the aluminum face ($Dt_s$). The slope of the resulting approximately straight line yields the value of R = 1,250,000. Hence, Equation (5.8) becomes:

$$P/\delta = 325{,}000D^{7/4} + 1{,}250{,}000Dt \qquad (5.13)$$

Then an attempt was made to find the values of z and w if they were different than one. For that a family of curves was plotted, one for each aluminum thickness $t_1$, $t_2$, $t_3$ and $t_4$. This family of curves (Fig. (5.7)) yields the stiffness of the aluminum alone which is that given by the K values of curves $t_1$, $t_2$, $t_3$ and $t_4$ of Fig. (5.6) minus the K values of curve ($t_o$). The curves of Fig. (5.7) give the stiffness of the aluminum versus the staple diameter for various aluminum facing thicknesses. The equations of these curves were found by trial and error, and they are:

$$K_{s1} = 62000\ D^{1.4} \quad \text{for } t_1$$

$$K_{s2} = 112000\ D^{1.4} \quad \text{for } t_2$$

$$K_{s3} = 182000\ D^{1.4} \quad \text{for } t_3$$

$$K_{s4} = 235000\ D^{1.4} \quad \text{for } t_4$$

where $K_s = K_{total} - K_{t_o}$

Now $$\frac{K_s}{D^{1.4}} = R_1$$

Where $R_1$ = coefficient of $D^{1.4}$

The values of $K_{s/D}{}^{1.4}$ or $R_1$ were plotted against the aluminum thickness. The slope of the resulting straight line is

$$K_{s/D}{}^{1.4}{}_t = R = 3{,}600{,}000$$

Hence

$$K_s = 3{,}600{,}000\ t\ D^{1.4}$$

which means that: $z = 1.4$

$w = 1.0$

$R = 3{,}600{,}000$ (lbs/in$^{3/4}$)

Hence, Equation (5.8) becomes

$$P/\delta = 3{,}600{,}000\ t\ D^{1.4} + 325{,}000\ D^{7/4} \qquad (5.14)$$

The values given by equation (5.13) and (5.14) differ by less than 5% for the range of the parameters in the tests. Since Equation (5.13) is simpler, it will be used hereafter.

The large flexibility at the beginning of loading is replaced by an initial slippage ($\delta_o$) (Fig. 5.8) which is given by the equations

$$\delta_o = \frac{3\text{-}43t_s}{1000} \qquad \text{for gages 15, 14} \tag{5.15}$$

$$\delta_o = \frac{6\text{-}80t_s}{1000} \qquad \text{for gage 16} \tag{5.16}$$

Equations (5.15) and (5.16) were found by plotting the initial slippage for each gage against the aluminum facing thickness.

Thus, the total deformation $\Delta = \delta + \delta_o$ is given by

$$\Delta = \frac{p}{(1{,}250{,}000\ Dt + 325{,}000\ D^{7/4})} + \delta_o \tag{5.17}$$

It should be noted that all the above formulae are empirical although based on a theoretical development. Thus, they can be applied only for the range within which they have been experimentally verified. The limits for the application of the above formulae are as follows:

a) Maximum aluminum face thickness = 0.07"

b) Staple diameter $0.05" \leq D \leq 0.09"$

The value of the initial slippage ($\delta_o$) given by equations (5.15) and (5.16) is zero for staple diameter greater than 0.08" and aluminum face thicknesses greater than 0.065".

It is suggested, based on the discussions and conclusions of the world symposium on nailed connections (2), that the allowable design load ($P_a$) be creep load divided by 2.5.

$$P_a = P_{cr}/2.5 \tag{5.18}$$

The formulae given in Chapter 5 give the capacity and the stiffness of a single staple. Another factor to be investigated is the effect of the length of the connection (where many staples are used in a row) on the capacity and stiffness per staple leg. This is done in Chapter 6.

For the purpose of comparison, the theoretical results of Eqns. (5.12) and (5.17) are plotted in Figures (5.9) and (5.10) respectively (dashed lines), along with the experimental values (solid lines).

The theoretical and experimental stiffness values in Fig. (5.10) vary from 0.0 to 10%. The theoretical and experimental capacity values vary from 0.0 to 15%.

## CHAPTER 6

## THE EFFECT OF THE CONNECTION LENGTH ON THE BEHAVIOUR OF THE INDIVIDUAL STAPLE

In order to be able to fully describe the behaviour and the capacity of a stapled connection, it is necessary to know the behaviour of the connection when many staples in a row are used. There is already an established and applied theory for many fasteners in a row, explained by Cramer (Ref. 18). This reference considers the load on each fastener as a percentage of the applied load. The distribution of the load to the fasteners depends on the number of fasteners, the fastener spacing and the dimensions of the connected parts.

Equations of Ref. 18 are presented below. Figure 6.1 identifies the notations employed in these equations.

For the left end of the connection:

$$\alpha P_1 - P_2 = K_w F \tag{6.1}$$

for the intermediate fasteners:

$$P_{i-1} - (1+\alpha)P_i + P_i + 1 = 0 \tag{6.2}$$

for the right end of the connection:

$$P_{n-1} - \alpha P_n = -K_p F \tag{6.3}$$

where:

$$K_w = \beta_w r / b_w t_w E_w y \tag{6.4}$$

$$K_p = \beta_p r / b_p t_p E_p y \tag{6.5}$$

$$\alpha = 1 + K_p + K_w \tag{6.6}$$

$P_i$ = load on fastener i

F = applied force

n = number of fasteners

r = fastener spacing

t = thickness of the connnected members

$\beta$ = Schulz multiplying factor

$y = \delta/P$ . This is the slope of the deformation versus load of the fastener. It indicates how flexible the fastener is.

Values of $\beta$ in Equations (6.4) and (6.5) are given in Fig. (6.2). The factors $K_w$ and $K_p$ can be considered as the combined flexibility of each connected member with the fasteners. The product b.t.E indicates the stiffness of the connected members.

For the size of the members and the material properties used in the present experimental program the value of $\beta$ for both members approaches one due to the very small value of $\mu$ (see Fig. (6.2)). The product b.t.E is of the order $10^7$.

The value of y which is the inverse stiffness of the staple leg is of the order of $10^{-4}$. The value of r, which is the spacing of the staple legs is of the order $10^{-1}$.

Thus, the $K_p$ and $K_w$ are of ther order $10^{-4}$, approaching zero. This means that the stiffness of the connected members is very large compared to the stiffness of the fasteners and the value of $\alpha$ approaches 1.0.

Referring to Equations (6.1), (6.2) and (6.3), it can be seen that when $\alpha = 1.0$ the distribution of the load is the same for all the fasteners in the row which means that for a given deformation of the connection, the load acting on it should be the load of the individual fastener corresponding to this deformation multiplied by the number of fasteners. In a case like that, the efficiency of the long connection is said to be one hundred percent.

## 6.1 Tests and Results for the Length Effects

In deciding the basic parameters whose effects are to be tested, the following reasoning was adopted. Since the stiffnesses of the connected members are very large compared to the staple stiffness, the effect of the properties and dimensions of the member is considered negligible. Thus, the only remaining parameters to be investigated were the number of staples and their spacing. The number of staples tested and their spaces are shown in Table 6.1.

There were four samples for each variation of parameters; a total of 32 samples.

TABLE 6.1

| Staple Gage Length Crown | Aluminium plate Thickness | Aluminium sheet Thickness | Staple Spacing | Number of Staples |
|---|---|---|---|---|
| 16<br>7/8"<br>7/16 | 0.064" | 0.032" | 7/16" | 2,5,8,12 |
| | | | 1 1/2" | 2,5,8,12 |

SELECTED NUMBERS AND SPACING OF STAPLES TESTED

The experimental procedure was the same as for the case of single staples presented earlier in Section 5.1. The results are presented in the following figures.

Figure (6.3) shows the load per staple leg versus the connection deformation ($\delta$) for various numbers of staples. Figure (6.4) shows the stiffness (k) of the connection per staple leg versus the number of staple legs (N), it is seen that the large drop of stiffness is between one and sixteen staple legs. The stiffness per staple leg is obtained from the slope of the average force per staple leg versus the deformation. Figure (6.5) shows the percentage drop of the stiffness per staple leg and the percentage drop of the staple leg capactiy (P.015) at $\delta$ = 0.015" versus the number of staple legs in a connection.

The following conclusions were drawn from the results. The ultimate capacity of the staples was not affected by the length of the connection, as shown in Fig. (6.3).

The stiffness per staple leg, however, was reduced with increasing number of staples, but it was not affected by the spacing of the staples.

According to the theory, there should not be any drop in the stiffness per staple leg with increasing number of staples due to the large stiffness of the connected members. The tests, however, showed that a substantial reduction of stiffness resulted as the number of staples increased.

This discrepancy is due to the fact that the theory assumes all the fasteners to have the same load deformation curve with the same initial flexibiltiy which, in practice, cannot be satisfied. Hence, for a given deformation of the connection, different staples have different load which results in a reduction

of the overall stiffness of the connection.

As a standard practice for design purposes, the deformations are limited either at $\delta$ = 0.15" or at $\delta$ = 0.030" depending on the purpose of the connection. It is thus necessary to show how the capacity at $\delta$ = 0.015" and $\delta$ = 0.030" varies with the number of staples in a row, and this is shown in Fig. (6.6) where the staple leg capacity is plotted versus the number of staple legs.

In order to formulate the capacity of the staple at $\delta$ = 0.015" for changing number of staples, the load deformation curve of Fig. (6.6) was approximated with two straight lines as shown in Fig. (6.7). The capacity at $\delta$ = 0.030" does not need to be formulated because it is always greater than $P_{cr}/2.5$ which is the design load. The equation (6.7) for the staple leg capacity (P.015) at $\delta$ = 0.015 is derived from Fig. (6.7) for changing N and are given below:

$$P.015 = f_1 - 0.034 f_1 N \qquad \text{for } N \leq 16$$

$$P.015 = 0.45 f_1 \qquad \text{for } N > 16 \tag{6.7}$$

where $f_1$ is the capacity of a single staple at $\delta$ = 0.015 and can be found from Equation (5.17).

## CHAPTER 7

## DESIGN LOADS

If the deformation must be limited to $\delta = 0.015"$ in a connection, then the allowable load per staple leg should be the lesser of Equations (5.18) and (6.7), given below:

$$P_a = P_{cr}/2.5 \tag{5.18}$$

$$P.015 = f_1 - 0.034\, f_1 N \qquad \text{for } N \leq 16$$

$$P.015 = 0.45 f_1 \qquad \text{for } N > 16 \tag{6.7}$$

If the allowable deformation can be extended to $\delta = 0.030"$ then the allowable load per staple leg is given by Equation (5.18).

The ratio (L/D) of the length of the staple inserted in the wood to its diameter must always be greater than 14. The application of the formulae will be demonstrated with the following numerical equation:

Given:

staple gage -15

N = 12, number of staple legs

$t_s = 0.050"$

Find the allowable load per staple leg for $\delta = 0.015"$ and $\delta = 0.30"$ and the total allowable load for the connection.

Solution:

From Eqn. (5.12):

$P_{cr} = 15{,}750\ (.070)(.050) + 2700\ (.070)^{3/2} = 105$ lbs.

From Eqn. (5.18):

$$P_a = 105/_{2.5} = 42 \text{ lbs.} \qquad (A)$$

Using Equation (5.17) and $\Delta = 0.015"$ one can find $(f_1)$.

$$f_1 = [0.015 - (\frac{3-43(.05)}{1000}][(1,250,000)(.07)(.05) + 325,000(.07)^{7/4}]$$

$$f_1 = (.01415)(7470) = 106 \text{ lbs.}$$

$$f_1 > P_{cr} = 105 \text{ lbs}$$

which indicates that creeping for a single staple starts before $\delta = 0.015"$, as shown in Fig. (5.3).

Hence,

$$f_1 = 105 \text{ lbs}$$

from Eqn. (6.7)

$$P_{.015} = 105 - 0.034(105)(12) = 43 > 42 \text{ lbs} \qquad (B)$$

Therefore

$P_a$ of Eqn. (5.18) governs

for $\delta = 0.015"$ and $\delta = 0.030"$

$P_a = 42$ lbs/per staple leg

Total $P_a = 42(12) = 504$ lbs.

# CHAPTER 8

## SUMMARY, CONCLUSIONS AND RECOMMENDATIONS

It was shown in Chapter 3 that the connection tested had some weakness which could be eliminated by changing its geometry. The new connection is a substantial improvement over the original one and can be used for many structural purposes such as space enclosures, including low rise buildings, warehouses, workshops, factories and any other kind of structure in which the behaviour of the connection can be accepted. A complete variation of the modified connection that will accommodate all possible panel arrangements is presented in the following figures.

Figures (8.1) and (8.2) show connection of two panels in the same plane and in perpendicular planes respectively. Figure 8.3 shows the connection of three panels and Figure (8.4) the connection of four panels. The bolts of the connections shown in Figures (8.2), (8.3) and (8.4) are used to take the tolerances and also transfer loads, which, if not resisted by the bolts, will be resisted by the staples as direct pull out loads.

In Chapters 4, 5 and 6, the behaviour of stapled connections between aluminum plates and aluminum faced panels was investigated theoretically and experimentally. The theoretical study included and examined all possible parameters, with respect to dimensions, material properties and geometry, which need to be considered in defining the behaviour and capacity of the connection. It is, therefore, considered complete regarding the behaviour of

of the connection under lateral load.

From the theoretical study it was found that for a particular type of aluminum and a particular type of wood, when steel staples are used, the behaviour and capacity of the staple depends on the diameter of the staple and the thickness of the aluminum facing. On that basis, the experimental program was planned and carried out using steel staples, utility aluminum and white pine for wood. There was a number of tests performed varying the staple gage and the aluminum facing thickness to verify the theory and determine the coefficients needed for the equations. These coefficients could not be found theoretically due to the distortion that the staple causes to the aluminum facing during insertion. The effect that the length of the connection has on the behaviour of the staple was investigated theoretically and experimentally in Chapter 6 and it was formulated. As a result of this investigation formulae, verified experimentally, were derived giving the capacity and the behaviour of the previously described stapled connection. These formulae can be used for design and suggested allowable loads are given in Chapter 7. The designer should keep in mind that with thicker aluminum facing and with larger diameter of the staples, the connection performs better and much closer to the behaviour given by the formulae in this thesis. It is vital that the extrusion or aluminum connecting plate is kept tightly attached on the face of the panel since this gives the opportunity for the staple to develope a very high capacity and eliminates the slippage of the connection to the minimum. If the connection

is properly designed for spacing diameter and length of staples and if the connecting plate is kept tightly attached on the panel face, the capacity of the panels could be fully utilized.

## 8.1 Recommendations for further Research

The experimental investigation was based on available commercial products, but it does challenge the industry to increase the sizes of staples and expand their use in construction. A complete experimental investigation of the behaviour of a stapled connection under lateral load must include varying strengths of aluminum face, varying hardness of steel used for staples, create larger staples than those commercially available, and use of different species of wood. Another investigation required which should include both theoretical and experimetnal approaches is the determination of staple leg length, crown width, diameter, point and steel types that can be used to penetrate different types of aluminum sheets of varying thicknesses attached to various wood species. This investigation would determine the appropriate staple to efficiently penetrate the members of the connection and thus complete the study required to provide sufficient information for the design of the stapled connections examined here.

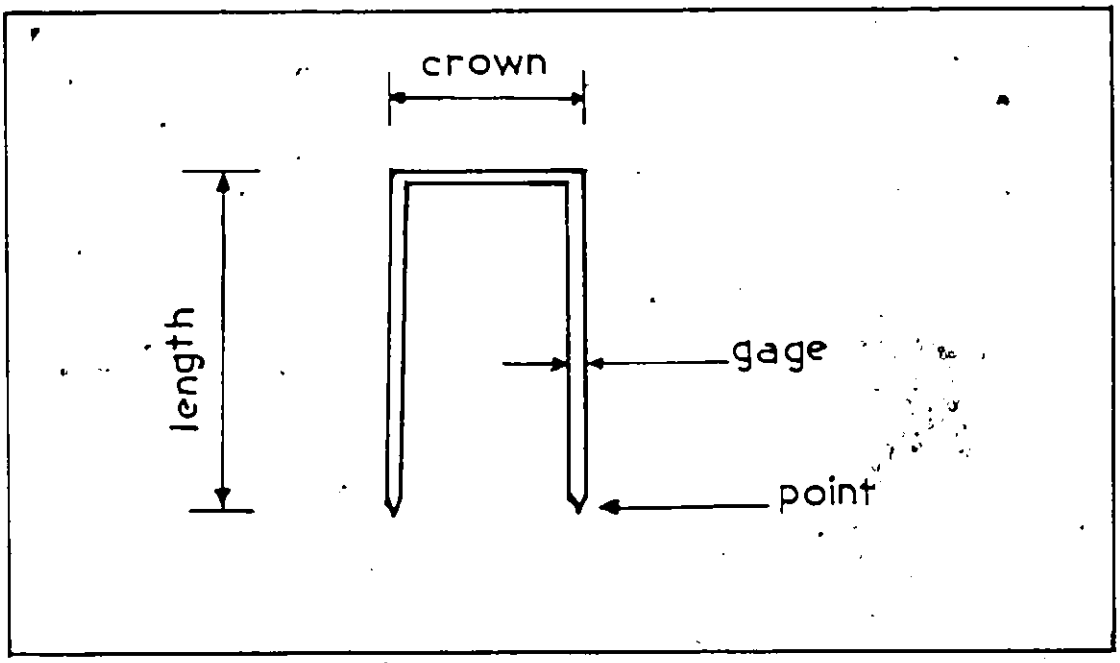


FIG. 2.1 - STAPLE SPECIFICATIONS

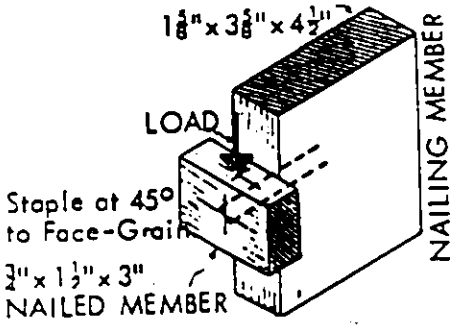


FIG. 2.2 - TEST SET-UP FOR DETERMINATION OF LATERAL LOAD TRANSMISSION EMPLOYED BY PR. STERN.

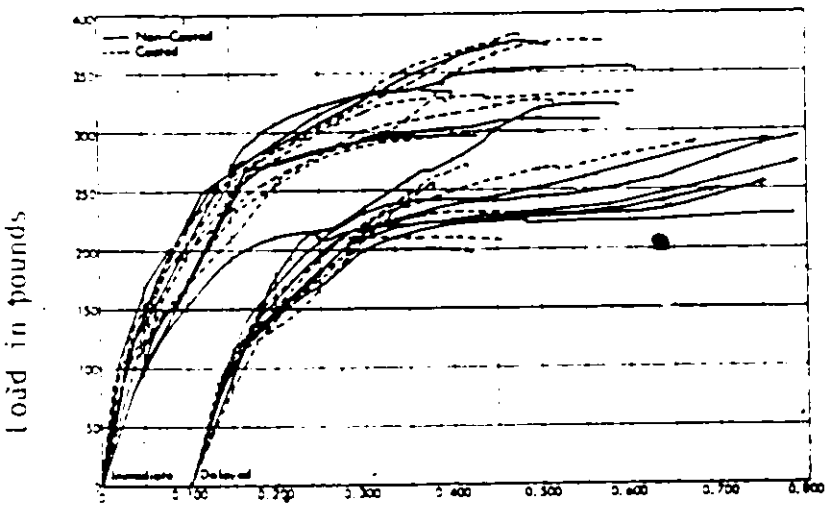


FIG. 2.3 - LOAD DEFORMATION CURVES FOR SOUTHERN PINE JOINTS ASSEMBLED WITH SINGLE 2 1/2"-LONG, 7/16"-CROWN, 15 GAGE SENCO STAPLE LATERALLY LOADED IMMEDIATELY AND SIX WEEKS AFTER ASSEMBLY IN THE DIRECTION PERPENDICULAR TO THE GRAIN OF THE FASTENED MEMBER AND PARALLEL TO THE GRAIN OF THE FASTENING MEMBER

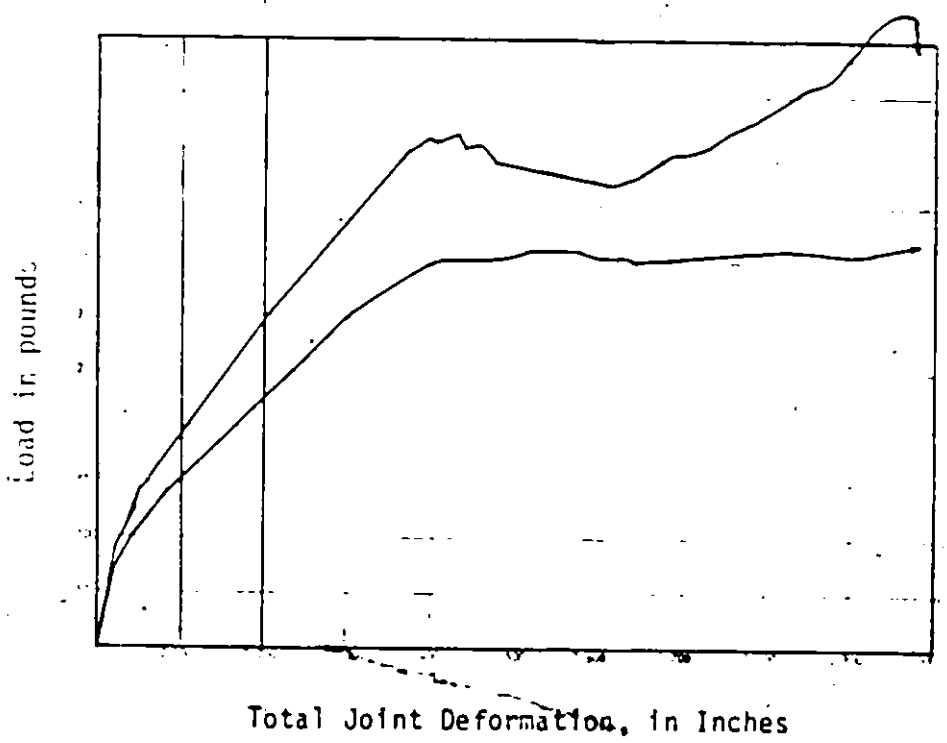


FIG. 2.4 - LOAD DEFORMATION CURVES FOR NAILED AND STAPLED JOINTS, CONSISTING OF 5/8" YELLOW POPLAR DECKBOARD FASTENED TO 1 1/4" x 3 5/8" HARD MAPLE STRINGER WITH THE FASTENER LOADED LATERALLY IMMEDIATELY AFTER ASSEMBLY.

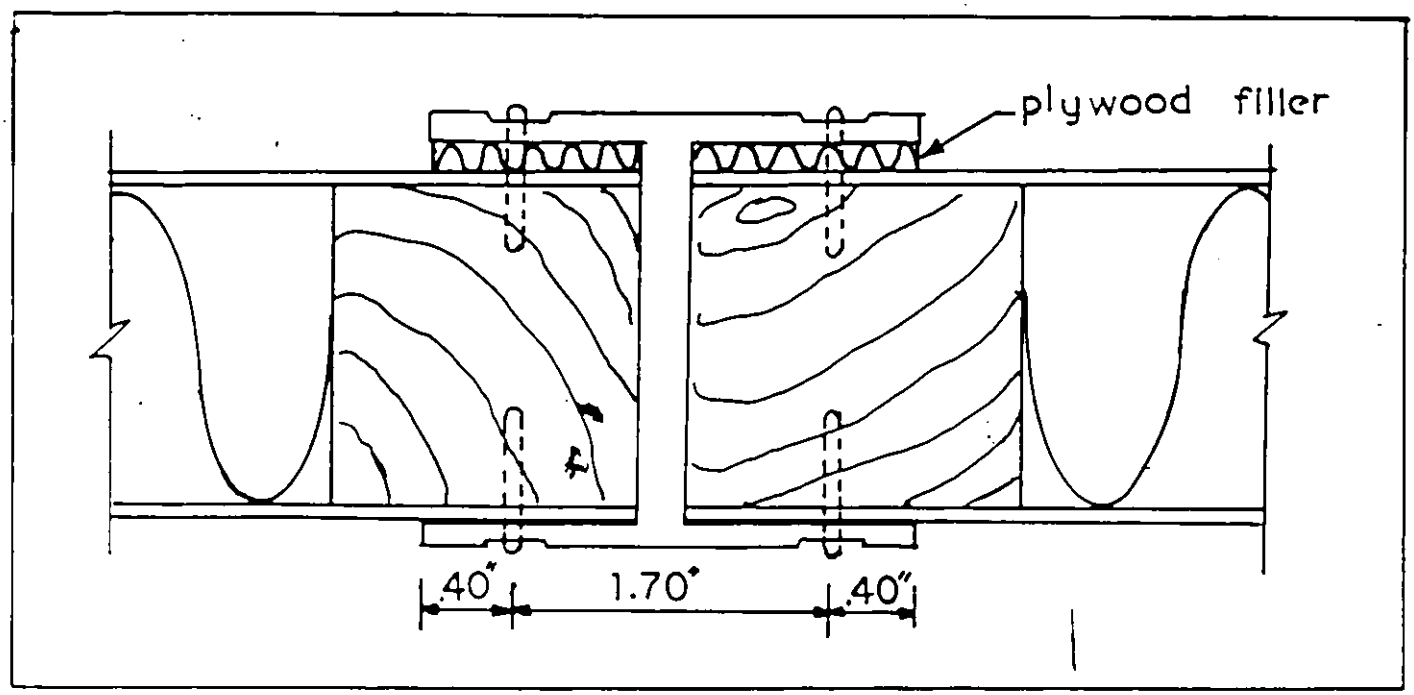


FIG. 3.1 - CROSS SECTION OF THE CONNECTION

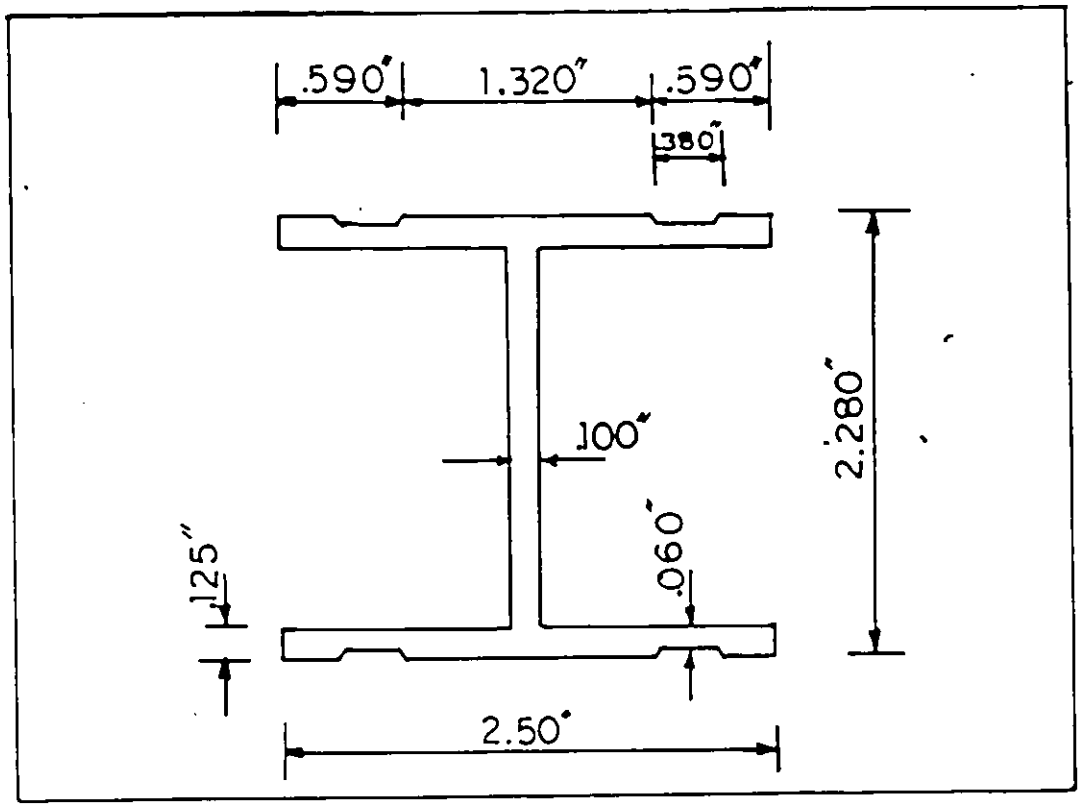


FIG. 3.2 - TYPE I EXTRUSION

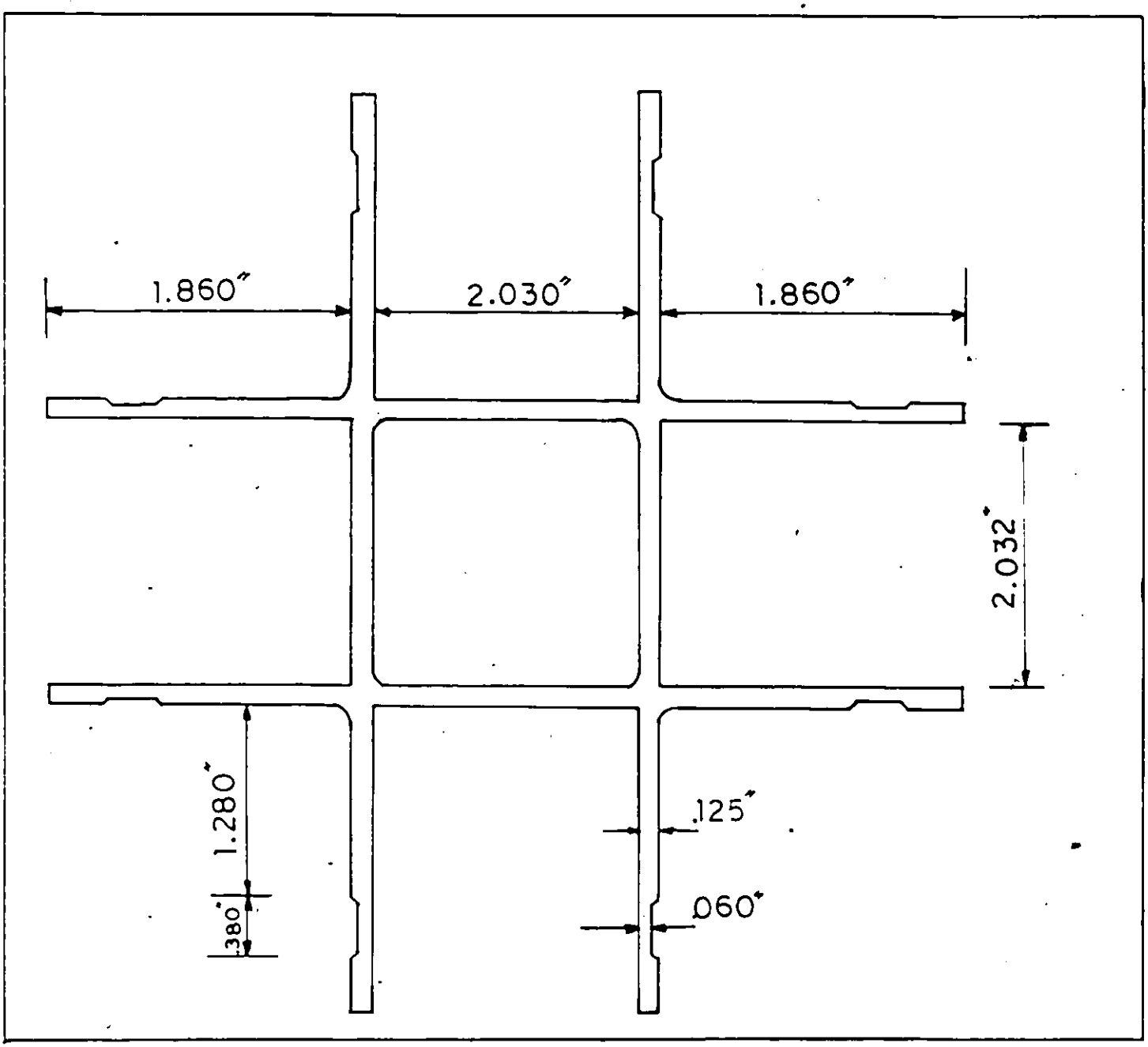


FIG. 3.3 - TYPE #-EXTRUSION TO ACHIEVE A FOUR-WAY CONNECTION.

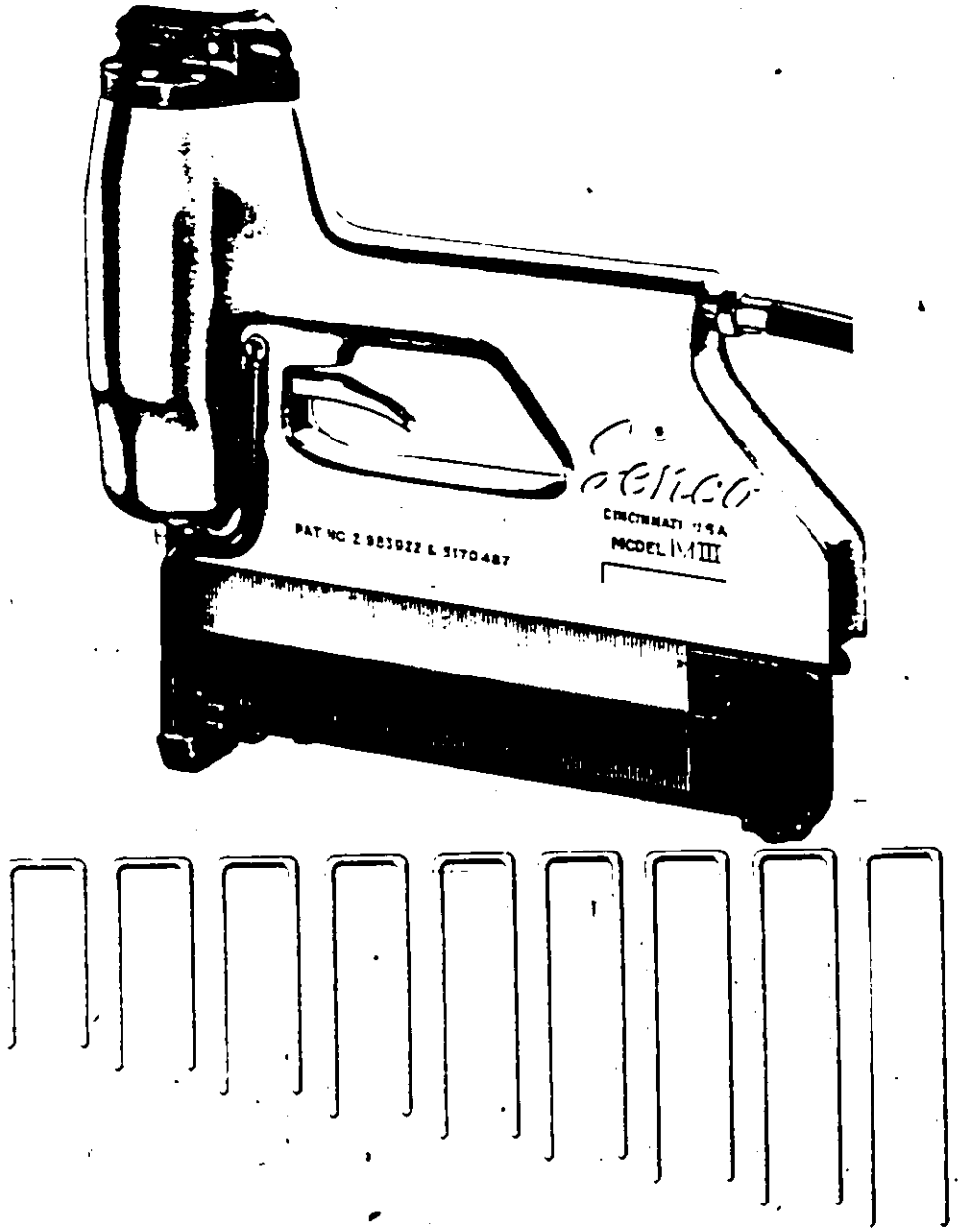


FIG. 3.4 - PNEUMATIC STAPLER AND STAPLES

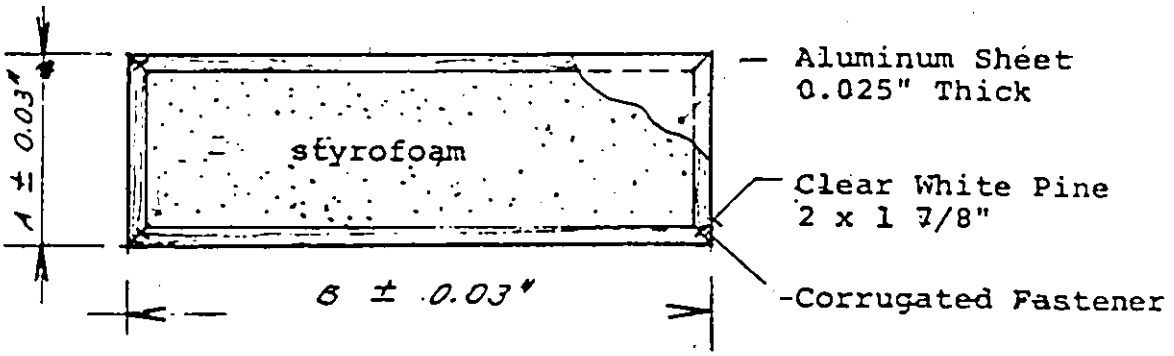


TYPICAL PANEL FRAME

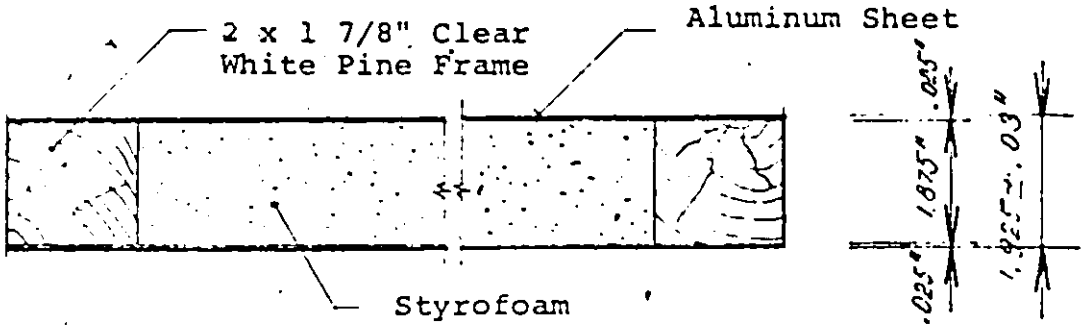


TYPICAL PANEL SECTION

FIG. 3.5 - TYPICAL PANEL FRAME AND SECTION

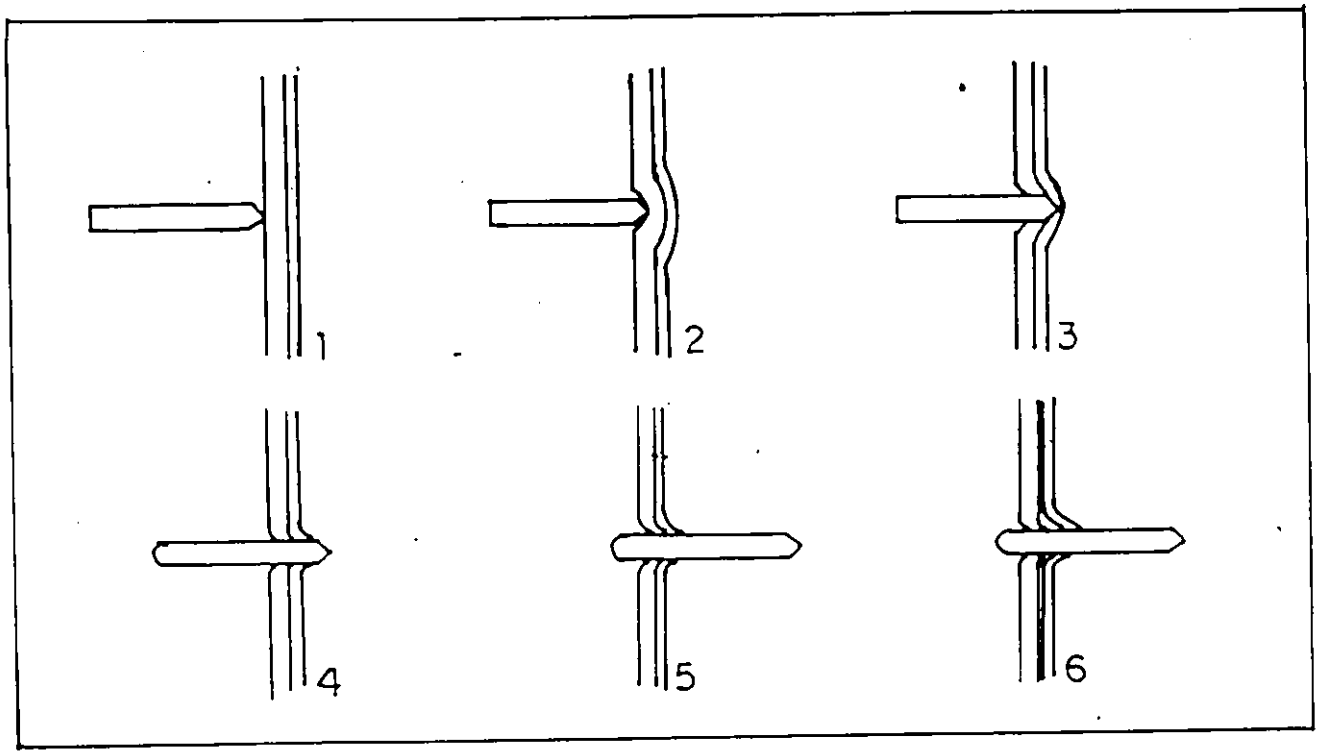


FIG. 3.6 - STAGES OF STAPLE PENETRATION THROUGH THE ALUMINIUM SHEETS

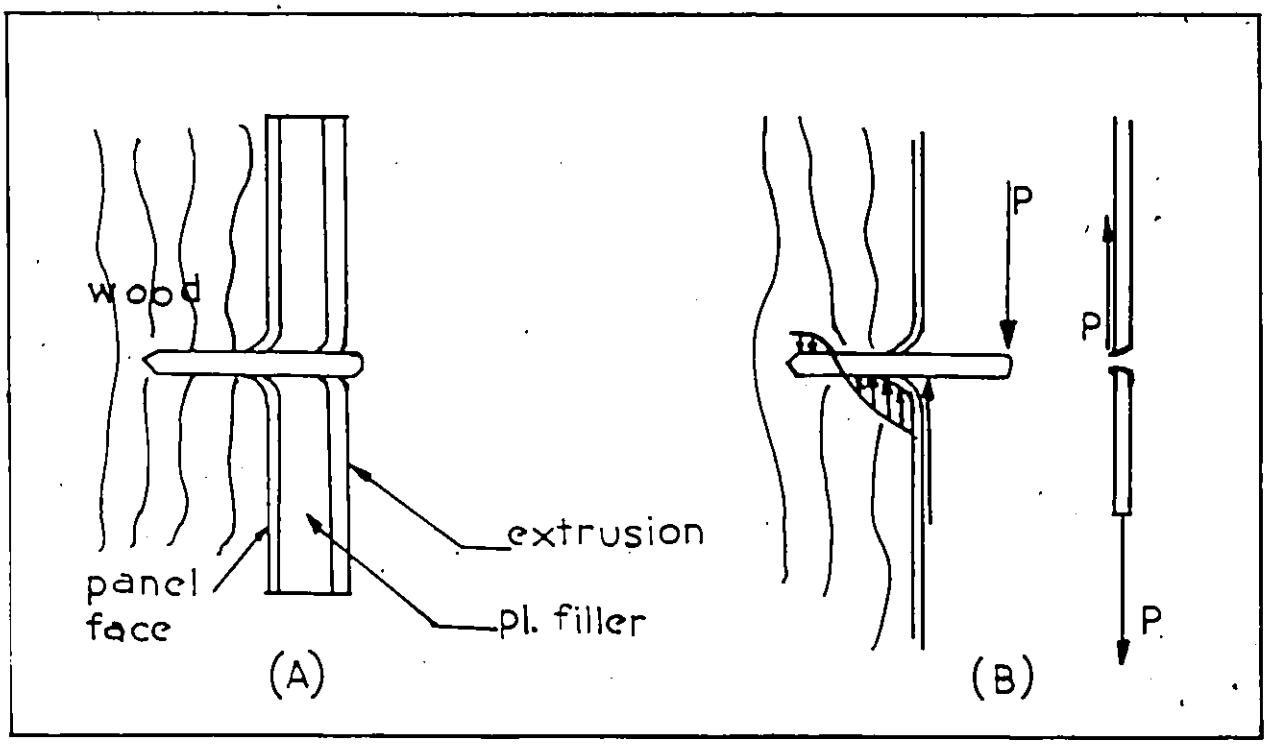


FIG. 3.7 - THE EFFECT OF THE PLYWOOD FILLER ON THE STAPLE LOADING

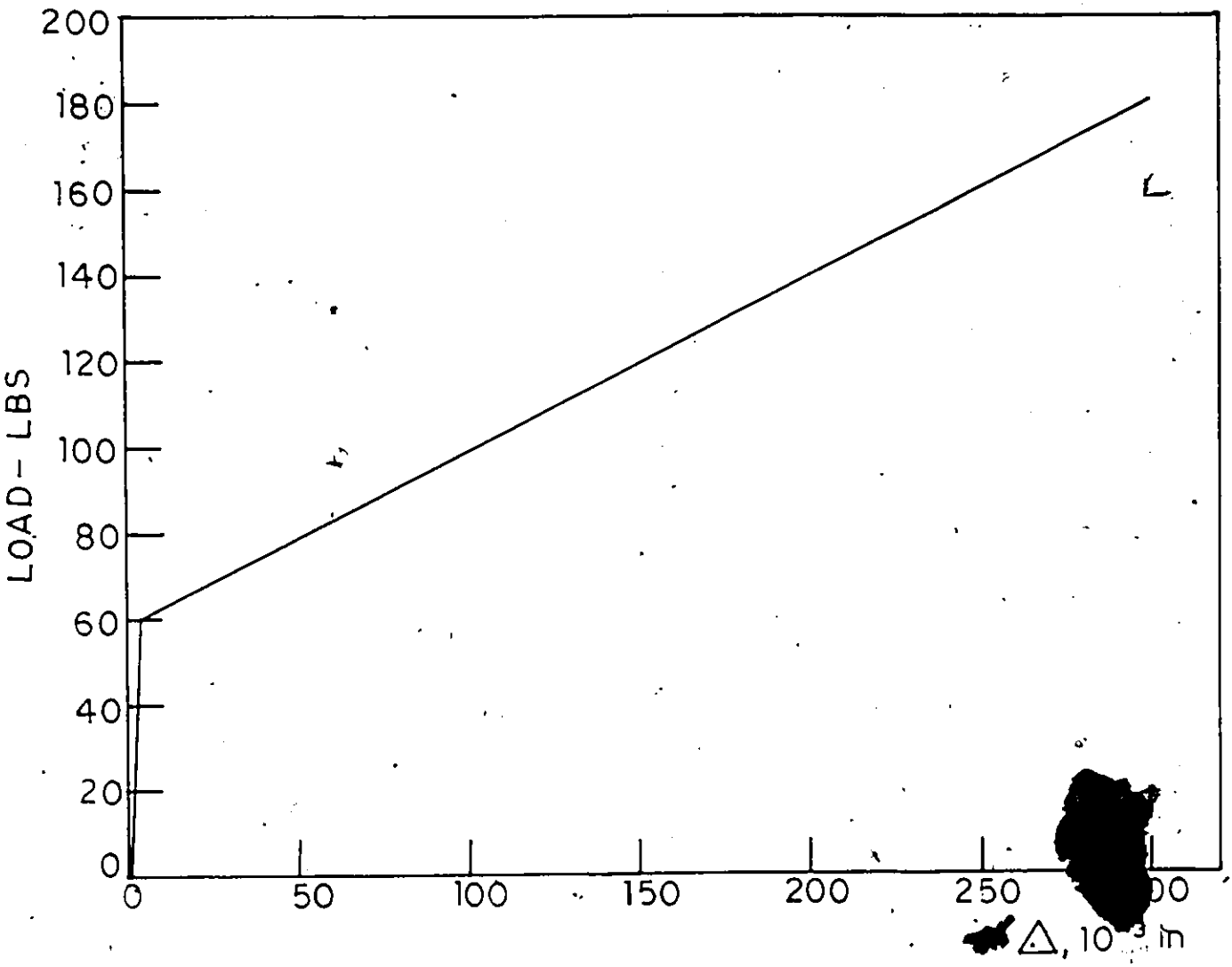


FIG. 3.8 - LOAD-DEFORMATION RELATION FOR BEARING ON THE ALUMINIUM SHEET USING A STAPLE LEG AS PIN.

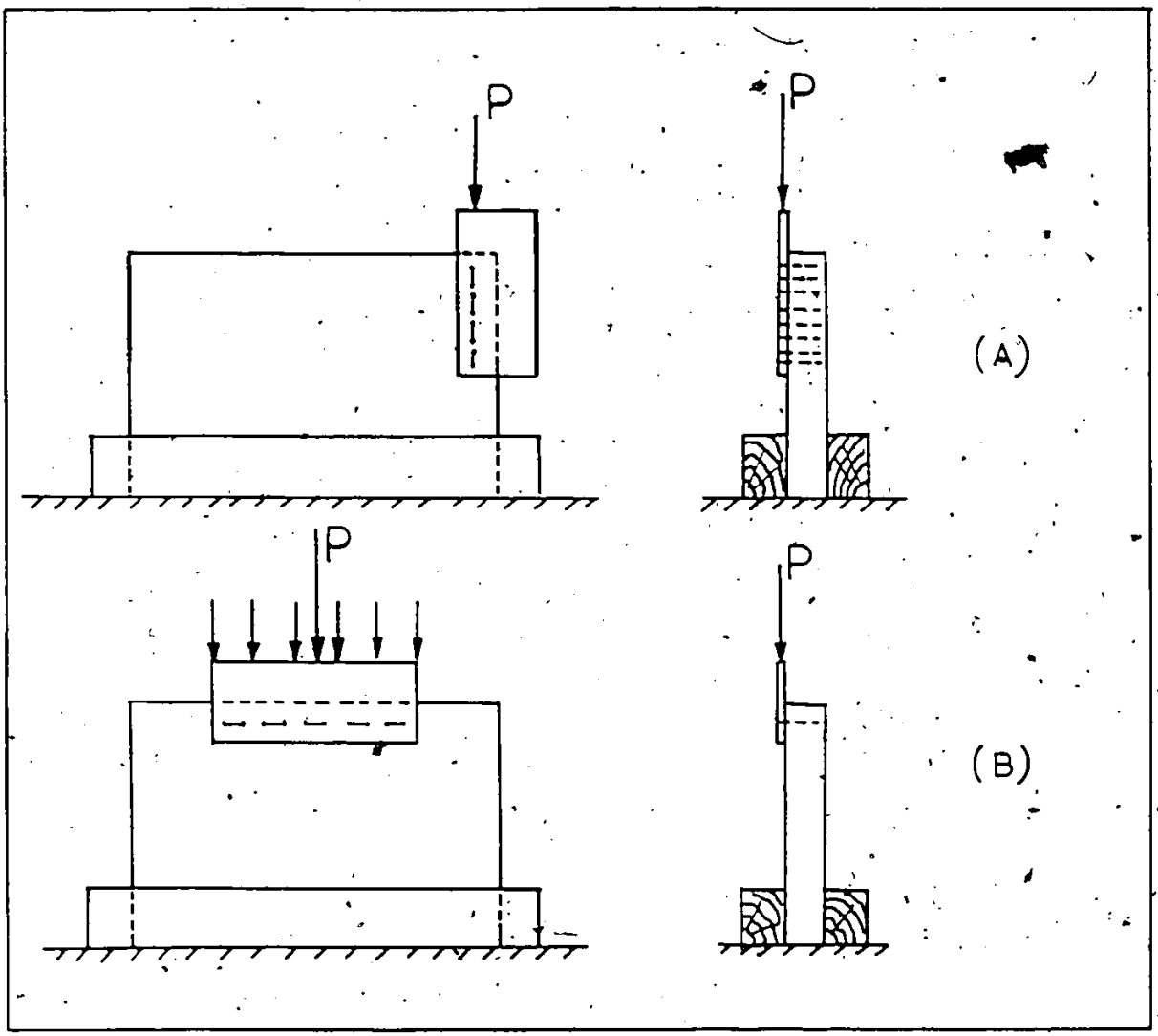


FIG. 3.9 – TESTING ARRANGEMENT FOR THE INVESTIGATION OF THE STAPLE BEHAVIOUR.

(A) LOAD APPLIED IN THE DIRECTION OF THE STAPLE LINE

(B) LOAD APPLIED PERPENDICULAR TO THE DIRECTION OF THE STAPLE LINE.

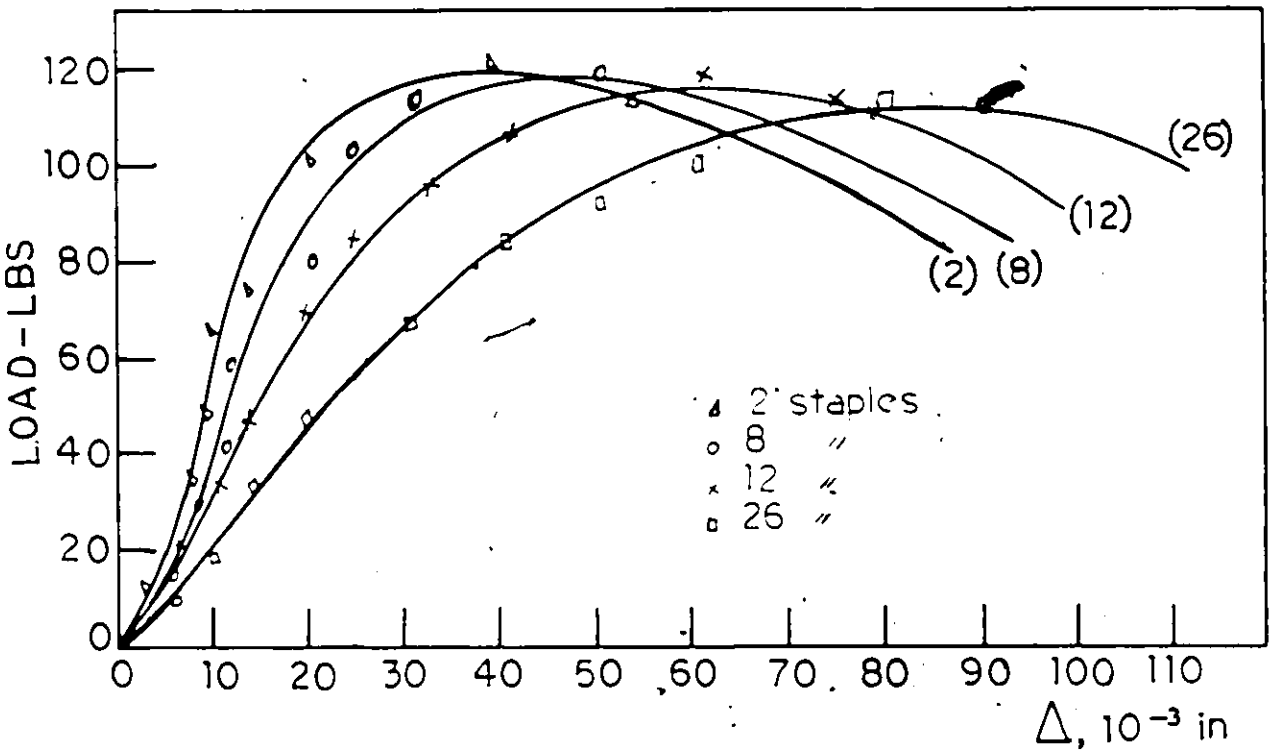


FIG. 3.10 - LOAD PER STAPLE LEG VERSUS THE DEFORMATION FOR DIFFERENT NUMBER OF STAPLES IN A ROW (AS SHOWN) WITHOUT PLYWOOD FILLER SUBJECTED TO LOAD IN THE DIRECTION OF THE STAPLE LINE.

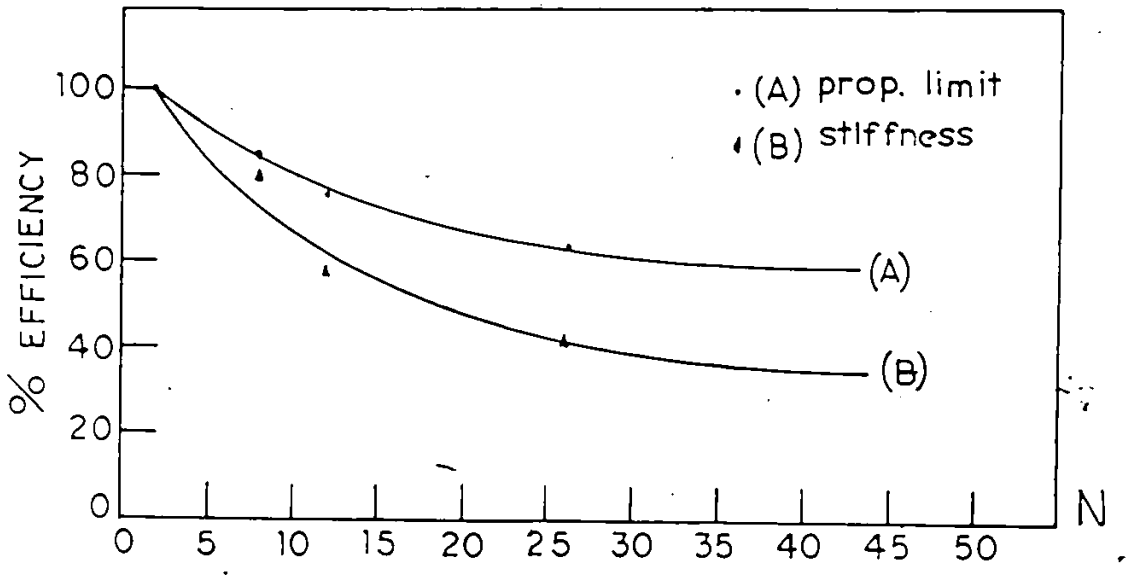


FIG. 3.11 - PERGENT EFFICIENCY PER STAPLE LEG RELATIVE TO TWO STAPLES VERSUS THE NUMBER OF STAPLES. FOR STAPLES WITHOUT PLYWOOD FILLER SUBJECTED TO LOAD IN THE DIRECTION OF THE STAPLE LINE.

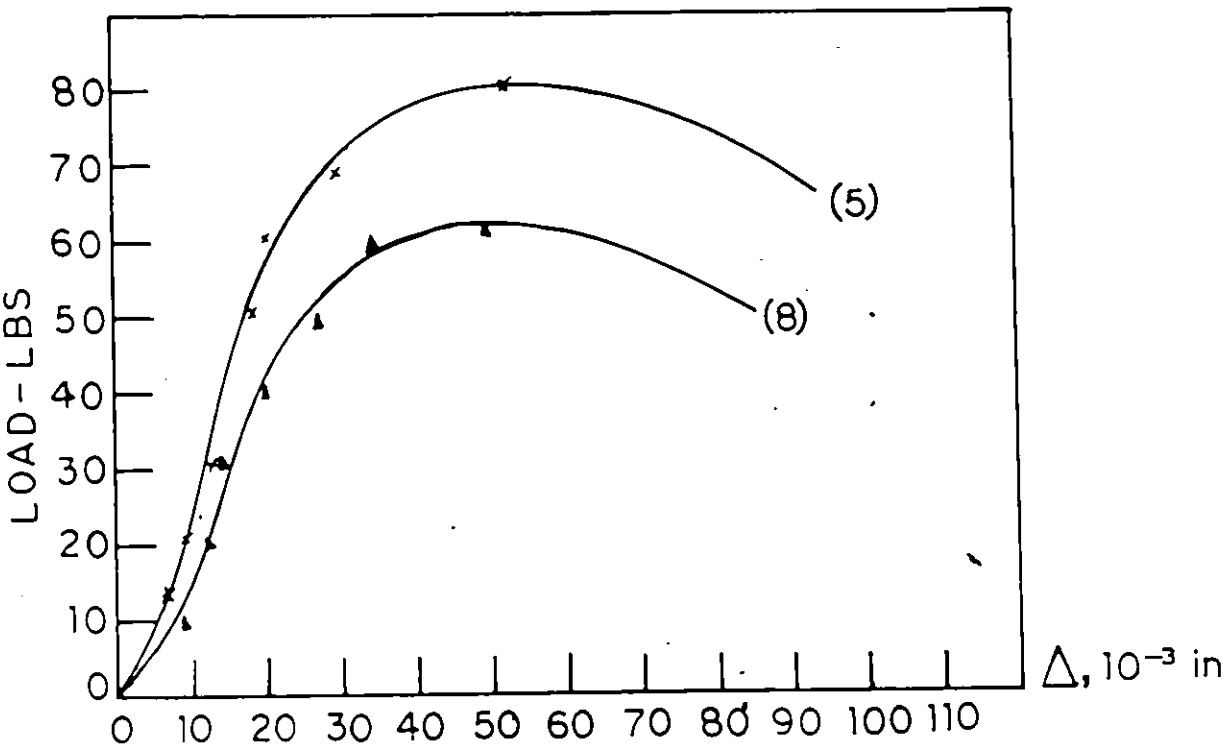


FIG. 3.12 - LOAD PER STAPLE LEG VERSUS THE DEFORMATION FOR DIFFERENT NUMBER OF STAPLES IN A ROW (AS SHOWN) WITH PLYWOOD FILLER SUBJECTED TO LOAD IN THE DIRECTION OF THE STAPLE LINE.

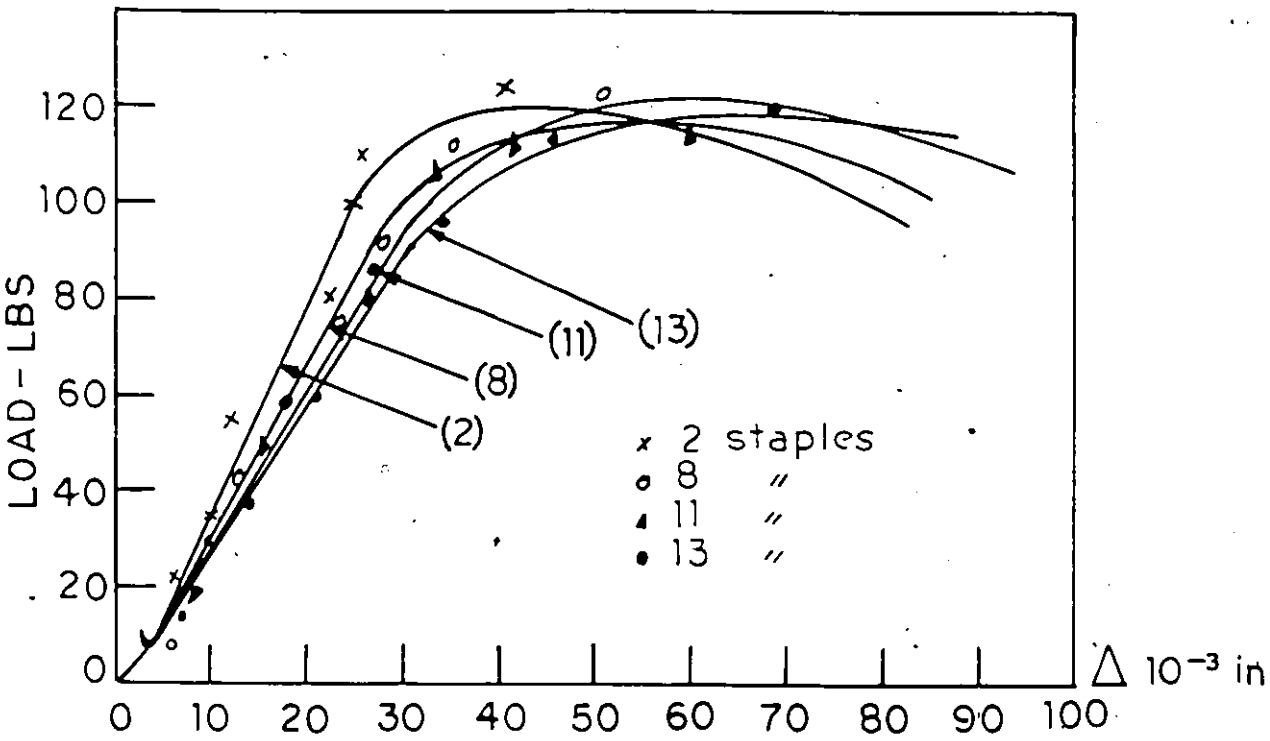


FIG. 3.13 - LOAD PER STAPLE LEG VERSUS THE DEFORMATION FOR DIFFERENT NUMBER OF STAPLES IN A ROW (AS SHOWN) WITHOUT PLYWOOD FILLER SUBJECTED TO LOAD PERPENDICULAR TO THE STAPLE LINE.

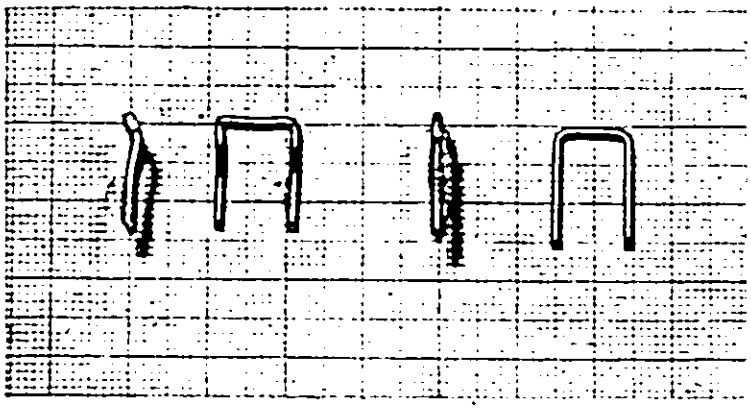

(A)

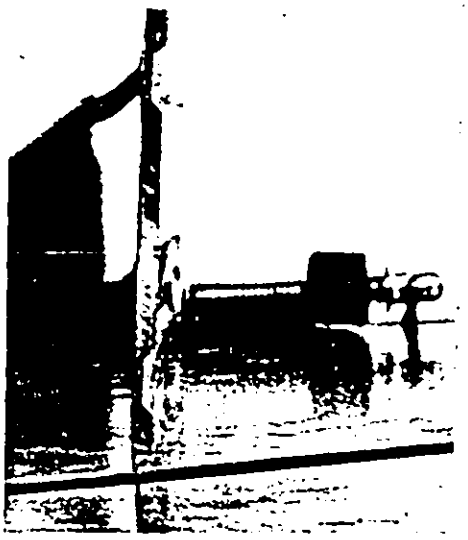

(B)

(C)

FIG. 3.14

A) Comparison of a staple after it pulled out (left) with an unused staple (right).

B) Staples deformed after having pulled out subjected to load perpendicular to line of staples.

C) Staples deformed after having pulled out subjected to load in the direction of staple line.

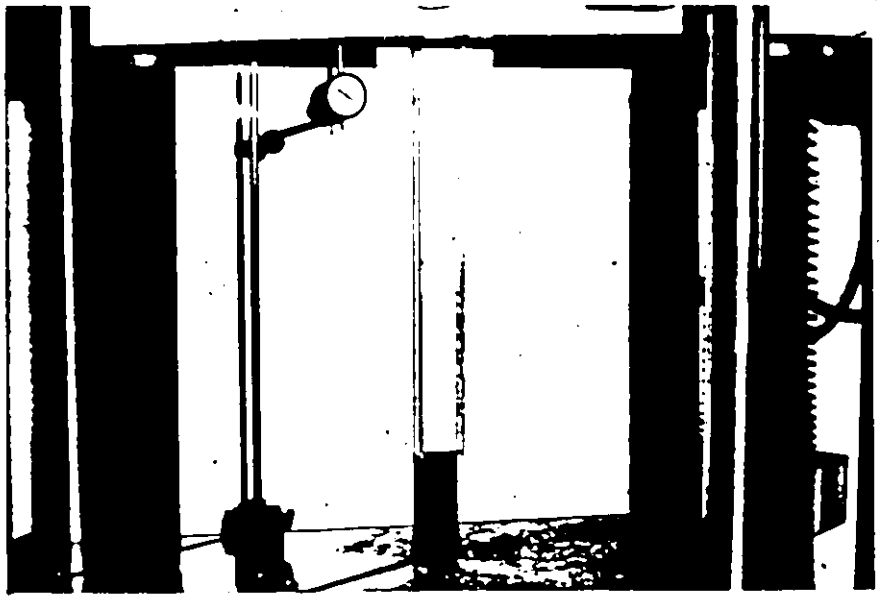

FIG. 3.15 - TESTING ARRANGEMENT FOR THE SHEAR TEST

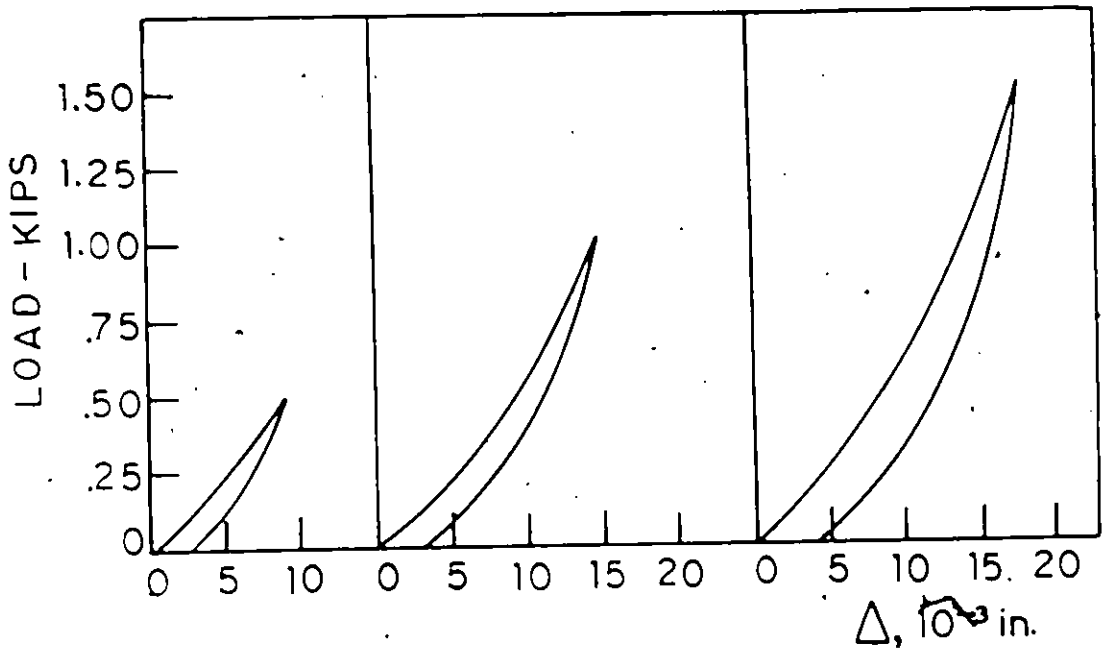


FIG. 3.16 - BEHAVIOUR OF THE CONNECTION IN LOADING AND UNLOADING UNDER SHEAR

NOTE: Different paths are followed in loading and unloading, with a permanent deformation left after the connection has been unloaded.

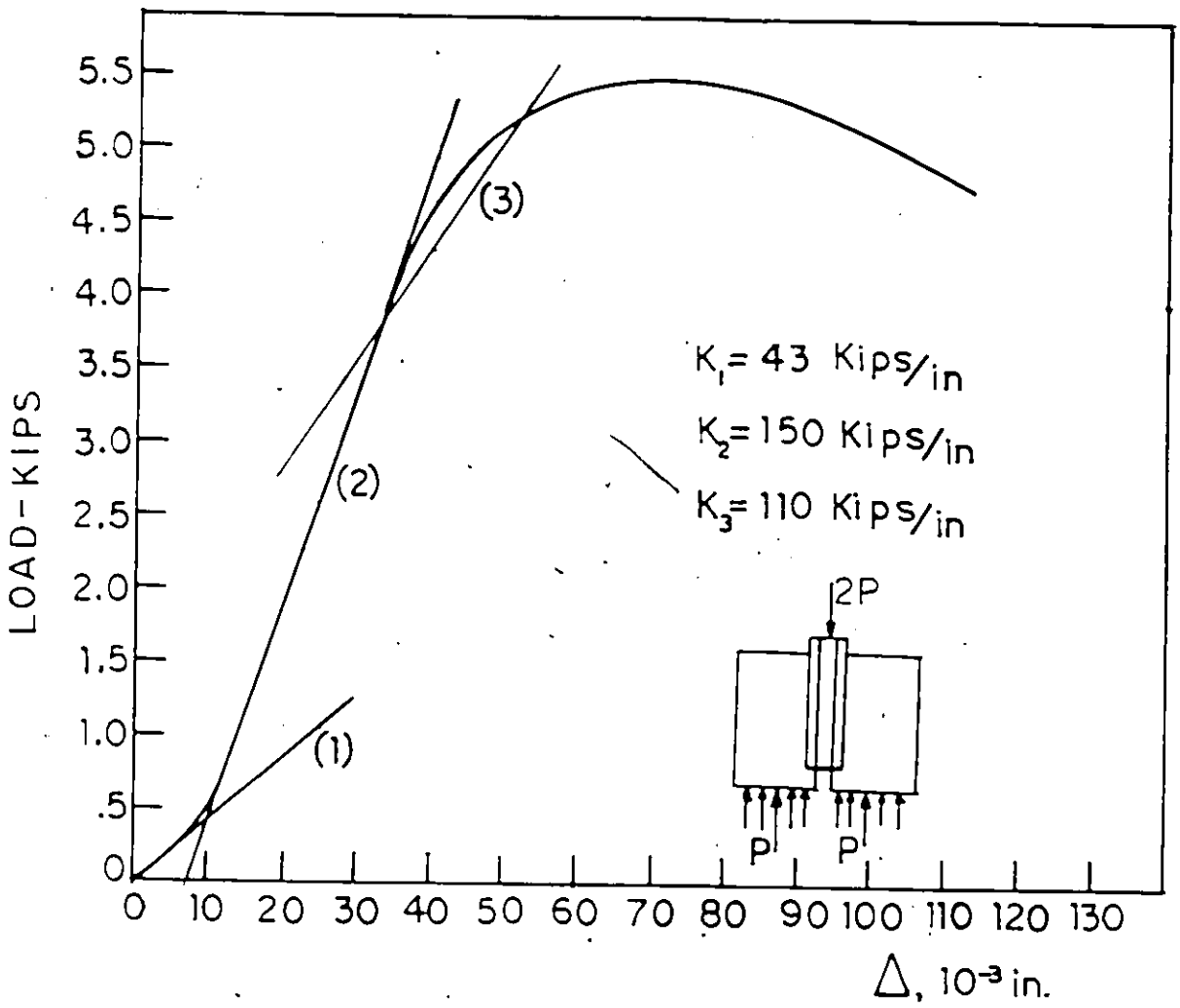


FIG. 3.17 - LOAD (P)-DEFORMATION (Δ) CURVE OF THE CONNECTION UNDER SHEAR

NOTE: The failure was reached with the staples pulling out. The curve can be approximated with three straight lines, the slopes of which are shown.

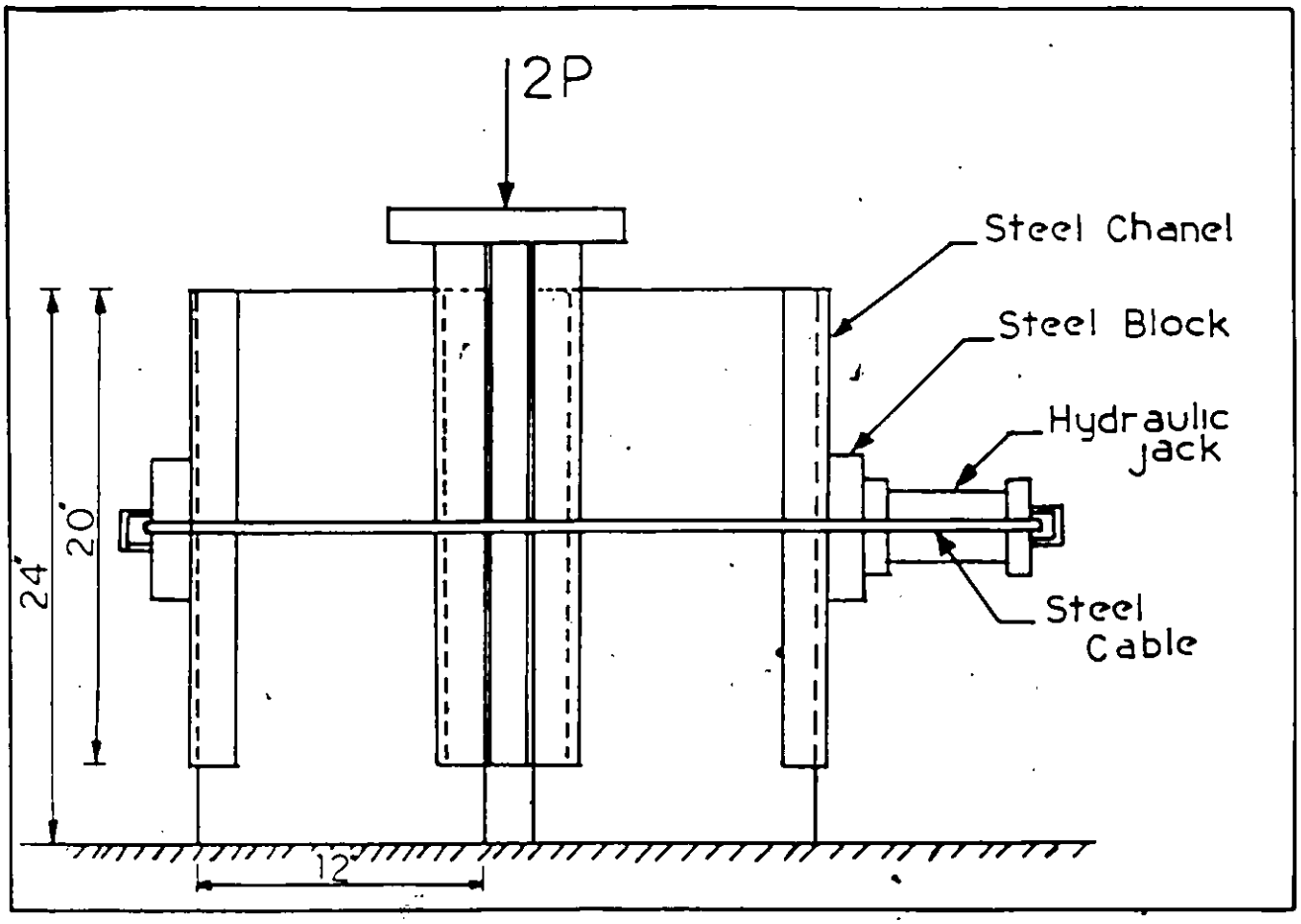


FIG. 3.18 - TESTING ARRANGEMENT FOR COMBINED SHEAR AND NORMAL LOAD

NOTE: The normal load was applied with the hydraulis jack and kept constant while the shear load was varied.

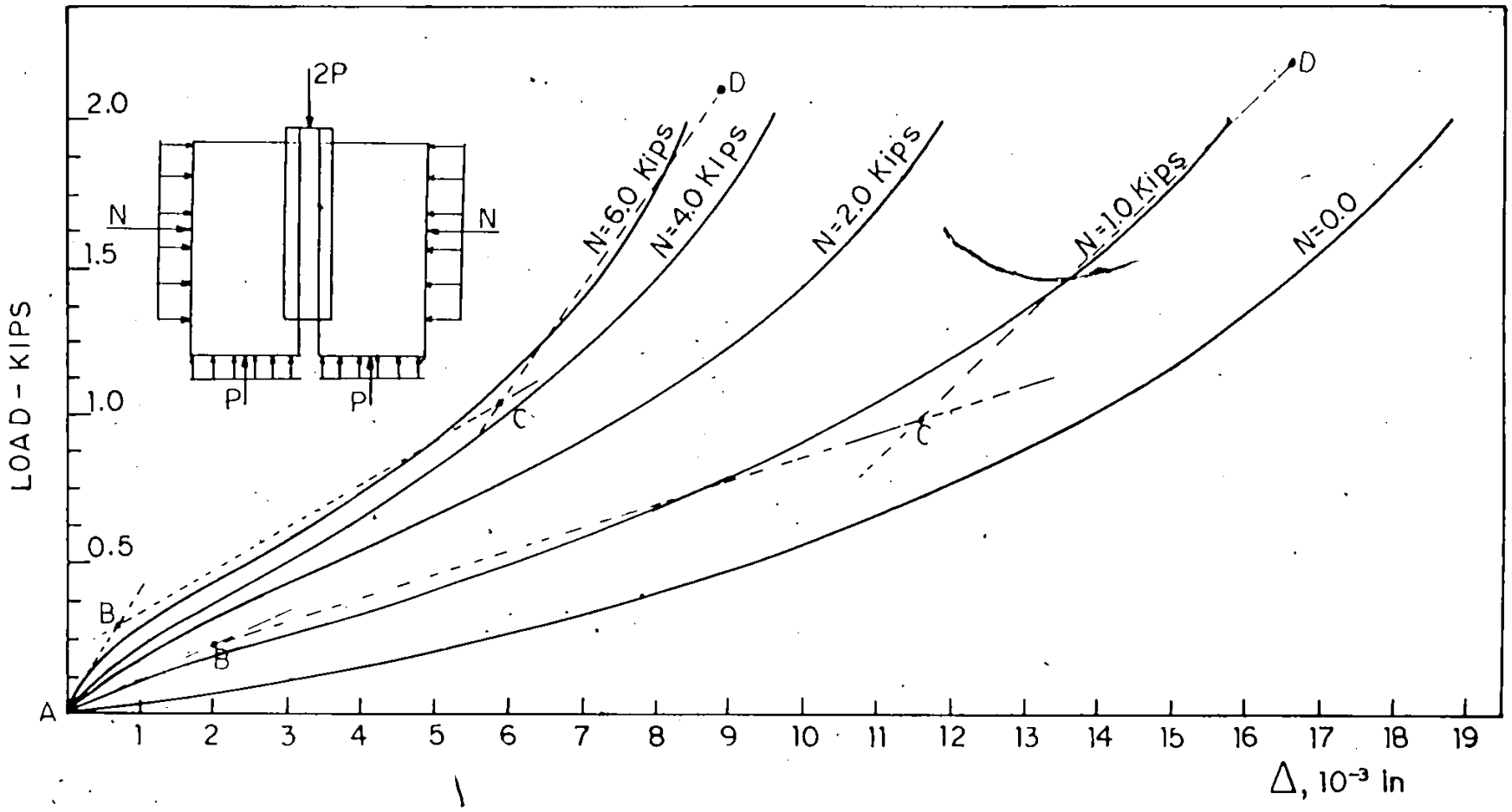


FIG. 3.19 - LOAD (P) -DEFORMATION (Δ) CURVES FOR COMBINED SHEAR (P) AND NORMAL LOAD (N)

NOTE: Each curve represents one value of the normal load (N).

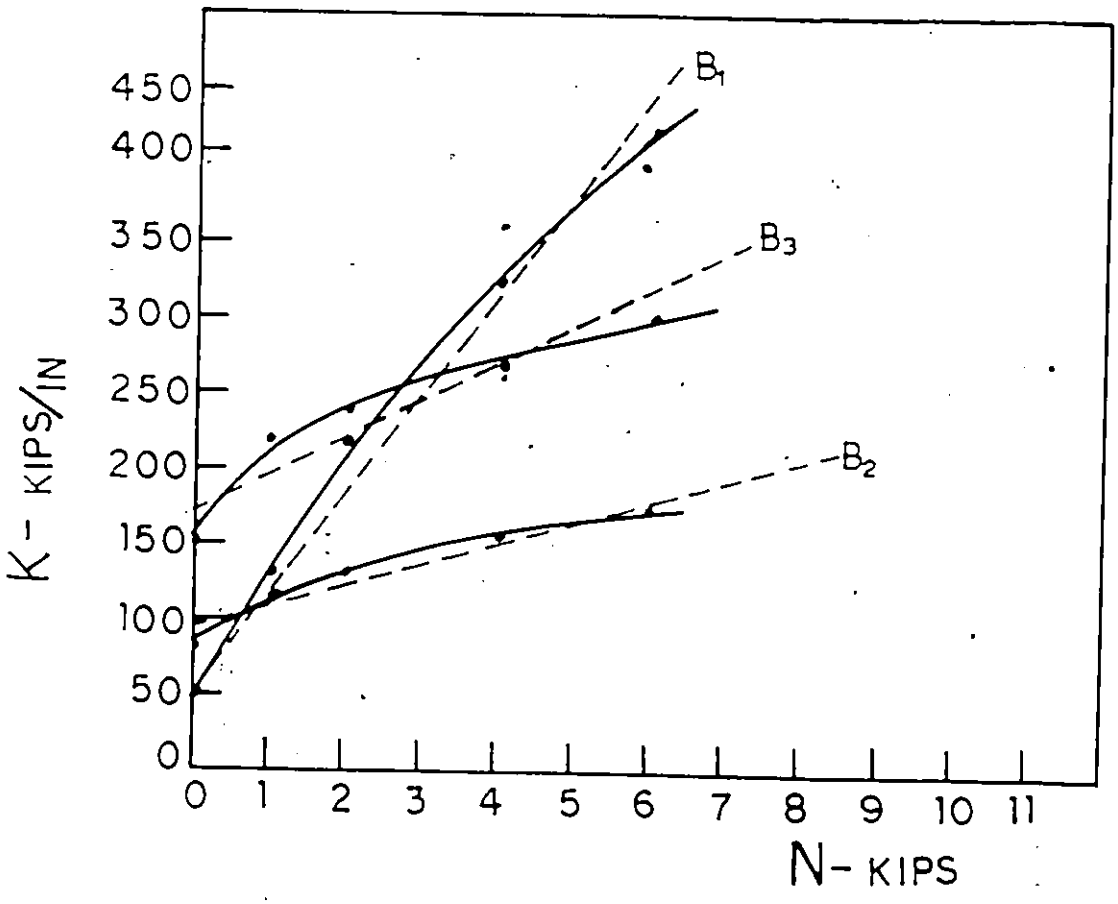


FIG. 3.20 - VARIATION OF THE STIFFNESS OF THE CONNECTION WITH THE NORMAL LOAD

NOTE: The three curves shown for the variation of the slopes, of the load deformation curves, with the normal load were derived after the load deformation curves of Fig. 3.19 were approximated with three straight lines.

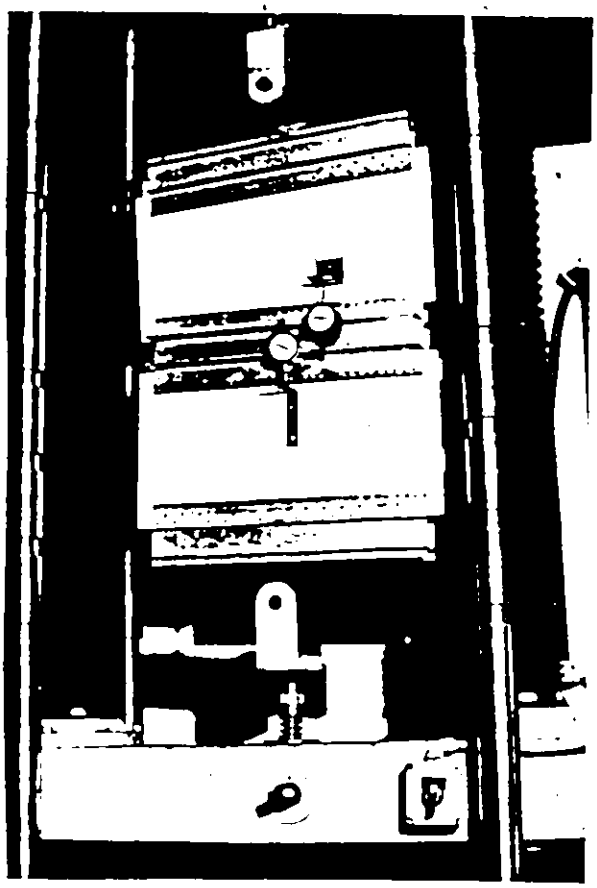

FIG. 3.21 - TESTING ARRANGEMENT FOR TENSION

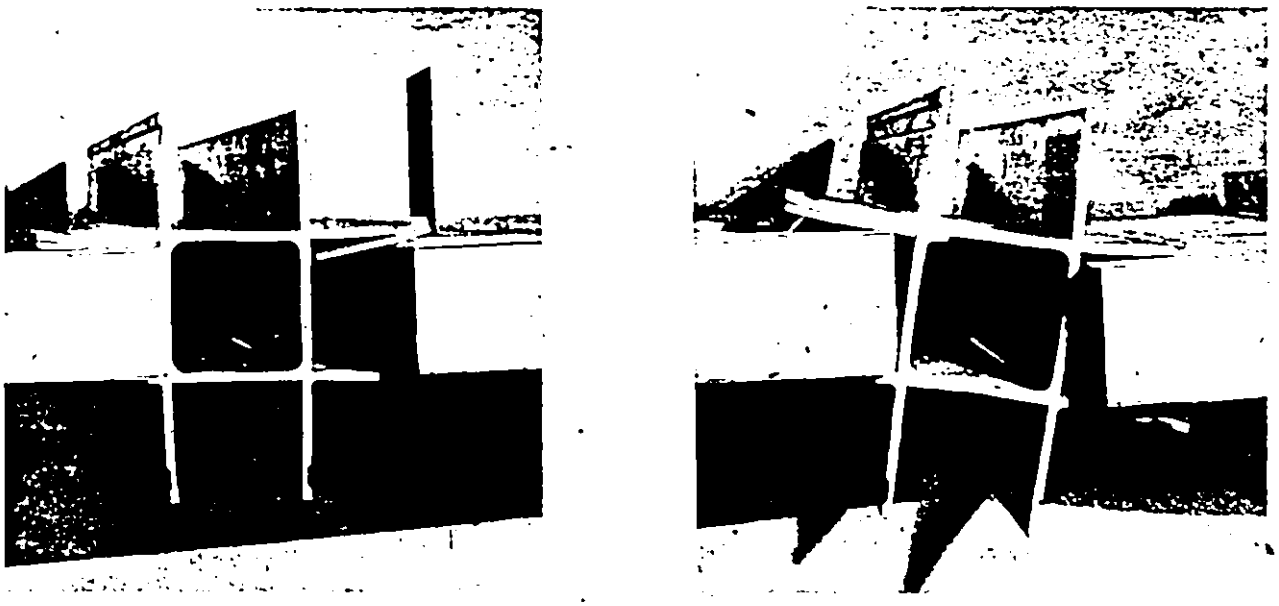

(A) (B)

FIG. 3.22 - FAILURE PATTERNS OF CONNECTIONS UNDER TENSION. (A) BOTH PLYWOOD FILLERS ON THE SAME SIDE OF CONNECTION, (B) FILLERS ON OPPOSITE SIDES OF CONNECTION.

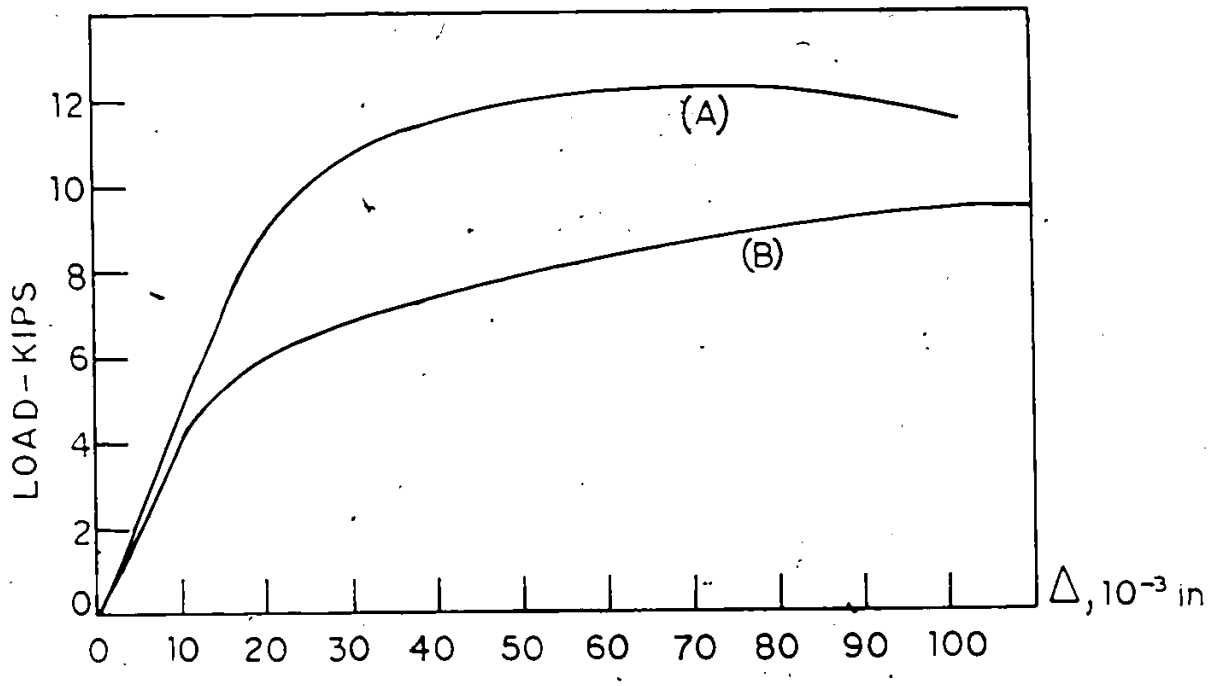


FIG. 3.23 - LOAD (P) - DEFORMATION (Δ) CURVES FOR THE CONNECTIONS UNDER TENSION

NOTE: Curve (A) is for the connection with both plowood fillers on the same side and curve (B) is for the connection with the fillers on opposite sides.

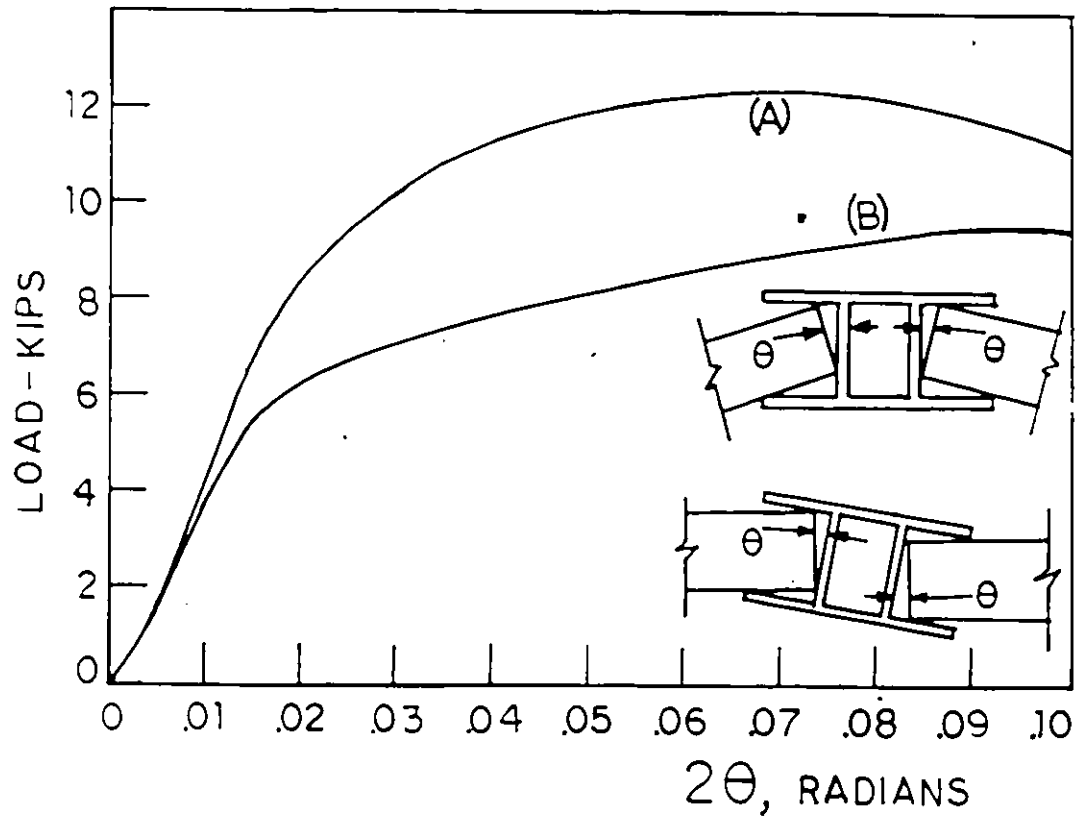


FIG. 3.24 - LOAD (P) - TOTAL ROTATION (2θ) CURVES FOR THE CONNECTIONS UNDER TENSION.

NOTE: Curve (A) is for the connection with both plywood fillers on the same side and curve (B) is for the connection with the fillers on opposide sides.

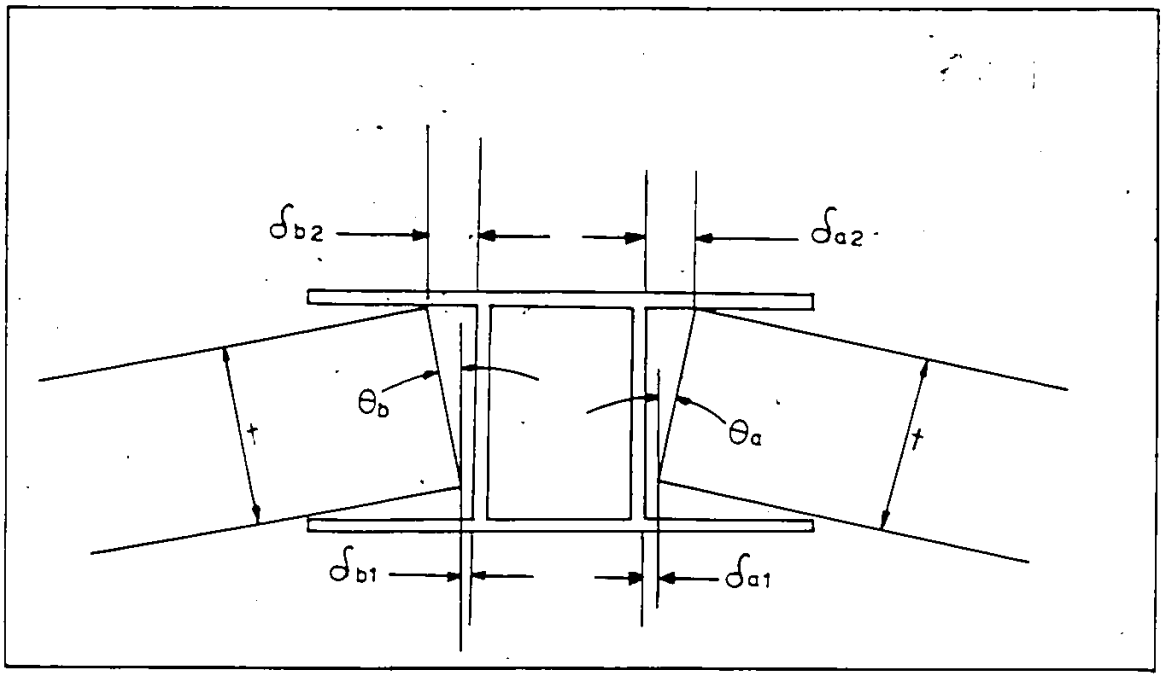


Measured $\delta a1$, $\delta a2$, $\delta b1$, $\delta b2$

$$\delta a = \frac{\delta a1 + \delta a2}{2} \qquad \delta b = \frac{\delta b1 + \delta b2}{2}$$

$$\Delta = \frac{\delta a + \delta b}{2}$$

$$\theta a = \frac{\delta a2 - \delta a1}{t} \qquad \theta b = \frac{\delta b2 - \delta b1}{t}$$

$$2\theta = \theta a + \theta b$$

FIG. 3.25 - CALCULATIONS OF THE DEFORMATIONS FROM THE MEASUREMENTS FOR THE TENSION TEST

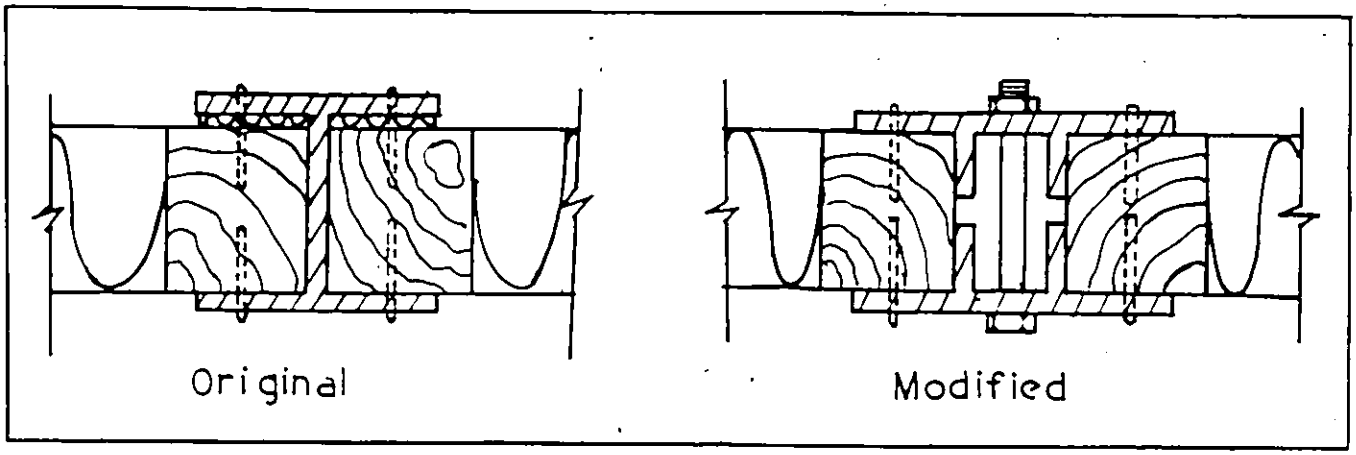


FIG. 3.26 - COMPARISON OF THE ORIGINAL AND THE MODIFIED CONNECTION

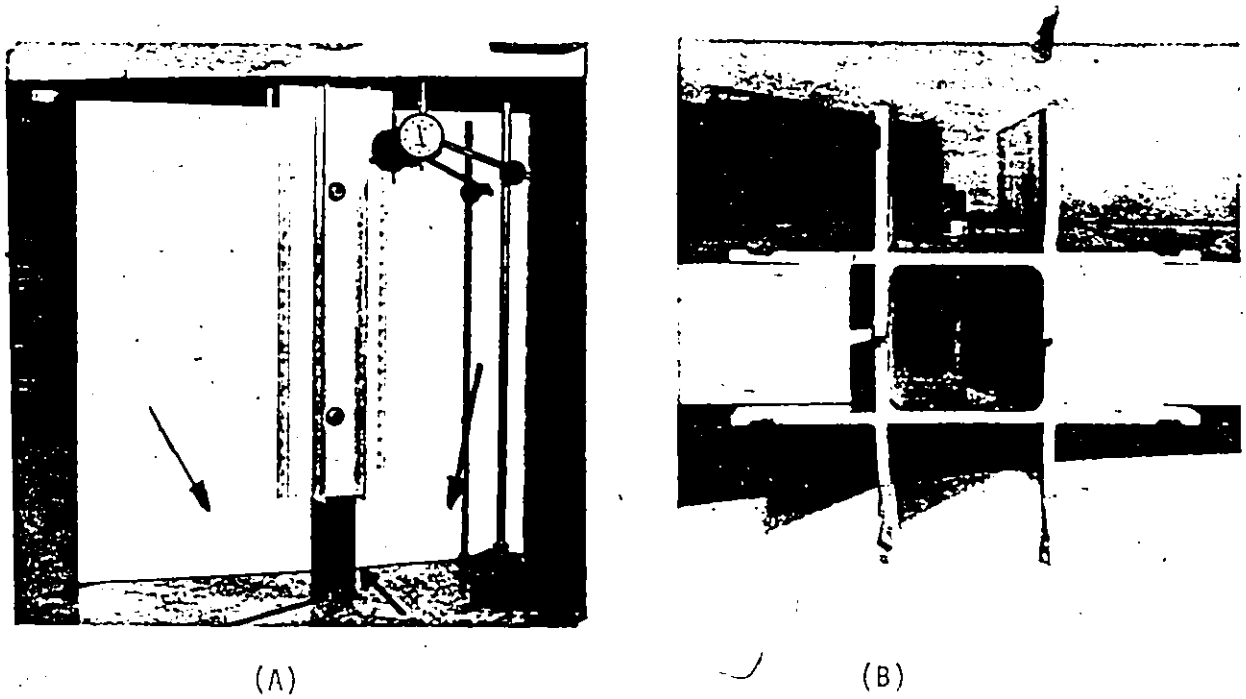

(A) (B)

FIG. 3.27

(A) Testing arrangement of the modified connection under shear.

(B) Cross section of the modified connection.

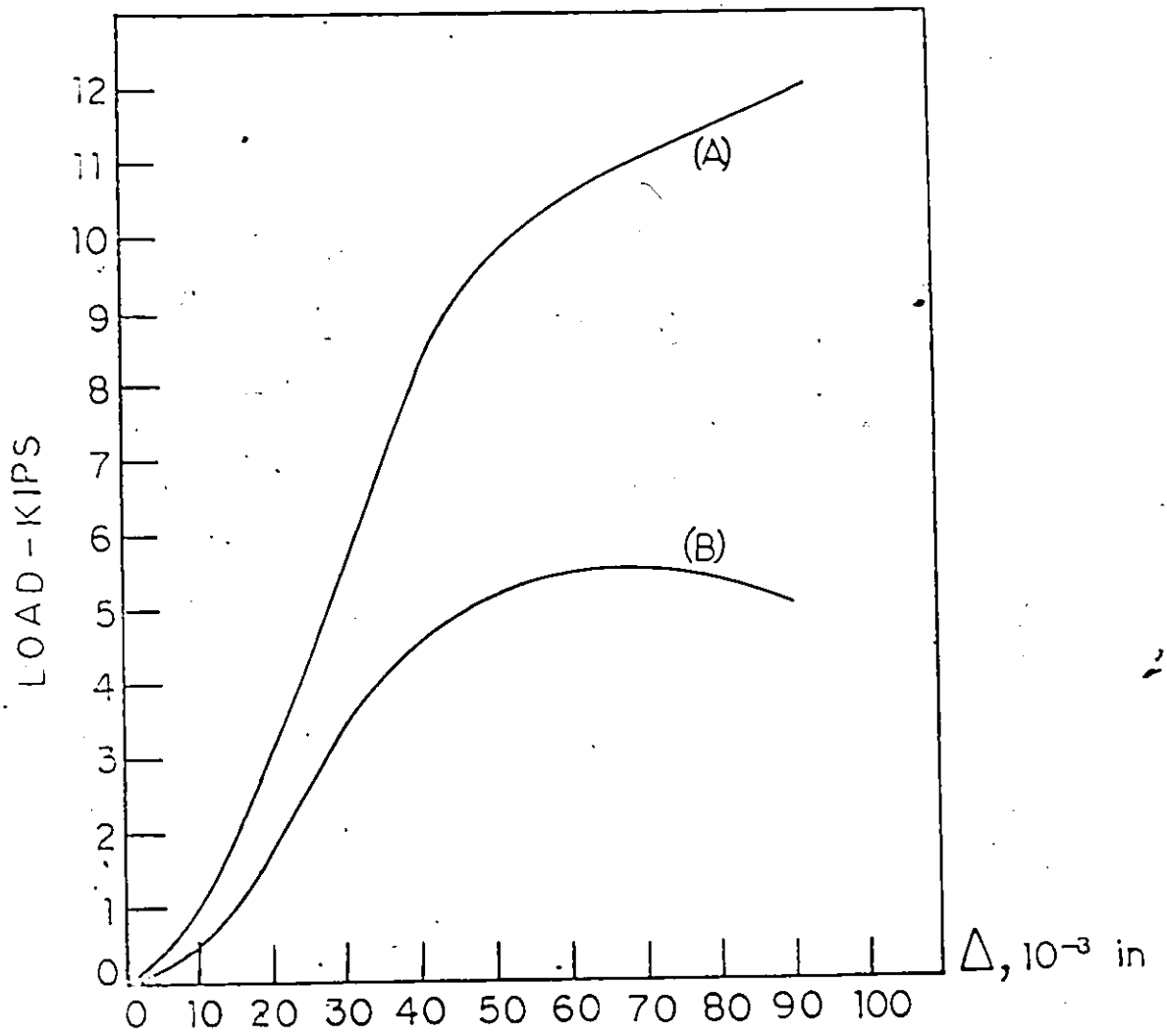


FIG. 3.28 - LOAD - DEFORMATION CURVES FOR THE MODIFIED (A) AND THE ORIGINAL (B) CONNECTIONS

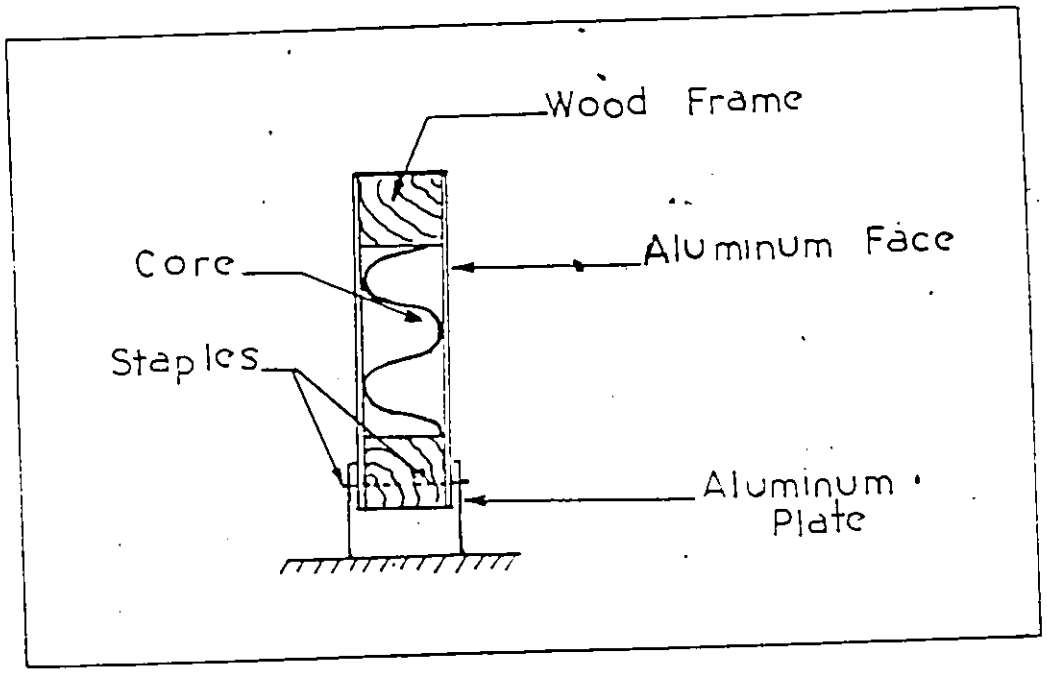


FIG. 4.1 - PICTORIAL CROSS SECTION OF THE CONNECTION JOINING THE PANEL TO THE ALUMINIUM EXTRUSION

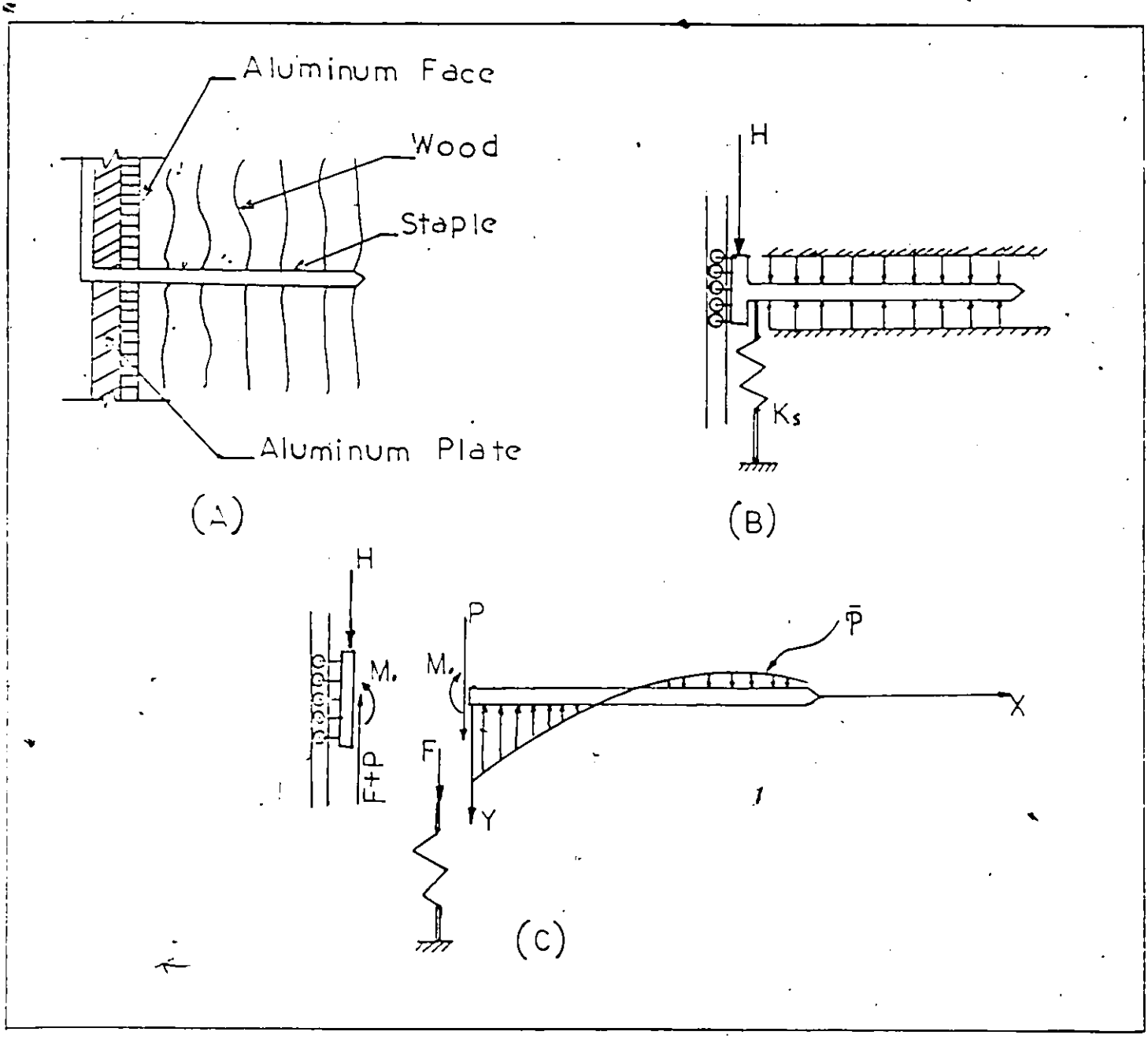


FIG. 4.2 - MODEL FOR THE STAPLE LEG

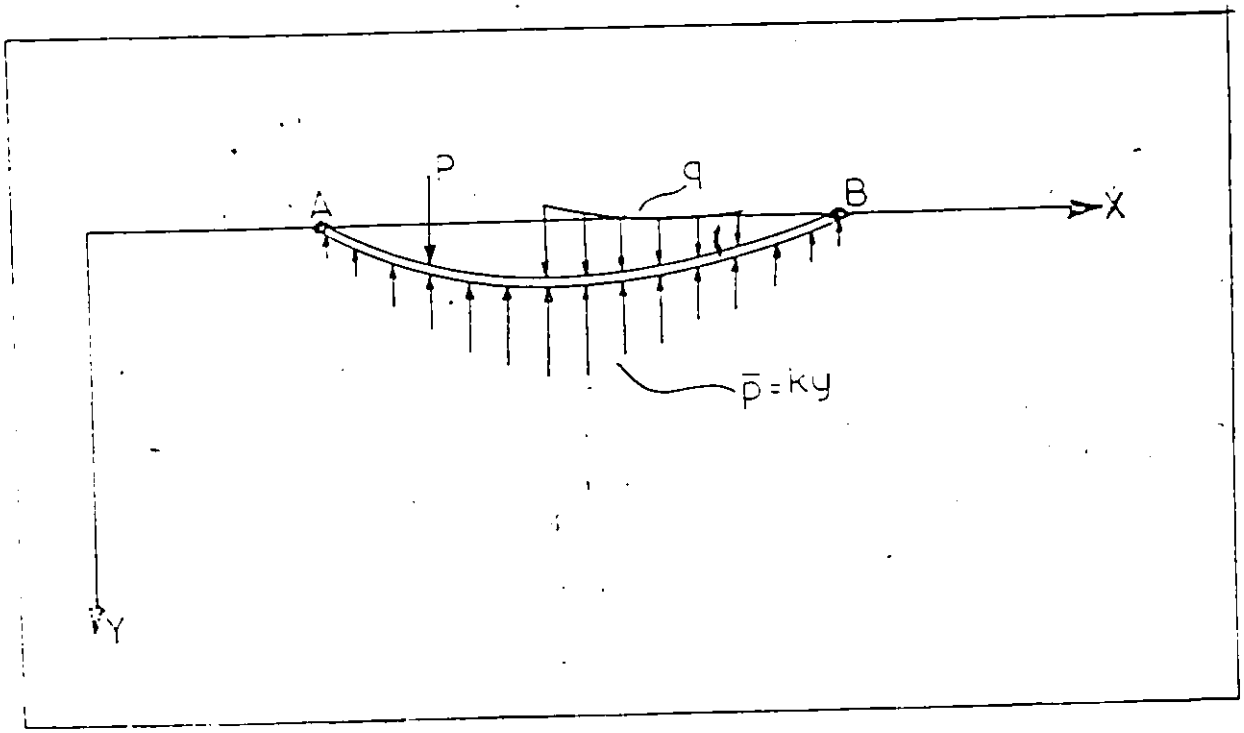


FIG. 4.3 - LOADED BEAM SUPPORTED BY AN ELASTIC FOUNDATION

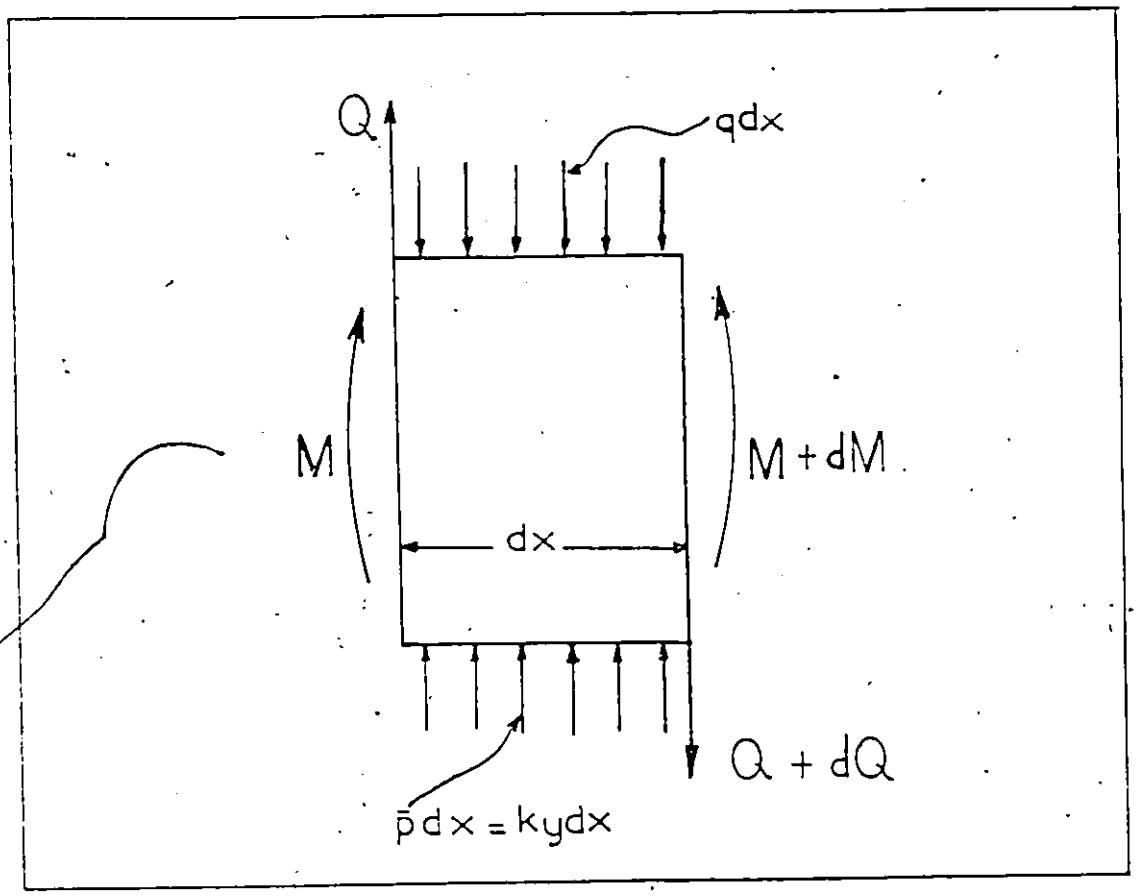


FIG. 4.4 - FORCES ACTING ON A SEGMENT OF A BEAM SUPPORTED BY AN ELASTIC FOUNDATION

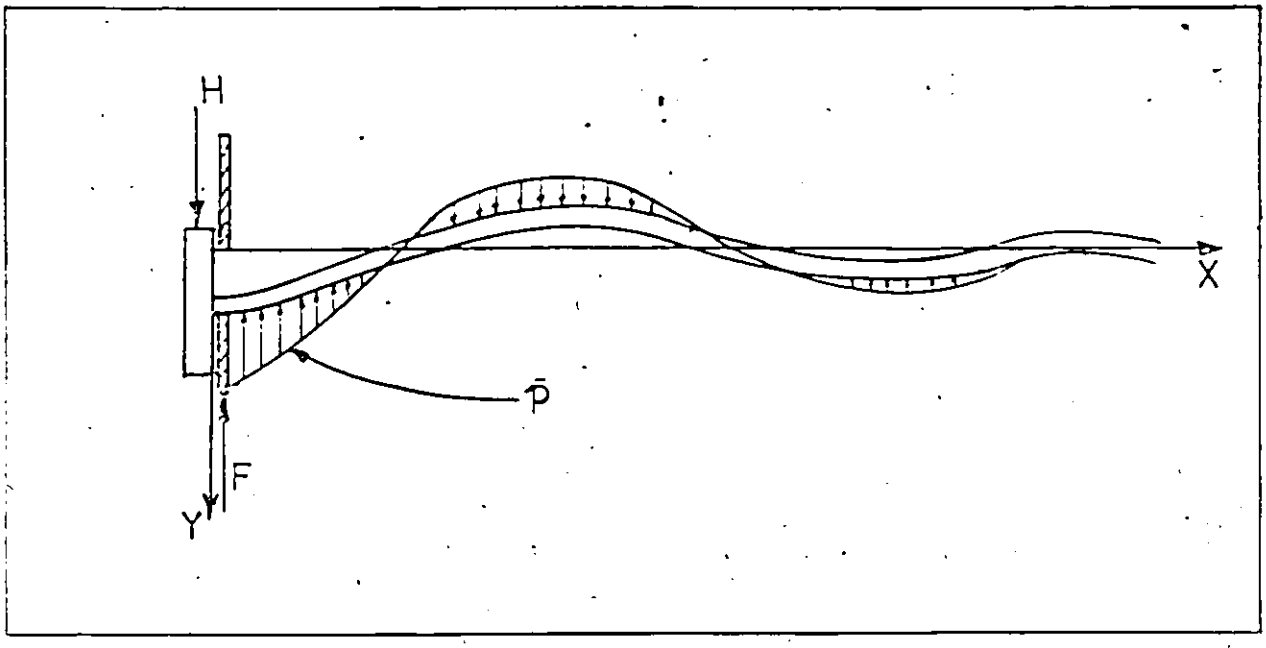


FIG. 4.5 - BEAM WITH INFINITE LENGTH SUPPORTED BY AN ELASTIC FOUNDATION

NOTE: The loaded end of the beam at x = 0.0 can translate but not rotate.

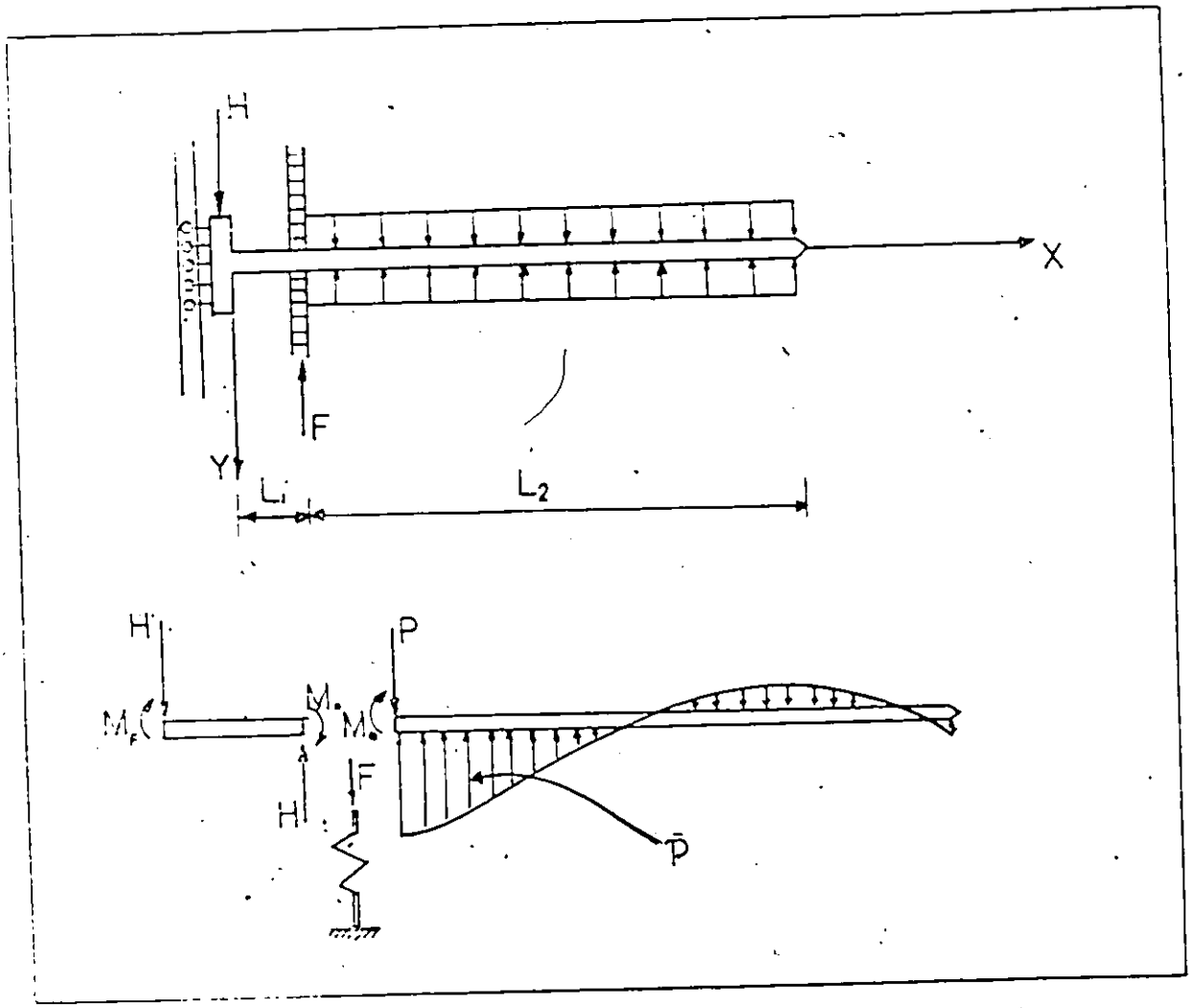


FIG. 4.6 - BEAM OF FINITE LENGTH WITH AN OVERHANG

NOTE: The supported part of the beam lies on the elastic foundation. The end of the beam where the load is applied can translate but cannot rotate.

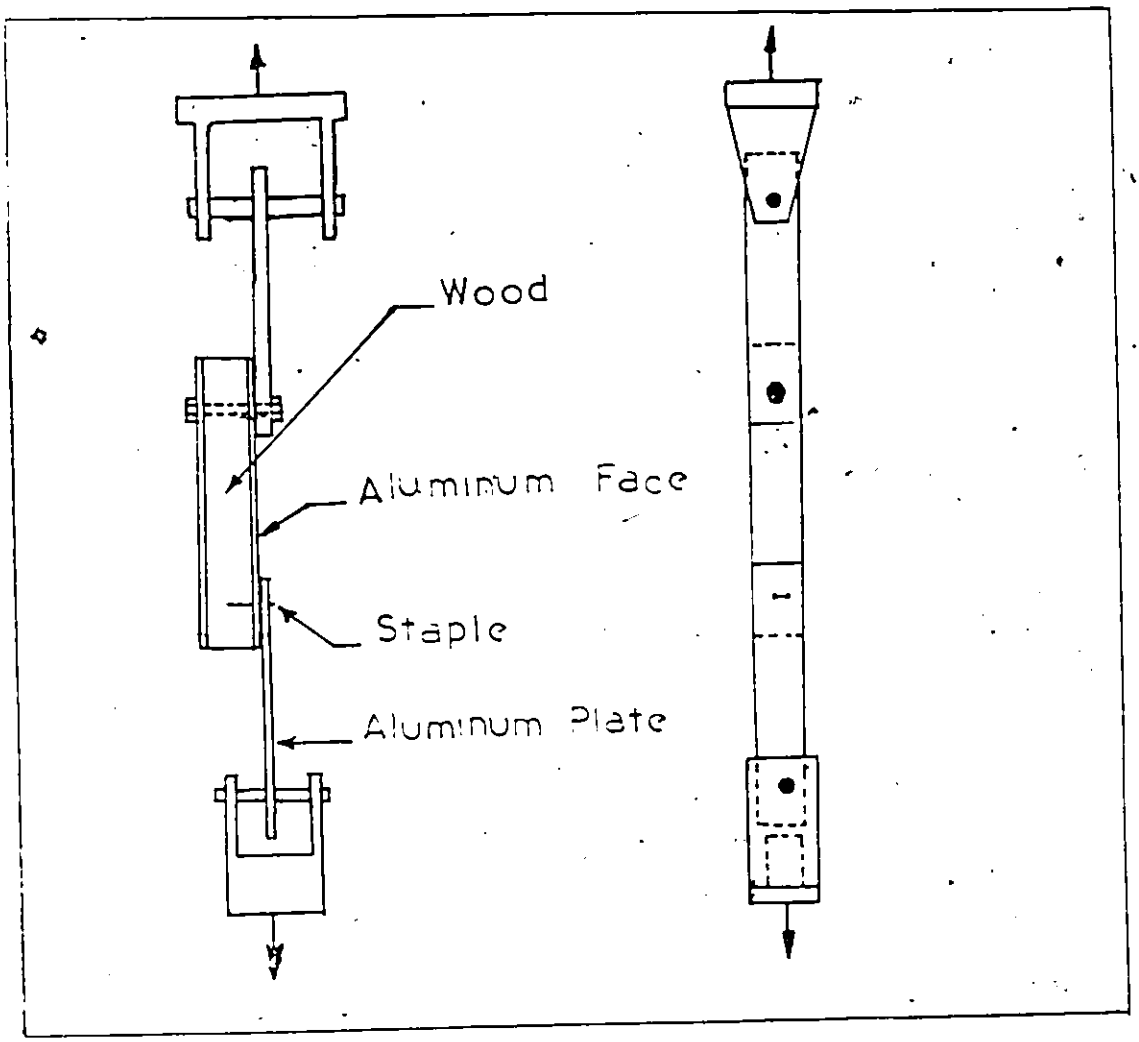


FIG. 5.1 - TESTING ARRANGEMENT FOR STAPLED CONNECTION TO DETERMINE THE EFFECT OF PARAMETERS VARIATION

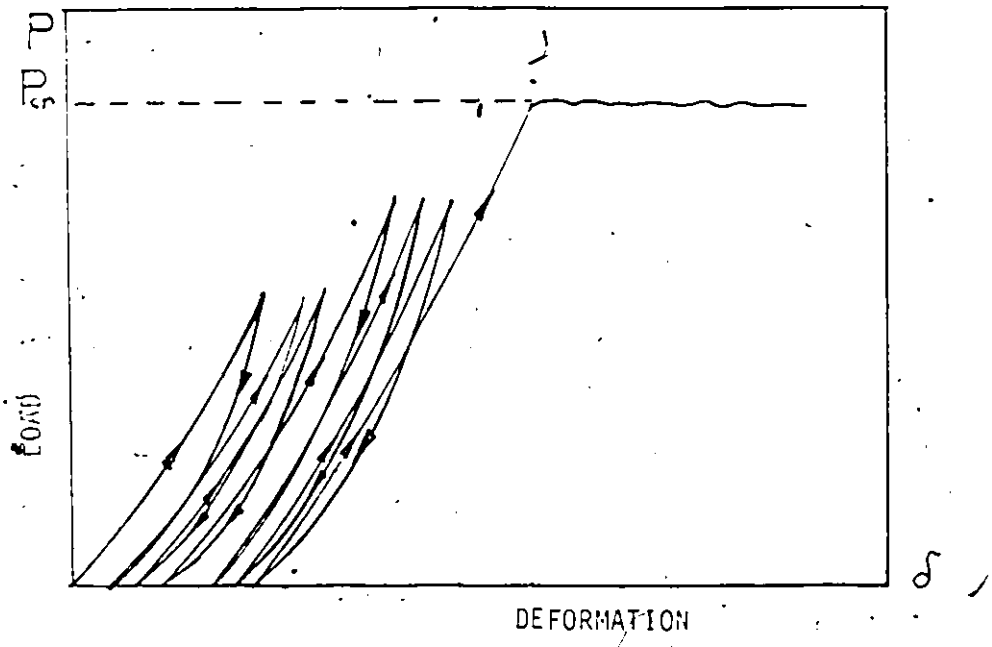


FIG. 5.2 - TYPICAL LOAD-DEFORMATION CURVES OF A STAPLED CONNECTION SUBJECTED TO CYCLES LOADING

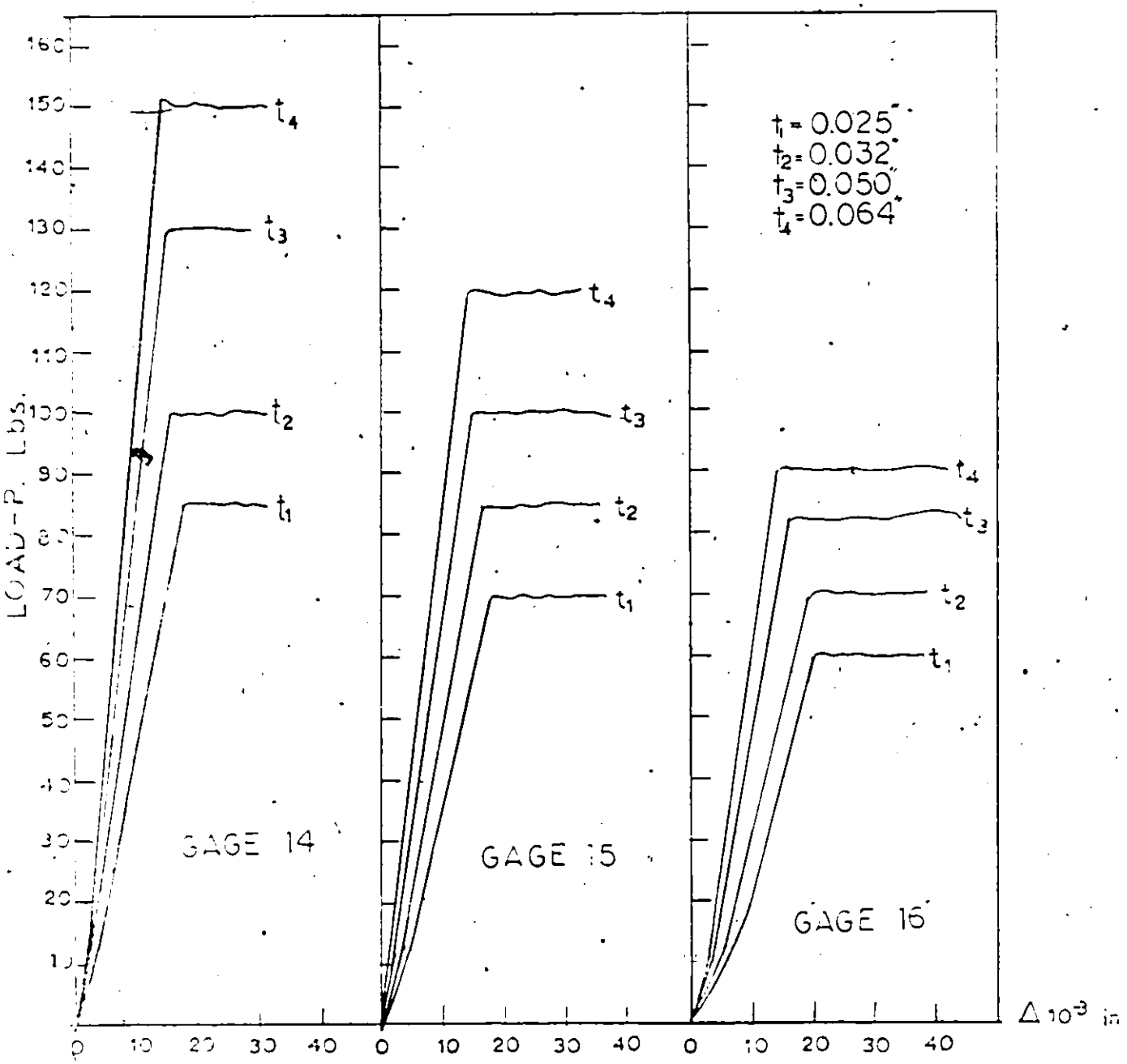


FIG. 5:3 - LOAD PER STAPLE LEG VERSUS THE DEFORMATION OF A STAPLED CONNECTION WITH VARYING STAPLE GAGE AND THICKNESS OF ALUMINIUM FACING

(a) gage 14
(b) gage 15
(c) gage 16

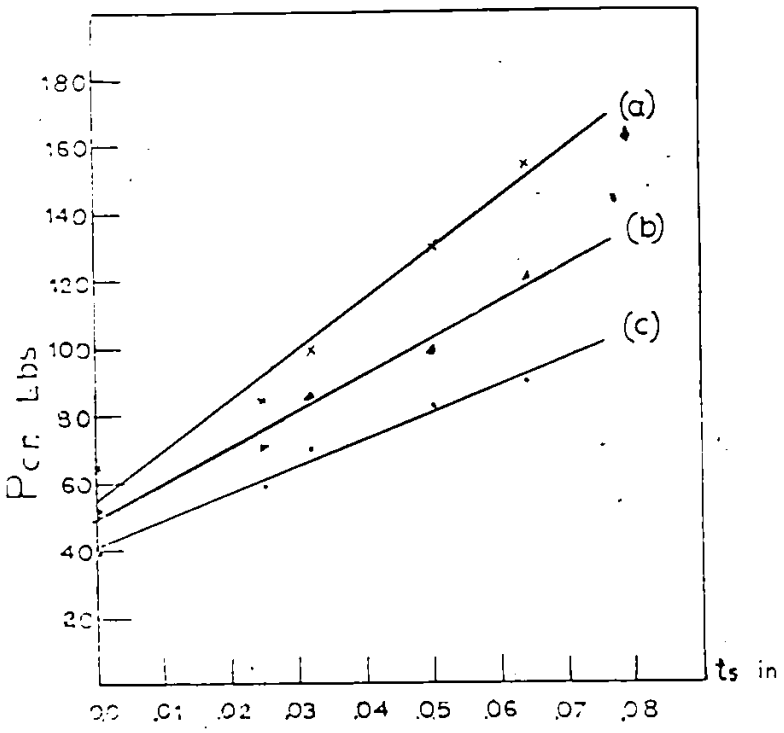


FIG. 5.4 - CREEPING LOAD PER STAPLE LEG VERSUS THE THICKNESS OF THE ALUMINIUM FOR VARIOUS STAPLE GAGES.

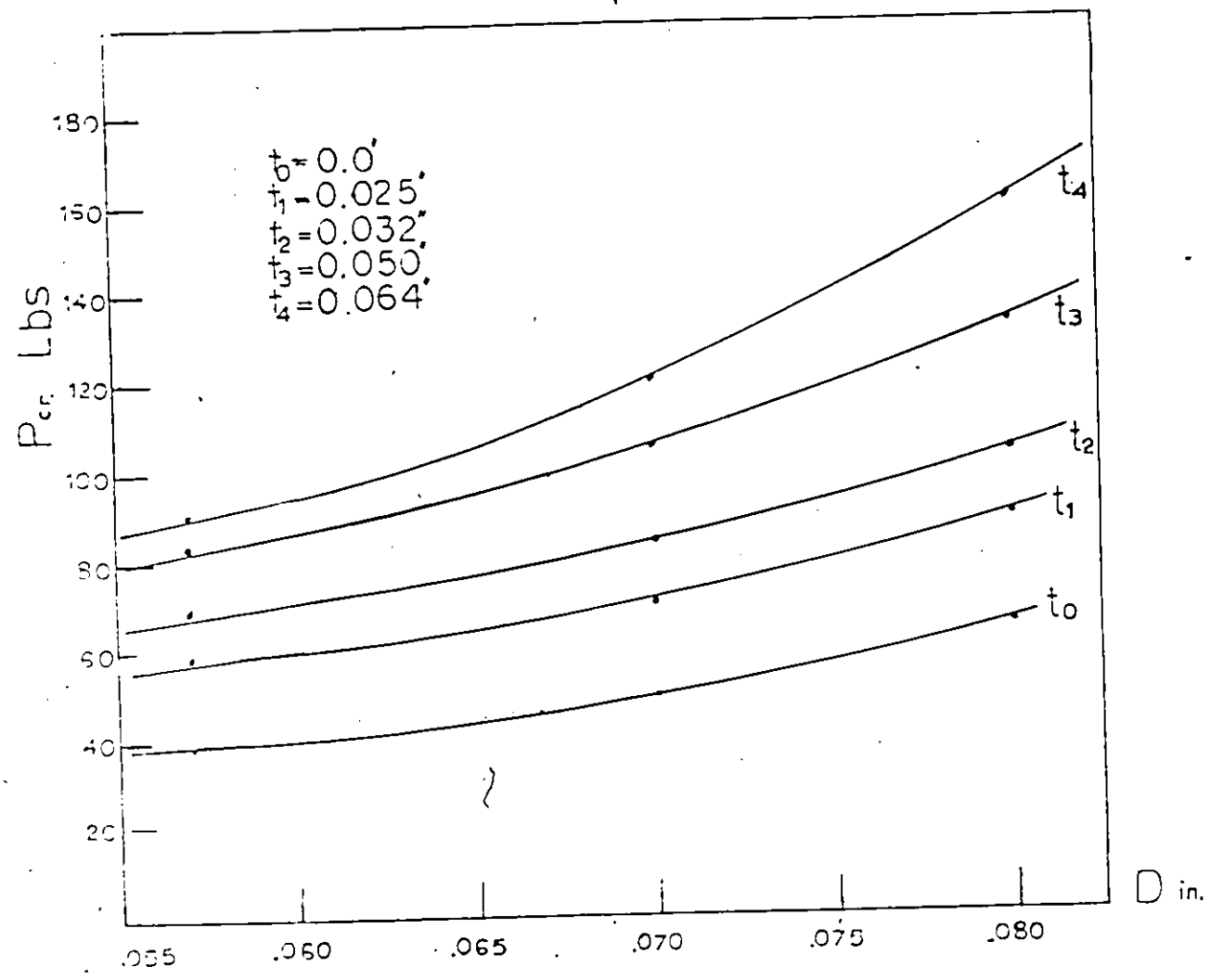


FIG. 5.5 - CREEP LOAD PER STAPLE LEG VERSUS THE STAPLE DIAMETER FOR VARIOUS ALUMINUM FACE THICKNESSES

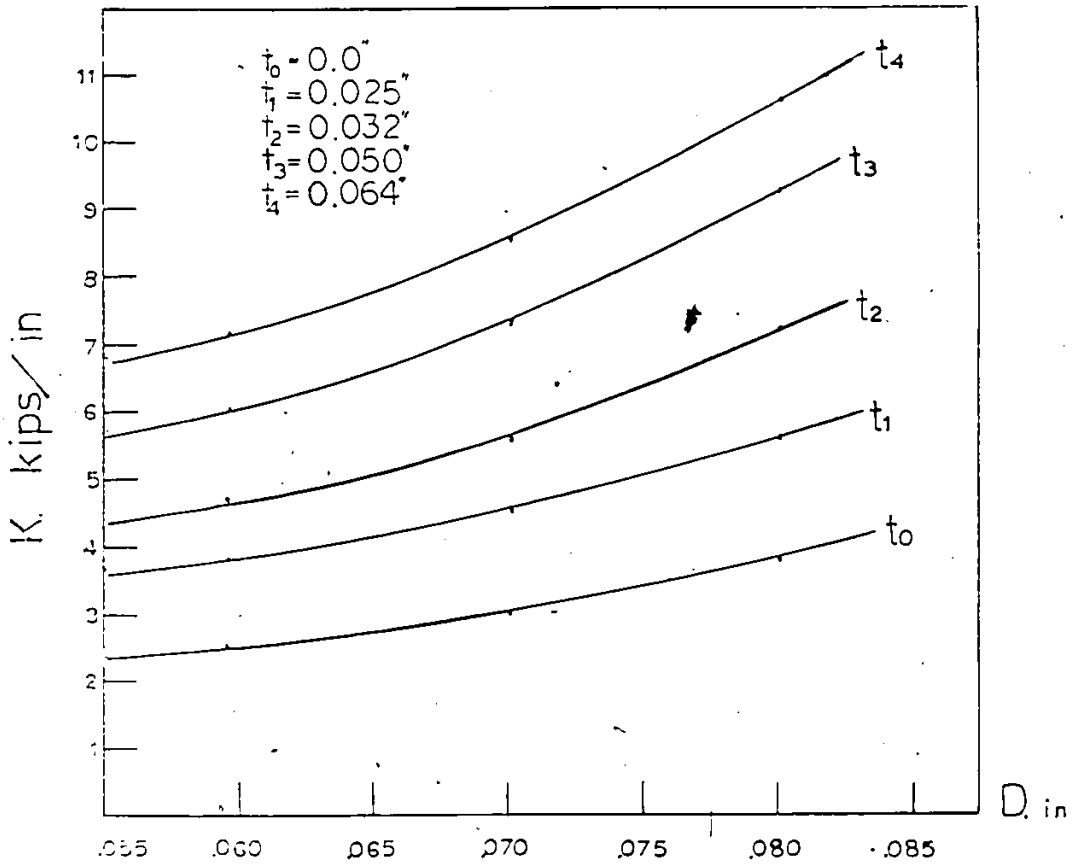


FIG. 5.6 - STIFFNESS VERSUS THE STAPLE DIAMETER FOR VARIOUS ALUMINIUM THICKNESSES -

NOTE: Stiffness is the slope of the curve: load-per-staple-leg vs deformation

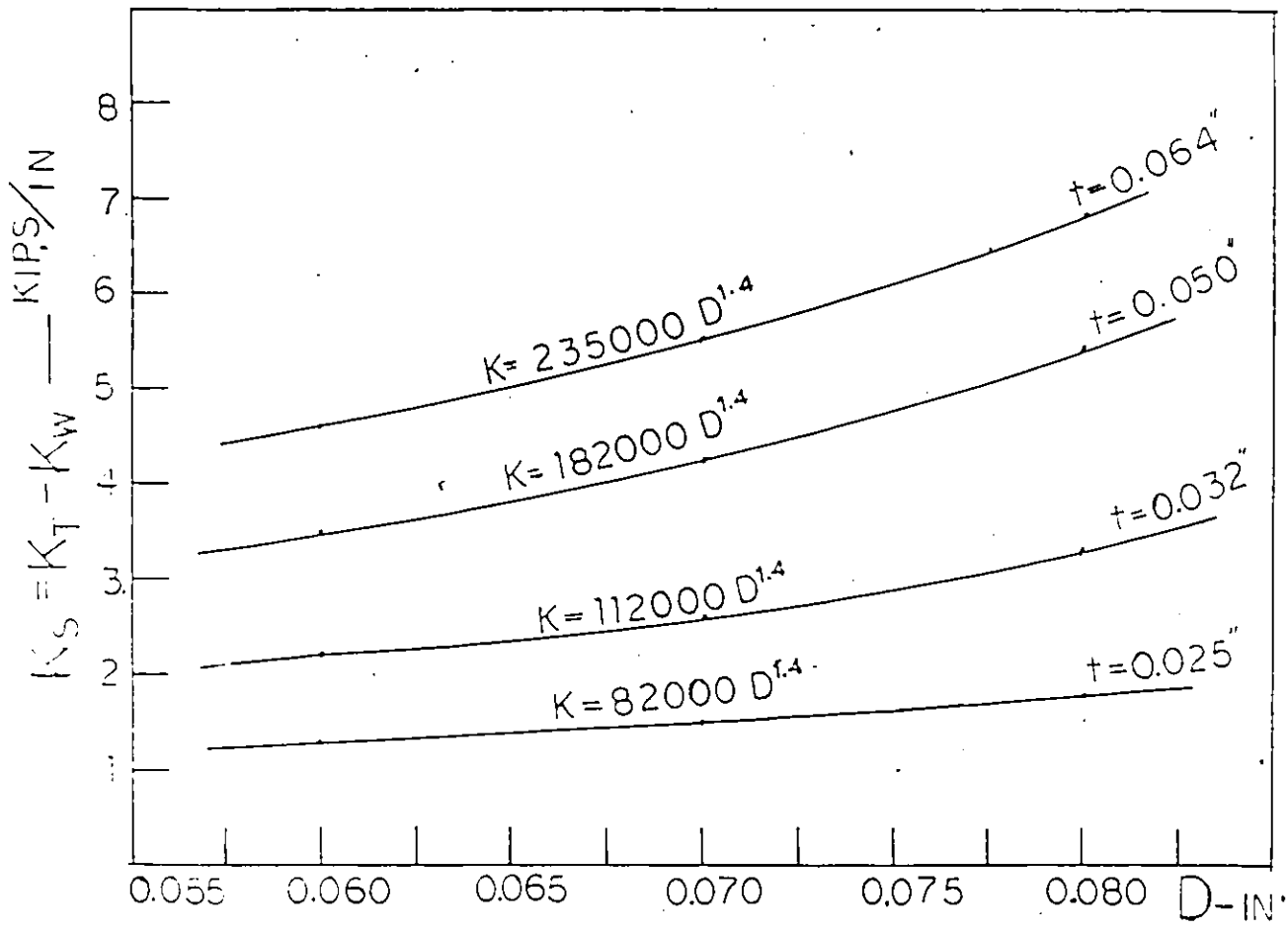


FIG. 5.7 - BEARING STIFFNESS OF THE ALUMINIUM FACING VERSUS THE STAPLE DIAMETER FOR VARIOUS ALUMINIUM FACING THICKNESSES

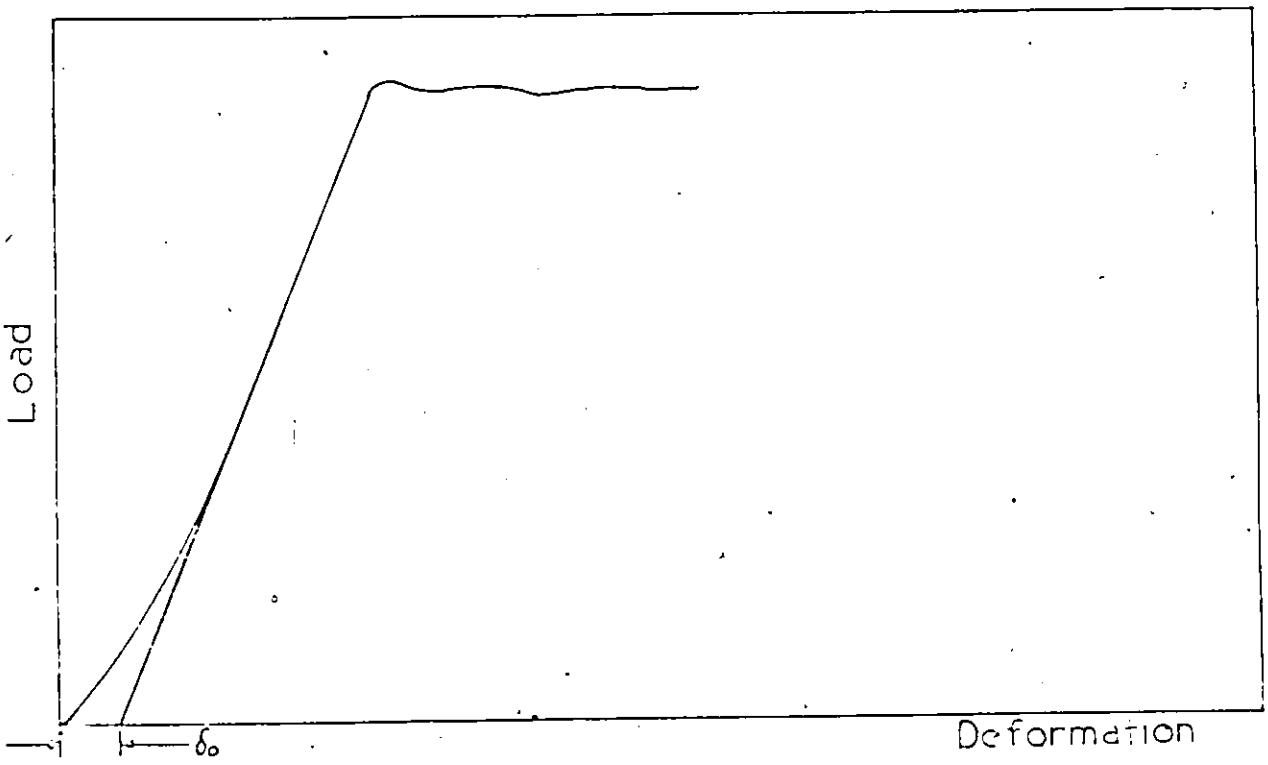


FIG. 5.8 - REPLACEMENT OF THE CURVE WITH A STRAIGHT LINE AND AN INITIAL SLIPPAGE.

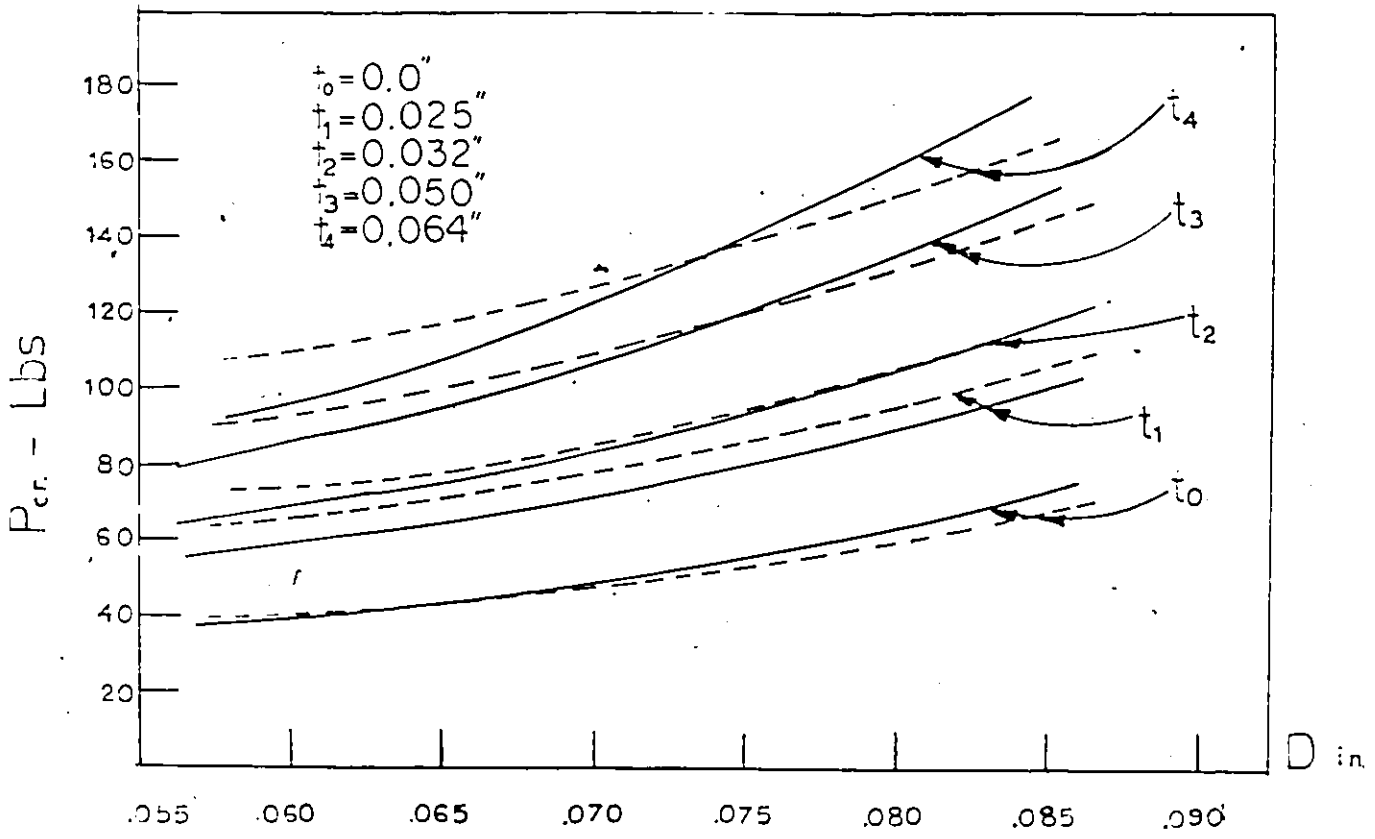


FIG. 5.9 - COMPARISON OF EXPERIMENTAL CURVES (SOLID LINES) FOR THE CREEPING LOAD WITH THE THEROETICAL RESULTS GIVEN BY EQUATION (5.12) (DASHED LINES).

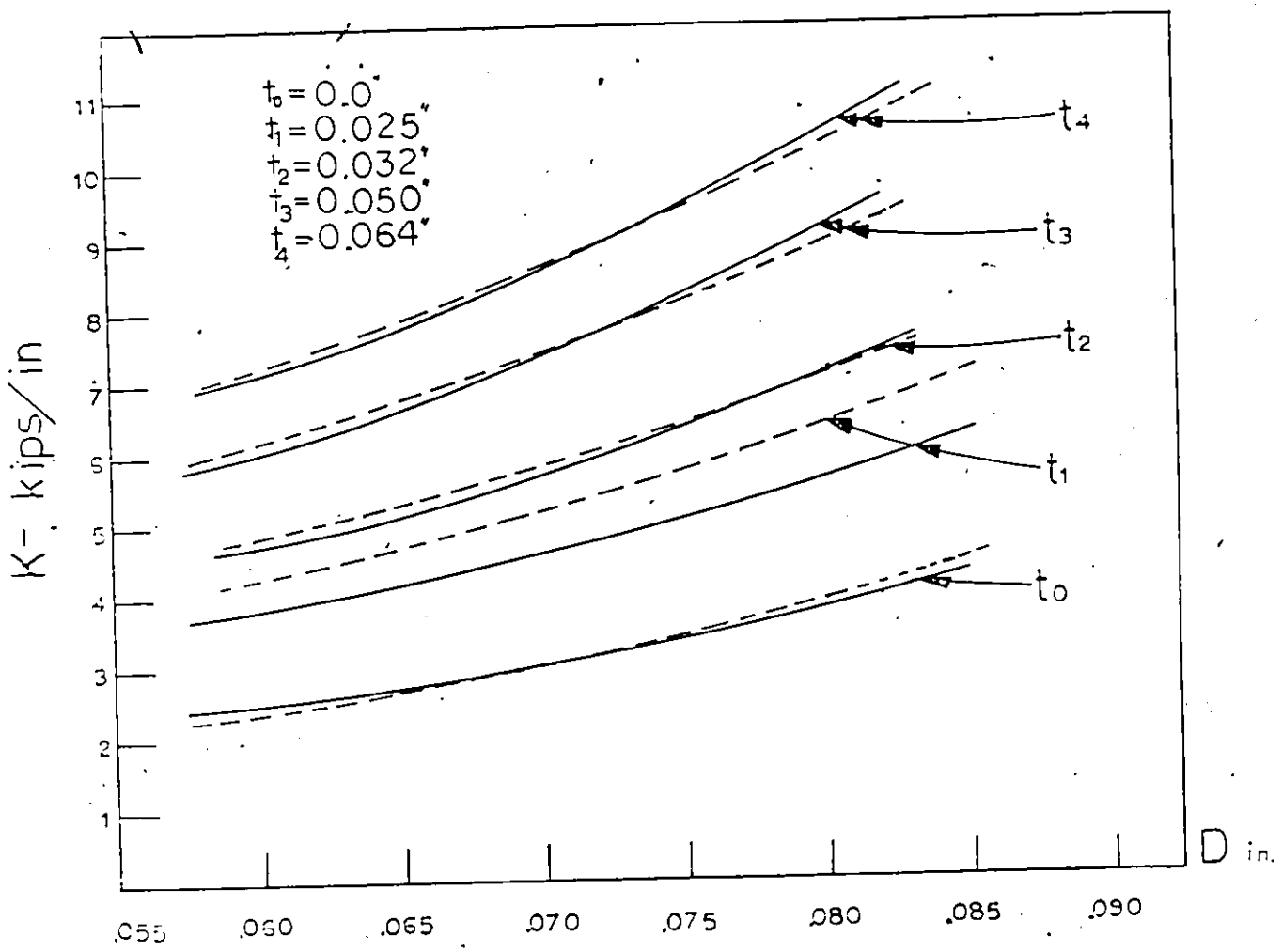


FIG. 5.10 - COMPARISON OF THE EXPERIMENTAL CURVES (SOLID LINES) FOR THE STAPLE LEG STIFFNESS WITH THE THEORETICAL RESULTS GIVEN BY EQUATION (5.17) (DASHED LINES).

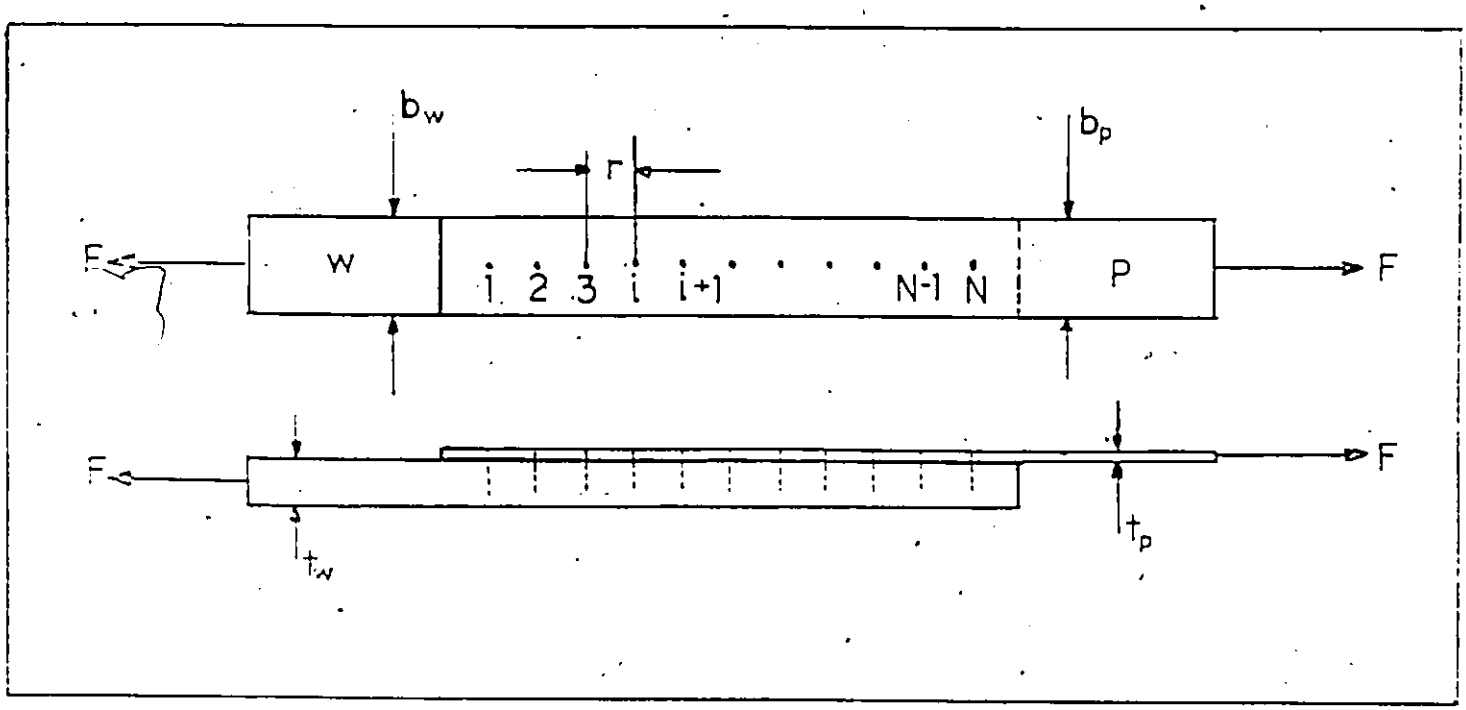


FIG. 6.1 - LONG JOINT WITH EQUALLY SPACED FASTENERS IN LINE WITH THE LOAD

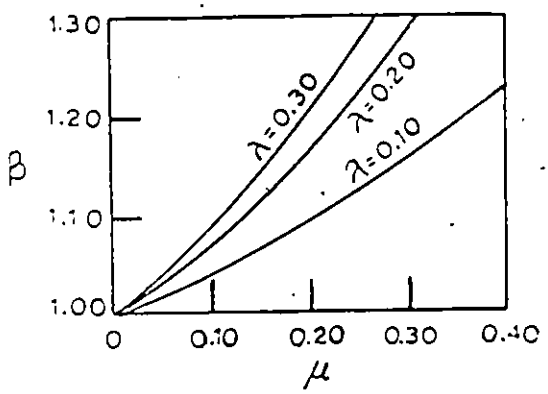


$\mu = d/D$

$\lambda = c/2r$

FIG. 6.2 - SCHULZ MULTIPLYING FACTOR

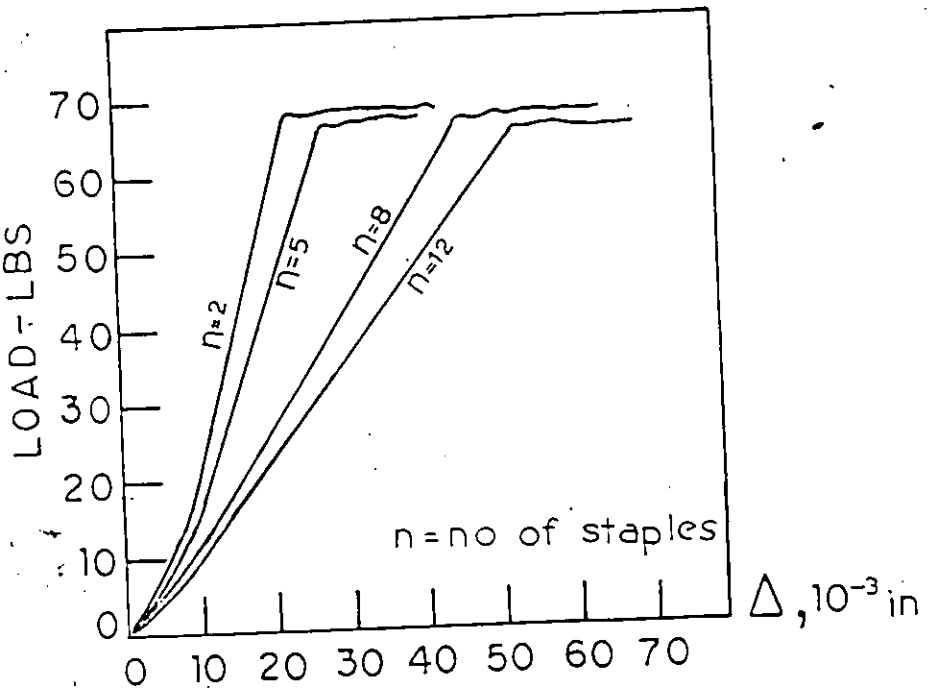


FIG. 6.3 - AVERAGE LOAD PER STAPLE LEG VERSUS DEFORMATION IN A LONG JOINT FOR VARIOUS NUMBERS OF STAPLES, AS SHOWN IN THE BRACKETS, AND FOR GAGE 16 STAPLES AND ALUMINIUM THICKNESS 0.032"

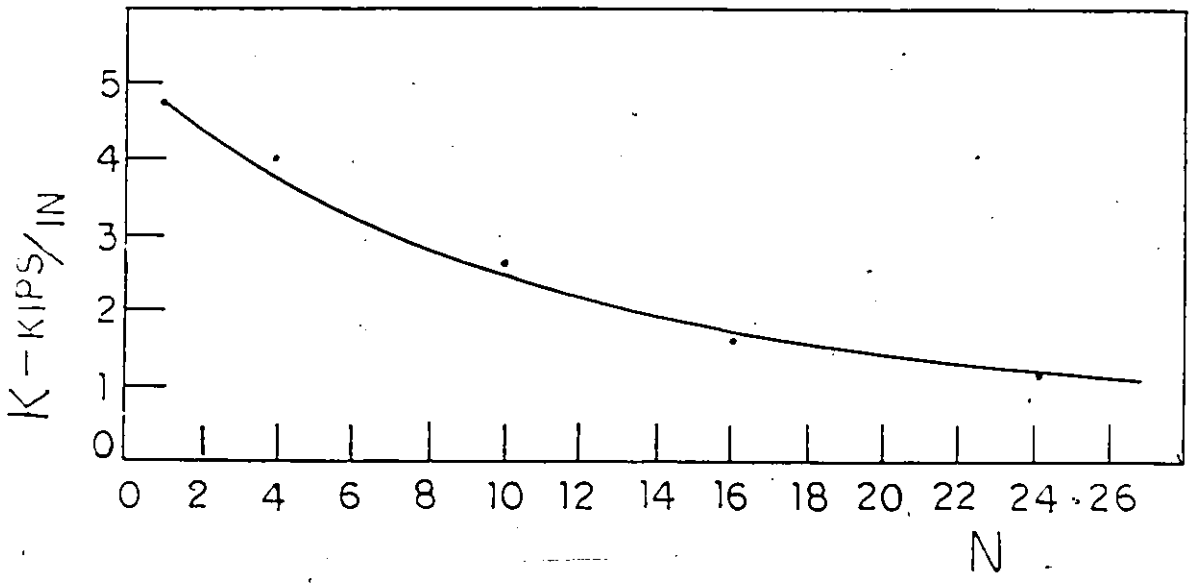


FIG. 6.4 - STIFFNESS PER STAPLE LEG VERSUS THE NUMBER OF STAPLE LEGS IN A LONG JOINT

NOTE: Stiffness is the slope of the average load per staple leg versus the defromation of the joint.

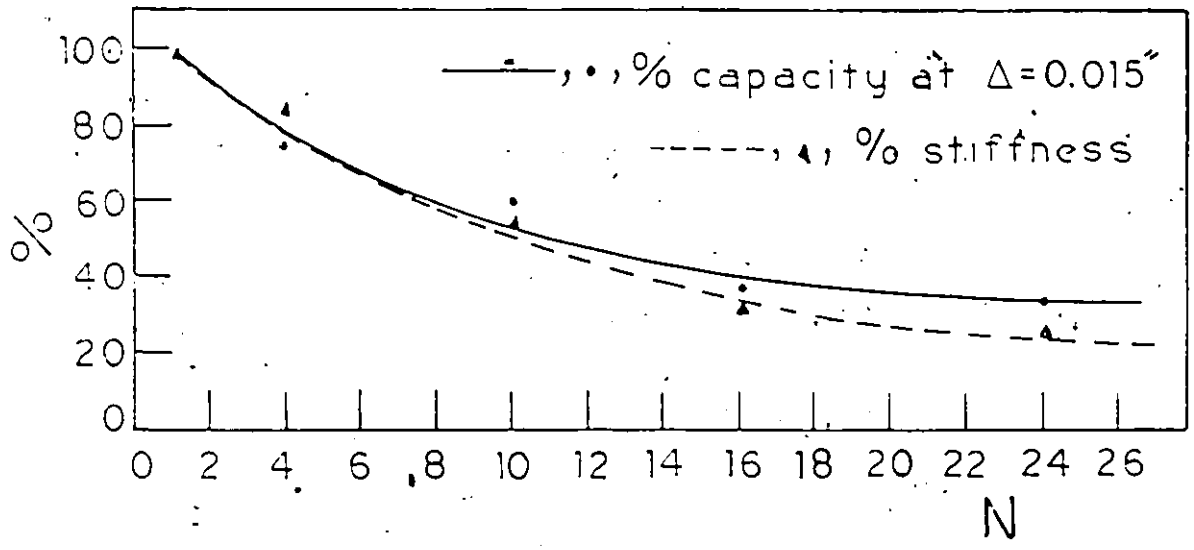


FIG. 6.5 - PERCENT STIFFNESS AND CAPACITY OF A STAPLE LEG AT Δ = 0.015" VS THE NUMBER OF STAPLE LEGS IN A LONG JOINT. 100% IS FOR A JOINT WITH ONE STAPLE ONLY.

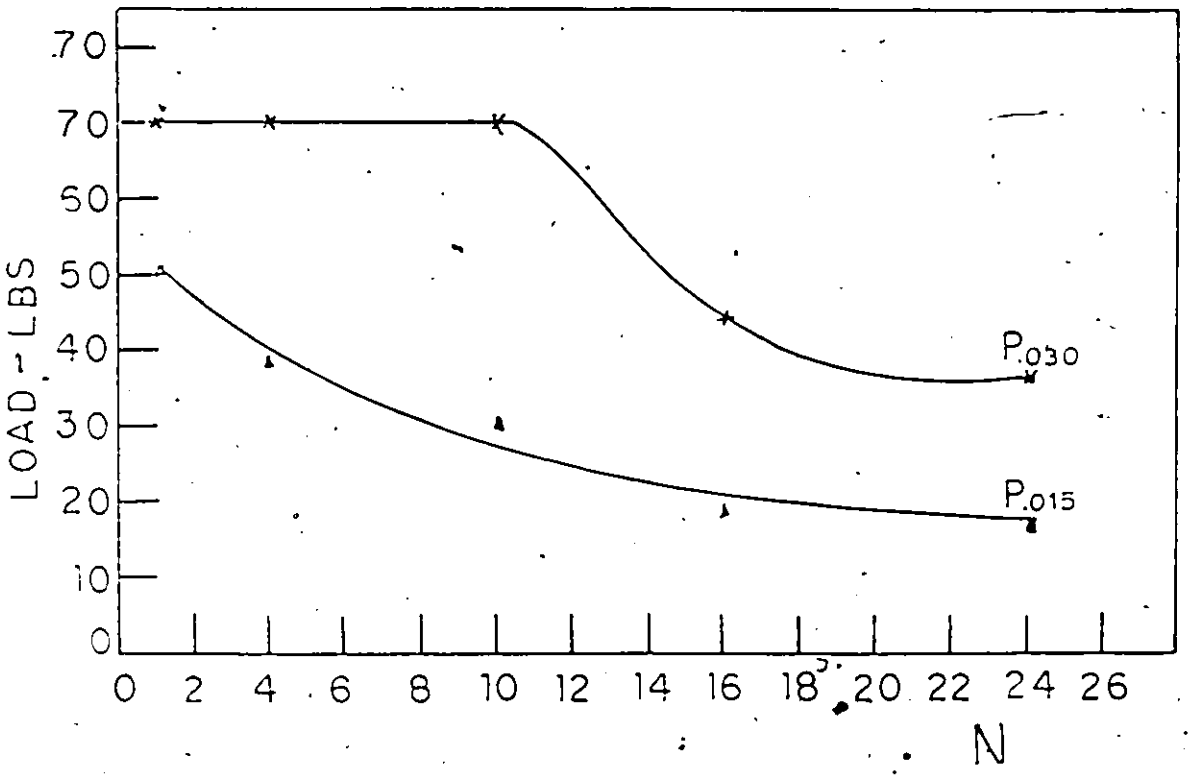


FIG. 6.6 - CAPACITY, AT $\Delta$ = 0.015" and $\Delta$ = 0.030" PER STAPLE LEG VERSUS THE NUMBER OF STAPLE LEGS IN A LONG JOINT FOR STAPLES OF GAGE 16 AND ALUMINIUM THICKNESS 0.039"

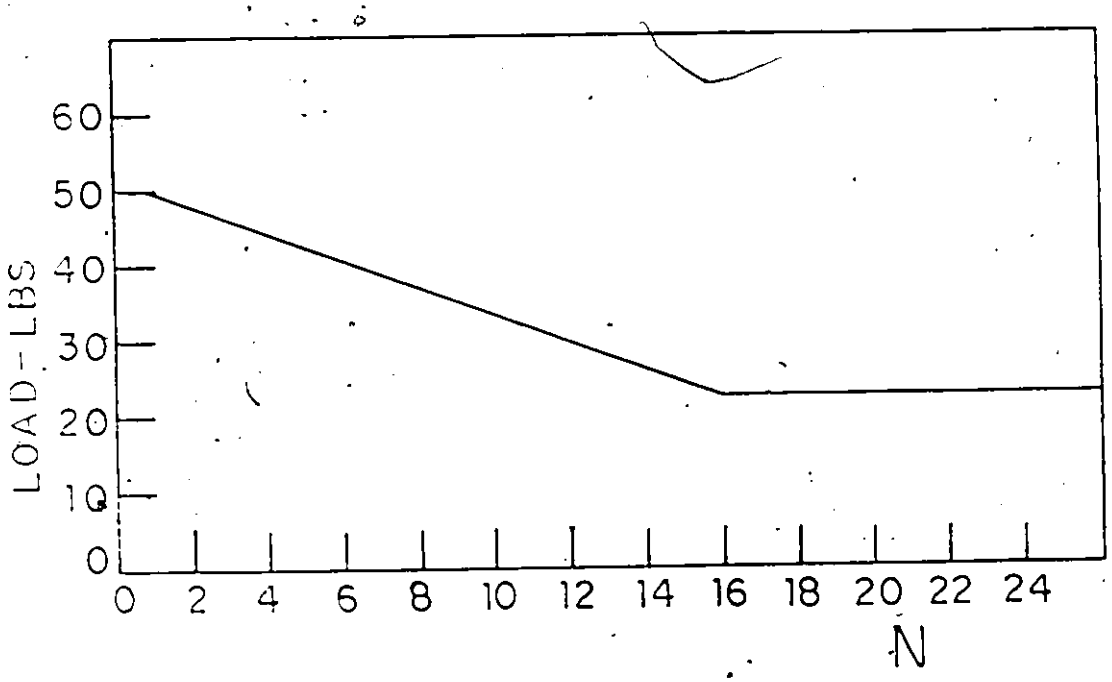


FIG. 6.7 - LINEAR APPROXIMATION OF THE CAPACITY PER STAPLE LEG AT $\Delta$=0.015" VERSUS THE NUMBER OF STAPLE LEGS FOR A LONG JOINT FOR STAPLES GAGE 16 AND ALUMINIUM THICKNESS 0.038"

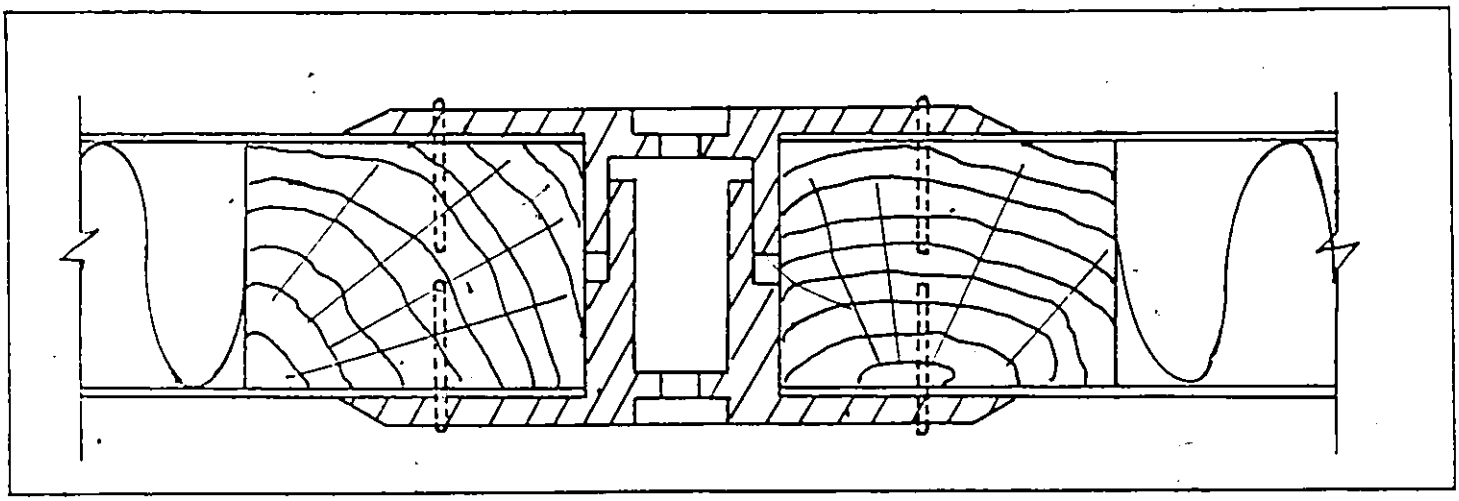

FIG. 8.1 - PROPOSED CONNECTION FOR TWO PANELS IN THE SAME PLANE

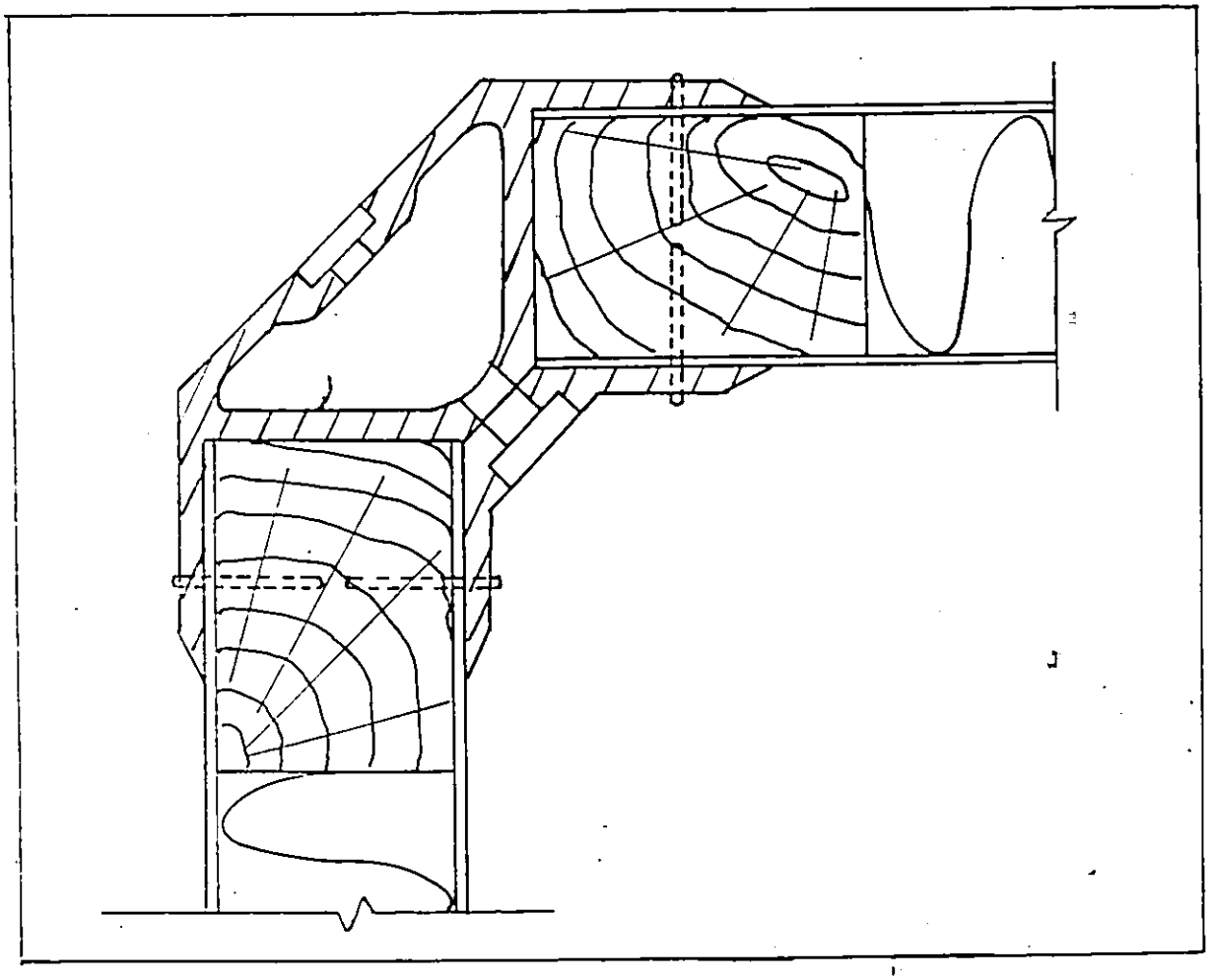

FIG. 8.2 - PROPOSED CONNECTION FOR TWO PANELS IN PERPENDICULAR PLANES

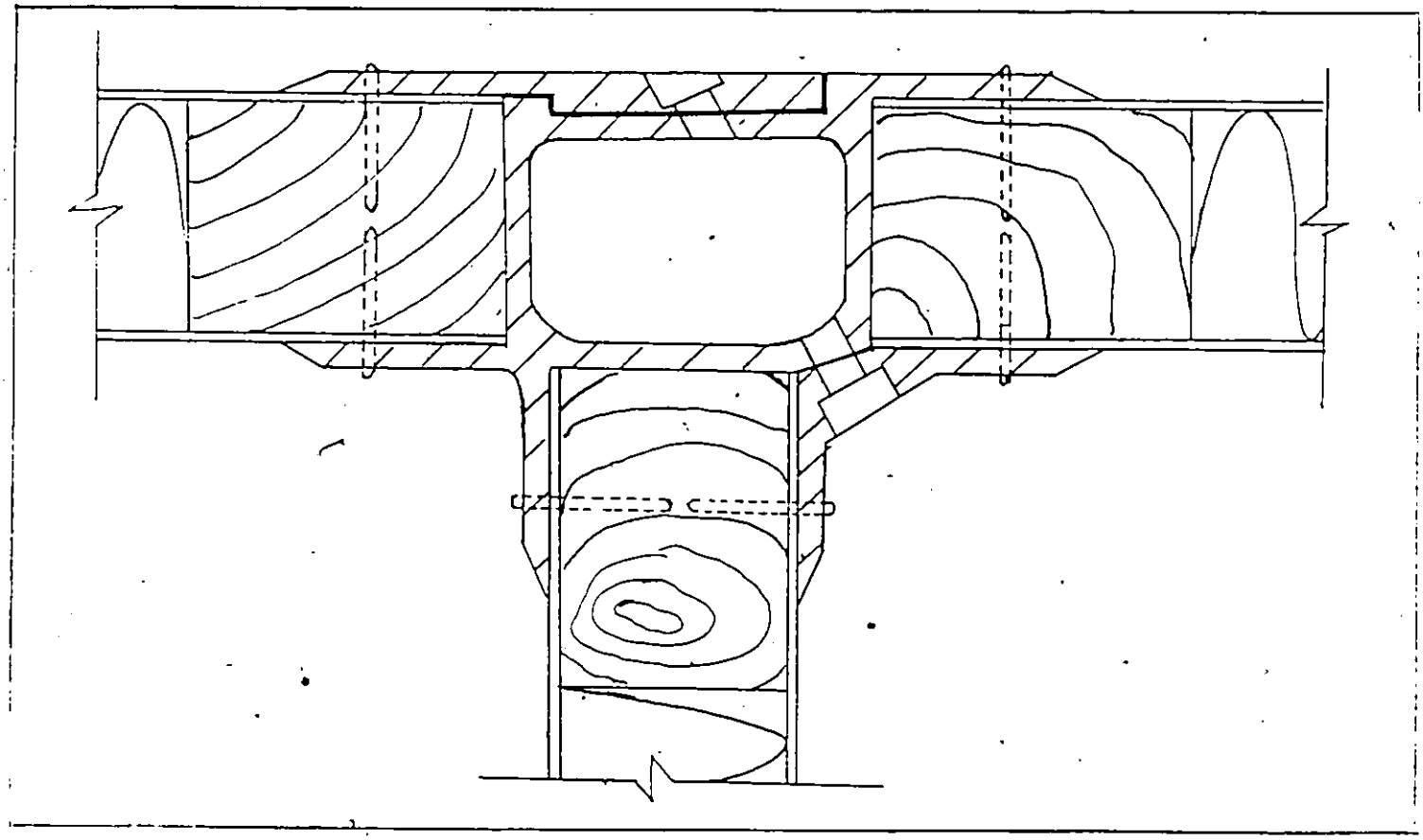

FIG. 8.3 - PROPOSED CONNECTION FOR THREE PANELS

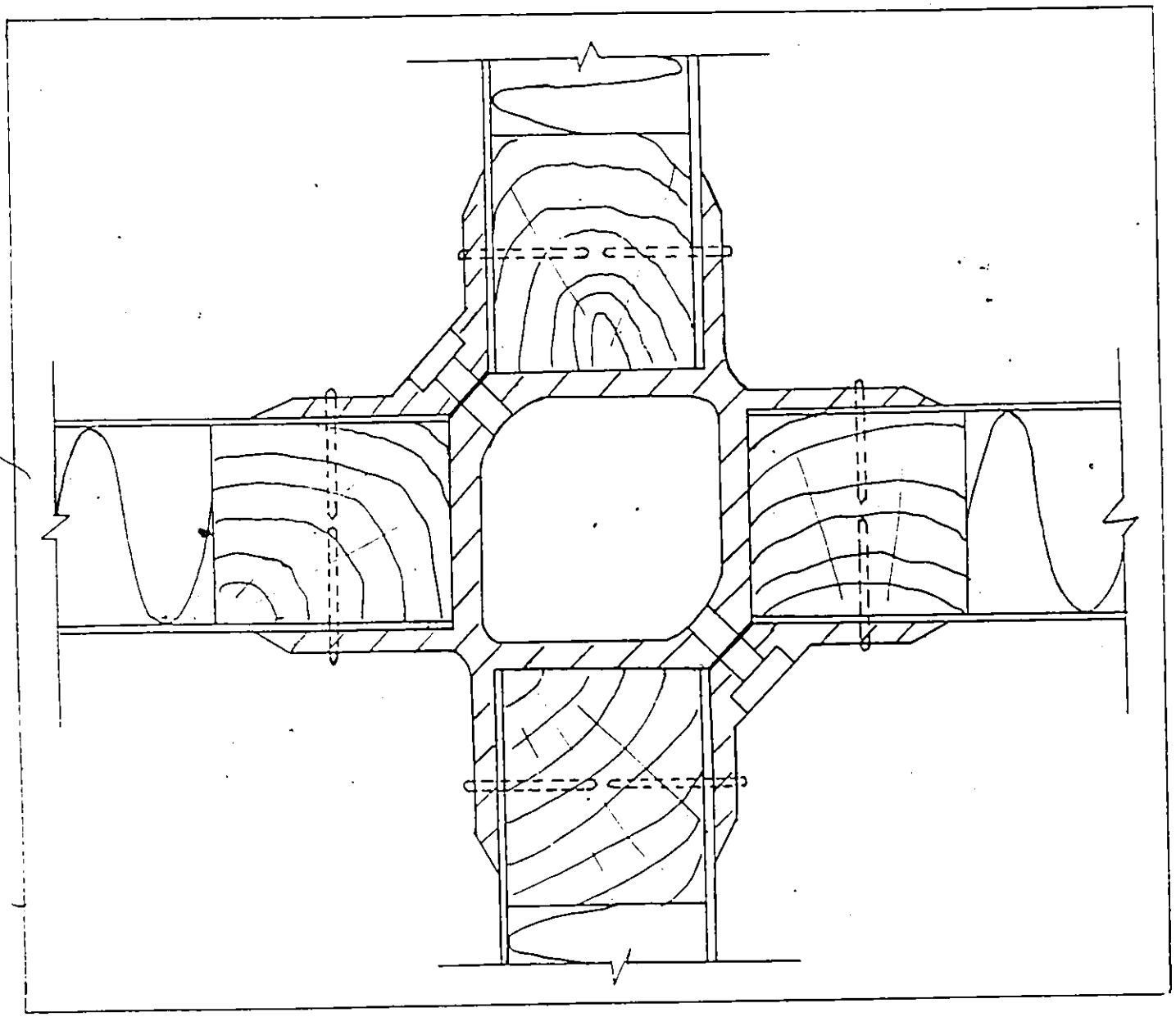

FIG. 8.4 - PROPOSED CONNECTION FOR FOUR PANELS

## REFERENCES

(1) Hetenyi, M., "Beans on Elastic Foundation", The warvely Press, Balitmore, Md., 1946, pp. 1-9.

(2) CIB, Modern Timber Joints, Report No. 8, by Trada-Rotterdam 1967.

(3) Stulka, R., "Theoretical Design of a Nailed or Bolted Joint under Lateral Load", thesis presented to the University of Winsconsin, at Madison Wis., 1960, in partial fulfillment of the requirements for the degree of Master of Science in Civil Engineering.

(4) Wilkinson, Thomas, "Theoretical Lateral Resistance of Nailed Joints", Journal of the Structural Division, proceeding of teh ASCE, No. ST5, May 1971, pp. 1381-1397.

(5) Wilkinson, Thomas, "Analysis of Nailed Joints with Dissimilar Members", Journal of teh Structural Division, Proceedings of the ASCE, No. ST5, Sept. 1972, pp. 2005-2013.

(6) ASTM Standard method of testing, metal fasteners in wood, D1761-68.

(7) U.S. Federal Specification FF-N-105B, Industrial Stapling and Nailing Technical Association, Chicago, Illinois, March 1971, pp. 21-27.

(8) Stern, George, Lateral Load Transmission by 2 1/2" x 15-gage Senco staples, Virginia Poltechnic Institute Research Division, Wood Research and Wood Construction Laboratory Bulletin, No. 92, June 1970.

(9) Stern, George, Staple versus Nail for Pallet Assembly, Virgiria Polytechnic Institute and State University Wood Research and Wood Construction Laboratory, Bulletin No. 102, April 1971.

(10) Stern, George, Performance of Pallet Nails and Staples in 22 Southern Hardwoods, Virginia Polytechnic Institute and State University, Wood Research and Wood Construction Laboratory, Pallet and Container Research Center, Bulletin No. 145, June 1976.

(11) Stern, George, Performance of 2 1/2" x 15-gauge Duo-fast Pallet Staples, Virginia Polytechnic Institute and State University, Wood Research and Wood Construction Laboratory, Pallet and Container Research Center, Bulletin No. 140, January 1976.

(12) Stern, George, Performance of 14-gauge Sencote staples, Virginia Polytechnic Institute and State University, Wood Research and Wood Construction Laboratory, Pallet and Container Research Centre, Bulletin No. 138, July 1975.

(13) Stern, George, Mibant Tests on Pallet Staples, Virginia Polytechnic Institute and State University, Wood Research and Wood Construction Laboratory, Bulletin No. 149, April 1977.

(14) Stern, George, Effectiveness of 2 1/2" Fasteners in Deckboard-stringer Joints for Permanent Warehouse Pallets, Virginia Polytechnique Institute Research Division, Wood Research and Wood Construction Laboratory, Bulletin No. 99, January 1971.

(15) Stern, George, Performance of 15-gauge Pas-Kote Pallet Staples, Virginia Polytechnic Institute and State University, Wood Research and Wood Construction Laboratory, Bulletin No. 137, June 1975.

(16) Stern, George, Qualtiy Control for 2 1/2" x 15-gage Seno staples, Virginia Polytechnic Institute Research Division, Wood Research and Wood Construction Laboratory, Bulletin No. 86, January 1970.

(17) Stern, George, Recent Pallet-fastening Research can Reduce Pallet Costs, Virginia Polytechnic Institute and State University, Wood Research and Wood Construction Laboratory, Bulletin No. 128, Sept. 1974.

(18) Cramer, C., Load Distribution in Multiple-bolt Tension Members, Journal of the Structural Division, Proceedings of the ASCE, No. ST5, May 1968, pp. 1101-1117.

(19) Fisher, J, Yoshida, N., Large Bolted and Riveted Shingle Splices, Journal of the Structural Division, proceedings of ASCE, No. ST9, Sept. 1970, pp. 1903-1918.

(20) Bendingo, R., Hansen, R., Rumof, J., Long Bolted Joints, Journal of the Structural Division, Proceeding of the ASCE, No. ST6, December 1963, pp. 187-213.

(21) Palmer, L., Brown, P., Piles Subjected to Lateral Thrust, ASTM Special Technical Publication No. 154-A, Publ. by ASTM, Philadelphia, Pa. 1955.

(22) Whitaker, Horizontal Forces on Piles and Pile Groups, Ch. 11 from the Design of Piles Foundations, 2nd Ed., Oxford, New York, Pergamon Press, 1976.

(23) Miranda, C., Nair., Finite Beams on Elastic Foundations, Journal of the Structural Division, Proceedings of the ASCE, No. 2, April 1966, pp. 131-142.

(24) Beaufait, F., Numerical Analysis of Beams on Elastic Foundations, Technical Notes, ASCE, No. EM1; February 1977, pp. 205-209.

(25) U.S. Forest Services, Wood Handbook, U.S. Dept. of Argriculture: 1955.

(26) Hansen, H, Modern Timber Design, 2nd Ed., New York, By John Wiley, 1962.

(27) Kuenzi E., Theoretical Design of a Nailed or Bolted Joint under Lateral Load, Forest Product Lab., Report No. D1951, Madison Wis., 1955.

(28) Fazio, P., Mikler, J., Modular Panelized Buildings, Concordia University, Montreal, Quebec, Canada, Report No. IV, July 1970.

(29) Strength of Aluminium, Alcan Canada Products Limited, April 1973.

(30) Fazio, P., Rizzo, S., Non Linear Elastic Analysis of Panelized Shear Sandwich Walls, Concordia University, Centre for Building Studies, Montreal, Quebec, Canada, Report November, 1977.

(31) Hrenikoff, A., Work of Rivets in Riveted Joints, Transactions, ASCE, Vol. 99, pp 437, 1934.

## APPENDIX I

## COMPARISON OF THE BEHAVIOUR OF A BEAM (STAPLE) OF INFINITE LENGTH WITH A BEAM (STAPLE) OF FINITE LENGTH

The behaviour of a beam of infinite length is given by Equation (5.2):

$$\frac{P}{\delta} = \frac{E^{1/4}\pi^{1/4}D^{7/4}K_o^{3/4}}{2} \qquad (5.2)$$

The behaviour of a beam of finite length is given by Equation (5.3):

$$\frac{P}{\delta} = -\frac{E^{1/4}\pi^{1/4}D^{7/4}K_2^{3/4}}{2}\left(\frac{F_1F_2 + 4F_3F_4}{-4F_2F_4 - F_1^2}\right) \qquad (5.3)$$

where

$F_1 = \cosh\lambda L \cdot \cos\lambda L$

$F_2 = 1/2(\cosh\lambda L \cdot \sin\lambda L + \sinh\lambda L \cdot \cos\lambda L)$

$F_3 = 1/2 \sinh\lambda L \cdot \sin\lambda L$

$F_4 = 1/4(\cosh\lambda L \cdot \sin\lambda L - \sinh\lambda L \cdot \cos\lambda L)$

$\lambda = \sqrt[4]{\frac{K}{4EI}}$

$K = K_oD$ lbs/in$^2$

$K_o = 2{,}114{,}000\ G$ lbs/in$^3$, G = specific gravity of wood

$I = \pi D^4/64$ in$^4$

$E = 30 \times 10^6$ psi

For varying diameter D, L/D rations, and wood species (varying G), find how the quotient of the F's in equation (5.3) varies, using the above equations for K, and $K_o$.

For G = 0.38

| D = 0.050" | | D = 0.080" | |
|---|---|---|---|
| L/D | F's quotient | L/D | F's quotient |
| 8 | -0.9445 | 7.5 | -0.9530 |
| 12 | -0.9957 | 12.5 | -0.9995 |
| 16 | -0.9990 | 15.0 | -0.9998 |
| 20 | -0.9999 | 20.0 | -1.000 |

For G = 0.45

| D = 0.50 | | D = 0.080" | |
|---|---|---|---|
| L/D | F's quotient | L/D | F's quotient |
| 8 | -0.9513 | 7.5 | -0.9600 |
| 12 | -0.9979 | 19.5 | -0.9997 |
| 16 | -0.9998 | 15.0 | -0.9999 |
| 20 | -1.000 | 20.0 | -1.000 |

For G = 0.57

| D = 0.050" | | D = 0.080" | |
|---|---|---|---|
| L/D | F's quotient | L/D | F's quotient |
| 8 | -0.9610 | 7.5 | -0.9694 |
| 12 | -0.9989 | 12.5 | -0.9998 |
| 16 | -0.9999 | 15.0 | -0.9998 |
| 20 | -1.000 | 20.0 | -1.000 |

From the above tables it can be seen that the value of F's quotient is equal to -1.0 for L/D > 14. This means that it can be eliminated and thus the equations of a beam of infinite length can be used for a beam of finite length, provided L/D > 14.